OPTICAL PROPERTIES OF RANDOM SEMICONDUCTING ALLOYS

by

BIPLAB GANGULI

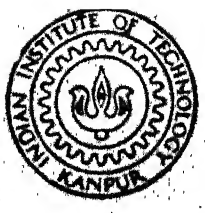

DEPARTMENT OF PHYSICS

INDIAN INSTITUTE OF TECHNOLOGY, KANPUR

SEPTEMBER, 1989

OPTICAL PROPERTIES OF RANDOM SEMICONDUCTING ALLOYS

A Thesis Submitted
In Partial Fulfilment of the Requirements
for the Degree of
DOCTOR OF PHILOSOPHY

by

BIPLAB GANGULI

to the

DEPARTMENT OF PHYSICS
INDIAN INSTITUTE OF TECHNOLOGY, KANPUR
SEPTEMBER, 1989

Dedicated To

My Parents

and

Susheela

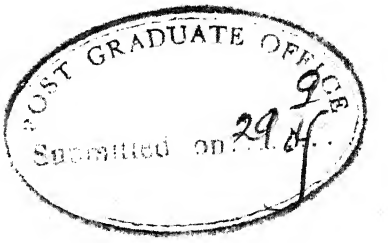

CERTIFICATE

This is to certify that the work of this thesis entitled : **OPTICAL PROPERTIES OF RANDOM SEMICONDUCTING ALLOYS** has been carried out by **BIPLAB GANGULI** under my supervision. No part of this work has been submitted elsewhere for a degree.

Abhijit Mookerjee
Professor
Department of Physics
Indian Institute of Technology
Kanpur 208016, INDIA

September, 1989

ACKNOWLEDGMENT

I gratefully acknowledge the able guidance and consta help of Professor Abhijit Mookerjee throughout my Ph.D. programme It is almost impossible to list out what all I got from him. short working with him has been a pleasant and memorable experienc of my life .

I am grateful to Professor R. Saran , Professor A.K Majumdar , Professor G.K. Mehta , Dr.V.A. Singh , and Dr.R. Prasa for many helpful discussions.

I am thankful to my colleagues Dr.P.K. Thakur , Aru Mishra , Samita Bardhan , S.S. Rajput , and S.S.A. Razee for mar useful discussions.

I am gratful to Dr.A.P. Shukla and Dr.Veenapani Shukla wh stood by me through testing times and provided me great moral ar emotional courage. It would have been almost impossible to pursue m research work without thier encouragement and support.

My special loving thanks goes to Susheela who has alway been the driving and inspiring force behind me.

I would like to thank all my family members and relative for their special love and concerns.

Many thanks to Abhay , Sandeep , Manoj , Mona , Mishraje , Vijay , Jagdish , and Videsh for being good friends , prompt wit encouragement and support and people with whom I could share so muc more than just academic committments.

It is a pleasure to thank my dear friends Anuradha , A , Sanjay , Manoranjan , Ganesh , Alok , Rita , Amitabh , Naveer Abhijit , Samir , Massood and many others.

Special thanks are due to Raghava Verma for the patier and sincerity which he showed during the correction of the thesis.

Thanks are due to Ranjan Basu who prepared the figures a N. Kumar and V. Seetharam for their kind help in proof reading.

I thank R. Khanna and Mr. Bajpai for typing the thesis.

Lastly I thank all the members of Jan Vigyan Samiti a Janta Pustakalya and all the students of Janta Vidyalya who provid me the sense of responsibility towards the society.

29th September

Biplab Gangul

CONTENTS

SYNOPSIS

This thesis entitled "**OPTICAL PROPERTIES OF RANDOM SEMICONDUCTING ALLOYS**" is submitted by Biplab Ganguli to the Department of Physics, Indian Institute of Technology, Kanpur in partial fulfilment of the requirements of the Ph.D. degree.

The problem of optical responses likeoptical conductivity, dielectric function etc. of disordered alloys is a matter of interest for a long time now both for theoretical and experimental physicists. The optical response of ordered systems is well understood on the basis of the formulation based on the Bloch's Theorem and band structure ideas. The electron photon interaction matrix element factor in the expression for optical conductivity is assumed to be slowly varying function of energy. It is found that for a large class of materials the electron-photon interaction matrix element is a slowly varyig function of energy over a large energy range and fairly independent of randomness. However, the need to go beyond these assumptions for disordered alloys was felt for a long time.

In Chapter II, we discuss optical response in general and find a basic formula for optical conductivity. In particular we set up expressions for the optical conductivity for ordered systems and disordered alloys for two cases, one with the assumption that electron-photon interaction matrix element is independent of energy and randomness and the other without this assumption.

In chapter III, we discuss a self-consistent coherent potential approximation (CPA) and cluster coherent potential approximation (CCPA) formalisms to obtain a configurationally averaged Green function. The cluster CPA formalism is based on the AUGMENTED SPACE METHOD introduced by Mookerjee (1973). The Augmented space method is by now a well established and powerful formalism for calculating various average properties of disordered systems. In CPA the correlated scattering from two or more sites are ignored. In the self-consistent cluster generalization (CCPA) of CPA statistical clustering effects and off-diagonal disorder over finite cluster sizes are successfully taken into account. Beside, it preserves the (Herglotz) analytic properties of the Green function which are essential for obtaining physically meaningful approximate results.

In this chapter the Augmented space method is used to obtain an expression for configurationaly averaged optical conductivity of random semiconducting binary alloys without making any assumption about the electron-photon interaction matrix element. Thus a genral formulation for optical conductivity of random semiconducting binary alloys is obtained. This genralization is the principal contribution of the thesis. The formulation is applied to a model case. We use CPA and CCPA to calculate density of states and the various optical response functions. The effects of various assumptions are also discussed within the model.

In chapter IV we make applications of the above formalism to realistic systems. The systems chosen are $GaAs_{1-x}Sb_x$ and $Ga_{1-x}In_xSb$. In order to compare with the older formalisms we

calculate various optical response functions for the two cases. Firstly using the above formalism and secondly making assumption that the electron-photon interaction matrix element is randomness independent and taken to be the averaged value. We also calculate the square of the electron-photon interaction matrix element and the product of this and the valence band density of states as a function of energy to accurately interpret the energy resolved photo-emission experiment. The calculations are done for two concentrations, i.e., $x = .5$ and $x = .2$.

In this chapter we also discuss molecular orbital basis (bond basis) which is used to generate Recussion coefficients for the calculation of valence band density of states. The Recussion method introduced by Haydock (1972) enables us to work on such realistic three-dimensional lattices. We discuss Recursion method in this chapter. The Recursion method is a well-established means of solving the Schrödinger equation for a system in which local interactions dominate. The local density of states and related quantities are calculated from the continued fraction expansion generated through the application of the Recursion method. We also discuss various terminator schemes to terminate the infinite continued fraction expansion. The Recursion method together with CPA is used to calculate the Green function, the density of states and the various optical response functions.

In chapter V, the achievements and shortcomings of the present work are discussed. Some of the problems in this field are also suggested.

LIST OF TABLES

LIST OF FIGURES

CHAPTER I

INTRODUCTION

The problem of optical response in disordered alloys has received the attention of solid state physicists with the extensive experimental works in that field for the last two decades (Nilsson, 1974 ; Závětova & Velický 1976). The theoretical understanding of optical response of periodic systems is well understood with the application of Bloch's theorem and band structure methods.

Optical conductivity is related to the product of the joint density of states and the electron-photon interaction matrix element (optical transition matrix). For a large class of ordered systems, it is found that the optical transition matrix element is a very slowly varying function of energy and, thus, can be thought of approximately as a constant. Therefore the optical conductivity is directly proportional to the product of the frequency of the incident photon and the integrated joint density of states.

The theoretical understanding of optical response of disordered alloys is not so satisfactory. The reason for this inadequacy is an additional problem related to the study of disordered systems : configurational averaging. In the case of ordered systems, once the Hamiltonian model is set up, the solution of quantum mechanical problems is essentially the solution of Schrödinger equation. However, with the introduction of disorder, we face a new problem, *i.e.* the lack of sufficient information about the sample in the Hamiltonian. This itself involves random parameters

and until information about the distribution of these parameters is supplied, the solution remains incomplete. One of the central problem in the study of disordered systems is configuration averaging.

Before going on to say anything about how we tackle the problem of configuration averaging, let us first understand what the term *configuration* implies, why configuration averaging is needed and what is it that we should average. In any substitutionally disorder system, the lattice sites are occupied by random potentials : random in space as in quenched disordered solids or random in time as in thermally disordered systems, (for example, electrons in contact with a phonon bath). There are examples where both spatial and temporal disorders are involved, for example dirty alloys at high temperatures (Mooij systems). A simple example of a spatially disorder system is a random binary alloy. Cu-Ni is a good candidate. At T = 0^{o}K the randomness is quenched and spatial. The potentials are characterized by random parameters. For example in a random binary alloy the potential, $V(r_i) = V_A N_i + V_B(1-N_i)$, is characterized by the random occupation number N_i (N_i = 0 if i^{th} site is occupied by an A atom and N_i = 1 if i^{th} site is occupied by a B atom). If short ranged order is absent, then the probability that N_i = 0 or 1 is directly proportional to the concentrations of the A or B species. A particular realization of these parameters, either in a given sample or at an instant of time is what we refer to as a configuration of the system.

Let us now understand why it is necessary to take configuration averaging. We shall start with the above example of a

random binary alloy. A configuration is determined by a particular assignment of 0's and 1's to the sequence $\{N_i\}$. Any one sample therefore corresponds to a particular configuration. For a sample containing N atoms there are 2^N configurations. This is a very large number for a macroscopic system. An experimentalist at the outset has no knowledge of the particular configuration of his sample. Nor is such a knowledge of much use. Evidently, every different sample of the alloy will give experimental information having different microstructure according to the particular configuration it has. The experimentalist, on the other hand, is primarily interested in the overall statistical trends of his results which he interprets as the *physical properties* of the random alloy. A theorist too can generate a number of results depending upon the particular configuration he chooses for his random parameters. This again is not very useful. He could try to derive properties of the most probable configuration and propose that these properties are highly likely. But, again, the number of different configurations as probable as the most likely and those with comparable likelihoods of occurrence, are intractably numerous. Therefore, we have to evolve a statistical description of the system. The most basic of these descriptions is the averaging over all possible configurations.

It is clear from the above why configuration averaging is required. It is also clear that it is the physically measured quantities which must be configurationally averaged. It was pointed out by Anderson in 1972 that the type of statistical description essentially depends on what we are trying to describe. He warned that only experimentally observable physical quantities related to

the response of a physical system to a probe must be averaged. This warning was necessary to explain the source of controversies that arose over non-physical results obtained because directly non-measurable quantities like self-energies, wave-functions etc. were being averaged. Whereas, it is quantities like the density of states, and response functions like optical conductivity or diffusion probabilities which should be averaged. Since the imaginary part of the Green function is directly related to the density of states, Green function techniques are favoured for the study of disorder systems rather than the Schrödinger equation approach.

Configuration averaging is a valid procedure only when the probability distribution of the property under consideration is sufficiently well behaved so that the average dominates over the higher moments. Interesting examples are the intensity of starlight transmitted through layered media with randomnly varying refractive indices studied by Chandrasekhar (1960) and the problem of the resistance of disordered chains. Kumar and co-workers (1985, 1986) have shown that the variance of the resistance of disordered chain diverges much faster than the average as the length of the chain increases. It is, therefore, not meaningful to talk in terms of the average resitance of a very long disordered chain.

Before we begin the discussion of how configuration averaging may be carried out, it is worthwhile to say something about spatial ergodicity. For a large enough systems, in the limit of infinite size, all possible environments are achieved even in a single sample. The figure (1.1) illustrates this idea.

A global probe samples all possible environments in the sample weighted with appropriate probabilities. A global property is thus automatically configuration averaged, even if it refers to a single sample. This sampling of the entire configuration by a spatially global probe is analogous to the sampling in statistical mechanics of all configuration space by a dynamically evolving system. Hence the name : *spatial ergodicity*. Such global properties need not be configuration averaged all over again. This idea is implicitly behind a large body of the "large cluster" calculations involving either isolated or immersed clusters. One example is the application of the Recursion method to large disordered clusters (Haydock, 1987).

In general, the exact calculation of configuration averages is an intractable problem. In §3.2 in chapter III, we shall discuss in detail how to configuration average any physical quantity in a simple tight-binding model for a substitutionally disordered alloy. We shall discuss the configuration averaging of optical conductivity and related response functions.

Various mean field approaches, like the self-consistent coherent potential approximation (CPA)(Soven, 1967), provide powerful and physically meaningful methods for the study of configurationally averaged one and two particle Green functions for disordered systems which are directly related to the averaged density of states and response functions. The earlier works on optical properties of disordered systems (Závètova and Velicky (1976) ; Cody 1984; Pickett et.al. 1983; Zdetsin et.al. 1985, etc.)

used the mean field and other approaches without taking into account the vertex correction arising out of disorder dependence of the optical matrix element . That is, while doing the averaging, the average of the product of density of states and optical transition matrix element was replaced by the product of their averages. Pickett and co-workers (1983) used the virtual crystal approximation (VCA) to average the optical transition matrix element separately. They, then, took this factor as constant and finally used coherent potential approximation to get averaged density of states.

This procedure may suffice for large classes of systems, but for more accurate studies the full problem has to be tackled. Particularly, in the strong scattering cases, the vertex correction may be of importance and the optical transition matrix element may not be insensitive to energy variations.

The need was felt, therefore, to include the vertex corrections. Mookerjee (1973a, b, 1975 a,b,c) introduced a formalism called the **Augmented space formalism** (ASF) to calculate configuration average of a general function of many random variables. The formalism has been quite successful in making the generalization of single site CPAto Cluster Coherent Potential Approximation (CCPA) and also to include the off-diagonal disorder in a self-consistent manner (Kumar et.al. 1982). Nickel and Krummhansl (1971) tried to make such a generalization using a method based on the corrected cumulant expansion to find electronic density of states of a one dimensional model of an alloy. Butler (1972, 1973) calculated the real and imaginary parts of the Green function using a self-consistent cluster method. These generalizations posed

analytic problems, such as multivalued, discontinuous and negative density of states in certain energy regions.

Haydock *et.al.*(1972), Mookerjee (1973a,b), Müller-Hartmann (1973) and Mills and Ratanavararaksa (1978) pointed out that for any real potential function, the Green function must obey certain mathematical properties called the *Herglotz* properties. A complex function f(z) is defined as Herglotz if

(i) $\mathrm{Im}f(z) \leq 0$ for $\mathrm{Im}z < 0$

(ii) Singularities of f(z) lie on the real axis, and

(iii) $f(z) \longrightarrow \frac{1}{E}$ as $E \longrightarrow \infty$ (where $z = E + i0^{+}$)

In order to get physical results, Herglotzicity has to be retained in any approximation to the Green function. It has to be borne in mind that in the development of a theory which includes scattering from clusters, short ranged order, off-diagonal disorder or the effects of positional disorder, Herglotz property must be inherently retained.

The Augmented Space Formalism allows us to systamatically introduce approximations which retain such properties of Green function. The main aim of the present work is to extend the Augmented Space Formalism to obtain configurationally averaged optical properties including the vertex correction.

Chapter II deals with the detailed discussion on general optical properties of solids, response functions and their relations to one another. In chapter III we introduce the Augmented Space Formalism with its mathematical formulation. It is shown how we can

generate CPA and CCPA within the formalism. In §3.6 a general expression for the optical conductivity of random semiconducting alloys is formulated using the Augmented space formalism In §3.7 we apply the formalism to a model case. Chapter IV deals with the application of the formalism to the ternary systems $GaAs_{1-c}Sb_c$ and $Ga_{1-c}In_cSb$ for different concentrations c. In this chapter we also discuss molecular orbital (MO) or bond basis and Recursion method and its different terminator schemes which enable us to accurately calculate the constituent Green functions. These are used as essential inputs in our theory. Side by side, for comparison, we also calculate the various response functions without the vertex correction.

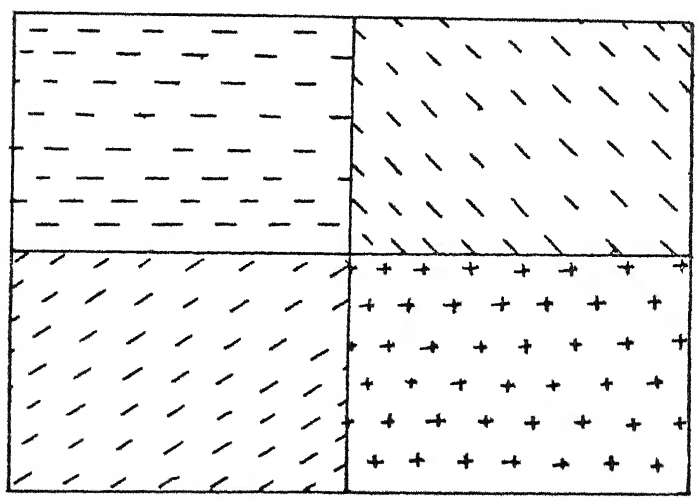

Figure 1.1 Representation of different environments within a sample. For $n \longrightarrow \infty$, all environments are realized.

CHAPTER II

THEORY OF OPTICAL PROPERTIES

2.1 INTRODUCTION :

The interaction between electromagnetic radiation and solids causes absorption of the radiation through microscopic excitations. The excitations can usually be described with quasiparticles like electrons, phonons, plasmons, magnons etc. For metals, the dominant absorption is caused by the electrons. In the infrared (IR) region (0.1 eV) the conduction or "free" electrons contribute to a strong absorption, the magnitude of which decreases smoothly with increasing photon energy. In the visible region (2 to 3 eV) it is usually comparatively small (Nilsson 1974). The microscopic process can be viewed as a electron-photon scattering process. The scattering occurs to a conduction or unoccupied band. Such excitations are called **intraband transitions**. This process is shown in the figure (2.1.1). The theory for such an absorption process was first given by Drude and the model is known as the Drude model (Animalu, 1978). In his model, Drude used a classical approach. The basic assumption was that the optical conductivity and the dielectric function could be determined by considering the motion of quasi-free electrons under the influence of the oscillating electric field vector of the electromagnetic wave.

The optical spectrum of a real crystal of a metal, a

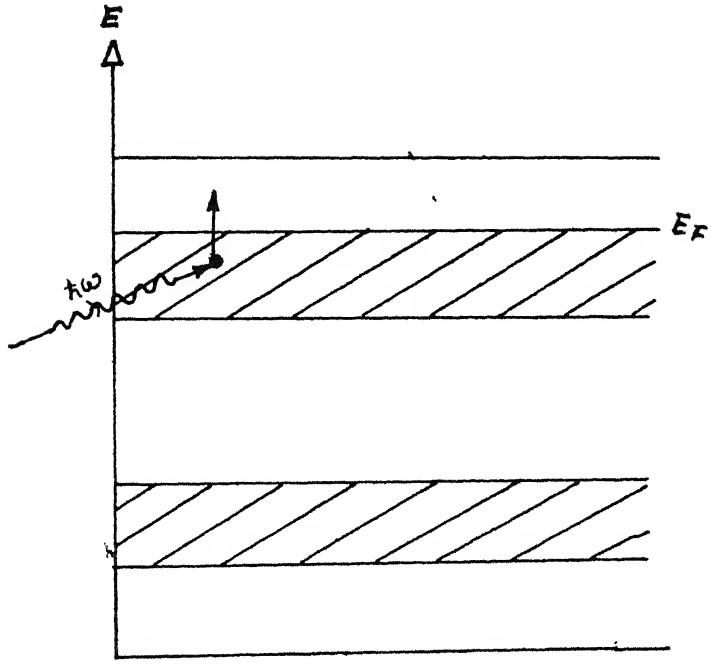

Figure 2.1.1 Intraband Transition in Metals

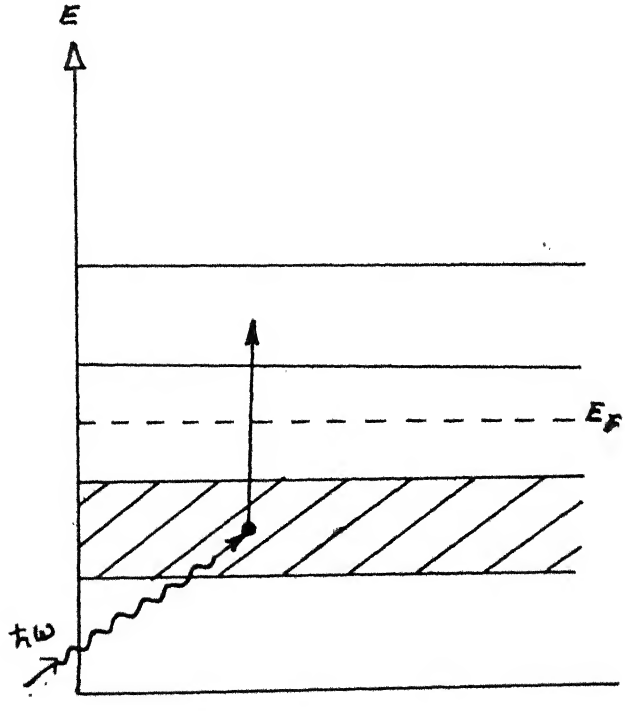

Figure 2.1.2 Interband Transition in Semiconductor

semiconductor, an insulator or a disordered system usually has mor structures in the visible region to far UV region (10 eV) than thos arising from Drude absorption and the occurence of plasm oscillations of free electrons accelerated by the electric field o the light wave. These structures are seen in the form of peaks, edges, etc., in the absorption versus frequency curve. Such structures arise due to the interaction of electrons only with the radiation. The electron is then directly excited from one electronic band to another. The process is called **interband transition**. This proccess is shown in the figure (2.1.2). In materials like insulators, semiconductors, or alloys of these, this is the only kind of absorption that takes place, because in such materials the valence band is completely filled and excitation can take place only to the completely unfilled conduction band. Drude absorption, therefore, is not possible. To understand these processes, we need to go beyond the classical approach and develop a quantum transport theory. In such a theory the electron-photon interaction is considered to be the exciting part of the Hamiltonian and a time dependent perturbation formalism is applied to obtain expression for the optical response functions of the system. Such a linear response theory was first suggested by Kubo (1957).

2.2 OPTICAL RESPONSE FUNCTIONS :

In this section we shall study the linear response of

electrons in a solid to external electromagnetic radiation, from the IR to the UV region (0.1 - 10 eV). In particular we shall describe the dielectric function $\varepsilon(\omega)$, optical conductivity $\sigma(\omega)$ and permeability $\mu(\omega)$ as the main properties usually studied experimentally. Here ω is the angular frequency of the external electromagnetic radiation. In the optical region (IR to UV) we shall choose non-magnetic systems where $\mu(\omega) \simeq 1$. The dielectric function $\varepsilon(\omega)$, conductivity function $\sigma(\omega)$ and permeability function $\mu(\omega)$ are defined through the response disturbance relations

$$\bar{D}(\omega) = \varepsilon(\omega)\ \bar{E}(\omega) \qquad (2.2.1)$$

$$\bar{J}(\omega) = \sigma(\omega)\bar{E}(\omega) \qquad (2.2.2)$$

$$\bar{H}(\omega) = \frac{1}{\mu(\omega)}\ \bar{B}(\omega) \qquad (2.2.3)$$

respectively, here $\bar{D}$, $\bar{E}$, $\bar{J}$, $\bar{H}$ and $\bar{B}$ are the displacement field, the electric field, the current density, the magnetic field and the magnetic induction vector respectively. A related response is the refractive index function $n(\omega)$ which is related to $\varepsilon(\omega)$ through :

$$n(\omega) = \sqrt{\varepsilon(\omega)} \qquad (2.2.4)$$

Another related response is the absorption function $\alpha(\omega)$. It is defined as the fraction of energy absorbedin passing through the unit thickness of the material.

Electromagnetic waves are the solutions of Maxwell's equations. For linear and homogeneous media these are written as

follows (In CGS units)

$$\text{Curl } \bar{H} = \frac{1}{c}\frac{\partial \bar{D}}{\partial t} + \frac{4\pi}{c}\bar{J} \qquad (2.2.5)$$

$$\bar{\nabla}.\bar{D} = 0 \qquad (2.2.6)$$

$$\text{Curl } \bar{E} = -\frac{1}{c}\frac{\partial \bar{H}}{\partial t} \qquad (2.2.7)$$

$$\bar{\nabla}.\bar{H} = 0 \qquad (2.2.8)$$

Eliminating the magnetic field vector between these Maxwell's equations for the electric field vector :

$$\nabla^2\bar{E} = \frac{\varepsilon}{c^2}\frac{\partial^2 \bar{E}}{\partial t^2} + \frac{4\pi\sigma}{c^2}\frac{\partial \bar{E}}{\partial t} \qquad (2.2.9)$$

This represents a wave propagating in a solid with dissipation (see figure (2.2.1)). If we choose the electric field of the type

$$\bar{E} = \bar{E}_o \exp(i(\bar{\varkappa}.\bar{r} - \omega t)) \qquad (2.2.10)$$

then our wave equation requires

$$-\varkappa^2 = -\varepsilon\frac{\omega^2}{c^2} - \frac{4\pi\sigma i\omega}{c^2}$$

i.e., $$\varkappa = \frac{\omega}{c}\left[\varepsilon + i\frac{4\pi\sigma}{\omega}\right]^{1/2} \qquad (2.2.11)$$

In general the propagation constant $\varkappa$ comes out to be a complex number. In free space we would simply have

$$\varkappa = \frac{\omega}{c} \qquad (2.2.12)$$

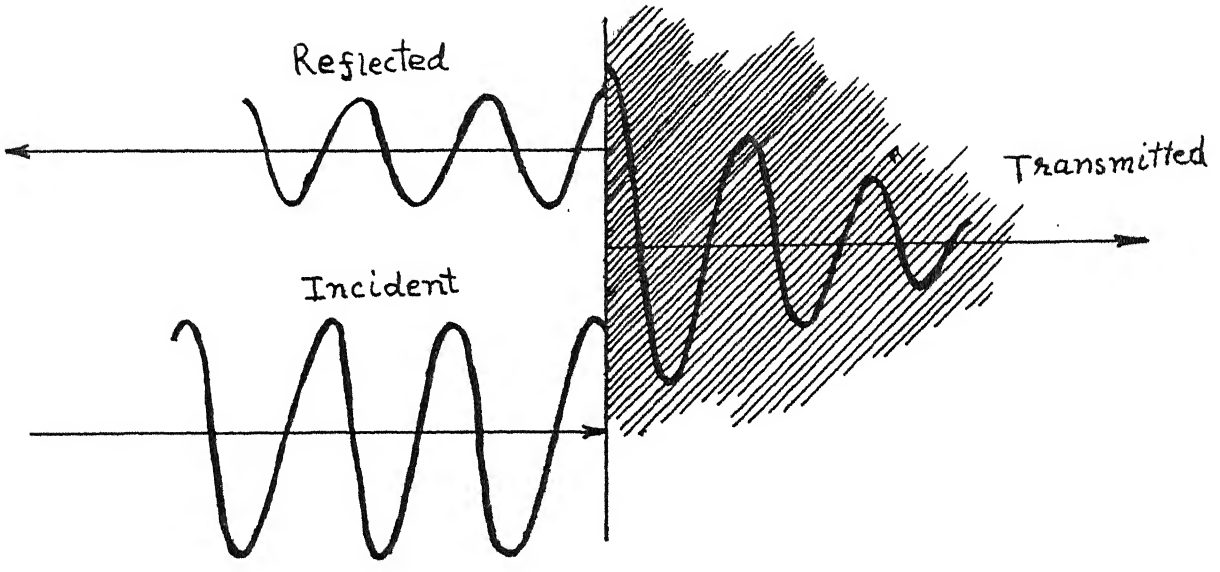

Figure 2.2.1 Damping of Electromagnetic Waves in Solid

In our medium the wave is travelling with the modified velocity v,

$$v = \frac{c}{n}$$

where n is the refractive index of the medium. Therefore

$$\varkappa = \frac{\omega}{c}\tilde{n} \qquad (2.2.13)$$

Comparing the relations (2.2.11) and (2.2.13) we find that the refractive index $\tilde{n}(\omega)$ comes out to be a complex function and is given by

$$\tilde{n}(\omega) = \left[\varepsilon(\omega) + i\,\frac{4\pi\sigma(\omega)}{\omega}\right]^{1/2} \qquad (2.2.14)$$

Comparing the relations (2.2.4) and (2.2.14), a complex dielectric function $\tilde{\varepsilon}(\omega)$ is defined as :

$$\tilde{\varepsilon}(\omega) = \varepsilon(\omega) + i\,\frac{4\pi\sigma(\omega)}{\omega} \qquad (2.2.15)$$

The real part of the complex dielectric function $\tilde{\varepsilon}(\omega)$ is the measured dielectric response of the medium and the imaginary part is related to the optical conductivity.

We may write $\tilde{n}(\omega)$ as

$$\tilde{n}(\omega) = n(\omega) + in_2(\omega) \qquad (2.2.16)$$

where $n(\omega)$ is the measured refractive index. Then

$$\kappa\hat{e}_\gamma = \frac{\omega}{c}\left[n(\omega) + in_2(\omega)\right]\hat{e}_\gamma$$

where $\hat{e}_\gamma$ is the direction of polarization of electromagnetic wave . Therefore the wave equation (2.2.10) becomes

$$\bar{E} = \bar{E}_o \exp\left[i\omega\left(\frac{n\hat{e}_\gamma \cdot \bar{r}}{c} - t\right)\right] \exp\left[-\frac{n_2\omega\hat{e}_\gamma \cdot \bar{r}}{c}\right] \qquad (2.2.17)$$

We see that the velocity of propagation in the medium is reduced to $\frac{c}{n}$, and the wave is damped as it progresses, by a fraction $\exp\left[-\frac{2\pi n_2}{n}\right]$ per wavelength. The damping of the wave is, of course, associated with the absorption of electromagnetic energy. To calculate this we should use Maxwell's equations to find the current associated with the equation (2.2.17). This is the right hand side of the equation (2.2.5)

$$\bar{J}_c = \left[-\frac{i\omega\varepsilon}{c} + \frac{4\pi\sigma}{4}\right]\bar{E}$$

or,
$$\bar{J}_c = -\frac{i\omega}{c}\tilde{n}^2\,\bar{E} \qquad (2.2.18)$$

where $\bar{J}_c$ is a complex current density. The rate of production of Joule heat is the real part of

$$\bar{J}_c \cdot E = -\frac{i\omega}{c}\tilde{n}^2\,|\bar{E}|^2 \qquad (2.2.19)$$

Thus the absorption coefficient $\alpha(\omega)$ is given by

$$\alpha(\omega) = \frac{\mathrm{Re}(\bar{J}_c \cdot \bar{E})}{n|\bar{E}|^2} = \frac{2n_2\omega}{c}$$

or, $$\alpha(\omega) = \frac{4\pi\sigma(\omega)}{n(\omega)} \qquad (2.2.20)$$

The optical absorption coefficient is perhaps most susceptible to simple experimental determination. Experimentally, it is measured as follows: when a beam of light of intensity I_o goes normally through a slab of a medium of thickness x, it attenuates in accordance with the exponential law, $I = I_o\exp(-\alpha x)$. Consequently, α can be obtained simply by measuring I_o/I of the intensities impinging and emerging from the sample.

It is seen that the whole game of optical response can be described by a single complex response function, *viz* the complex dielectric function $\tilde{\varepsilon}(\omega)$. The real and the imaginaryy parts are not independent. The analytic properties of $\tilde{\varepsilon}(\omega)$ lead to the Kramers-Krönig relation:

$$\varepsilon(\omega) = 1 + \frac{2}{\pi}\int_0^\infty \frac{(\omega'-\omega)\varepsilon_2(\omega')}{\omega'^2-\omega^2}\,d\omega' \qquad (2.2.21)$$

and optical sum rules

$$\int_0^\infty \omega\varepsilon_2(\omega)d\omega = \frac{1}{2}\pi\omega_p^2$$

(2.2.22)

$$-\int_0^\infty \omega \, \mathrm{Im}\, \tilde{\varepsilon}^{-1}(\omega)\, d\omega = \frac{1}{2}\pi\omega_p^2$$

where $\tilde{\varepsilon} = \varepsilon + i\varepsilon_2$ and ω_p is the plasma frequency.

We have already seen, the dielectric function relates the displacement current vector $\bar{D}$ and electric field vector $\bar{E}$. But in rapidly varying fields, such as the fields associated with electromagnetic radiation, the field strengths involved are fairly small. Now any variable field can be reduced by means of a Fourier expansion to a set of monochromatic components with a time dependence $e^{-i\omega t}$. For such a field the relation between $\bar{D}(t)$ and $\bar{E}(t)$ can always be taken to be linear. The most general linear relation between $\bar{D}(t)$ at all previous instants can be written in the integral form

$$\bar{D}(t) = \bar{E}(t) + \int_0^\infty f(\tau)\bar{E}(t-\tau)\, d\tau \qquad (2.2.23)$$

where $f(z)$ is a function of time and of the properties of the medium. Taking Fourier transform of the equation (2.2.23) and comparing with the equation (2.2.1), we get

$$\tilde{\varepsilon}(\omega) = 1 + \int_0^\infty f(\tau) e^{i\omega\tau}\, d\tau \qquad (2.2.24)$$

Thus for periodic fields the complex dielectric function may be regarded as a function of the field frequency as well as of the properties of the medium. The variation of $\tilde{\varepsilon}(\omega)$ on the frequency is called the dispersion relation for the medium. The function $\tilde{\varepsilon}(\omega)$ is in general complex for conducting media. From

the equation (2.2.24) we see that

$$\tilde{\varepsilon}(-\omega) = \tilde{\varepsilon}^{*}(\omega) \qquad (2.2.25)$$

Separating the real and imaginary parts, we have

$$\varepsilon(-\omega) = \varepsilon(\omega) \qquad (2.2.26)$$

and $\varepsilon_2(-\omega) = -\varepsilon_2(\omega)$

Thus $\varepsilon(\omega)$ is an even function of the frequency and $\varepsilon_2(\omega)$ is an odd function.

2.3 INTRABAND AND INTERBAND TRANSITIONS :

In section (2.1) we have already discussed about the two kind of transition processes : intraband and interband, and seen the distinction between these two. In this section we shall talk more about Interband transition. From figures (2.1.1) and (2.1.2), it is clear that intraband transition is possible only in a metal whereas interband transition is possible for all materials.

Interband transition takes place in the range of frequency $\omega_o \leq \omega < \omega_p$ where :

ω_o is the threshold value for interband transition-lies in the visible region, and

ω_p is the plasma frequency-lies in the far UV region.

The quantum transport theory for interband transition can

be developed for two different cases. First, at the temperature $0^{o}K$ and the other, at some finite temperature. The nature of interband electronic transition, in these two cases, is very different from each other. Since at $0^{o}K$ there is negligible number of phonons present, the electrons absorb only photon energy.

The momentum conservation requires

$$\hbar\bar{k}_f = \hbar\bar{k}_i + \hbar\bar{Q} \qquad (2.3.1)$$

where $\bar{k}_f$ and $\bar{k}_i$ are the final and initial wave vector of the electron and $\bar{Q}$ is the wave vector of the photon. But we are constraining ourselves only in the region of IR to UV light for which wavelength is much large compared to the lattice constant. Therefore, $\bar{Q}$ is much smaller than the $\bar{k}$'s. Thus the momentum of the photon may be neglected and finally we get

$$\hbar\bar{k}_f = \hbar\bar{k}_i \qquad (2.3.2)$$

or $$k_f = k_i. \qquad (2.3.3)$$

This shows that transition takes place vertically upward in the reduced Brillouin zone scheme as shown in figure (2.3.1). This kind of interband transition is called **direct transition.** The energy is also conserved during such a transition

$$E_f(\bar{k}_f) - E_i(\bar{k}_i) = \hbar\omega \qquad (2.3.4)$$

The other kind of interband transition is the indirect transition. This kind of transition process is observed in the higher temperature region. At finite temperatures there are sufficient phonons present. Therefore electron absorbs phonon energy as well as photon energy. Consequently, in this case, the conservation of momentum gives

$$\hbar\bar{k}_f = \hbar\bar{k}_i + \hbar\bar{Q} + \hbar\bar{q} \qquad (2.3.5)$$

where $\bar{q}$ is the phonon wave vector.

Since $\hbar\bar{Q} \simeq 0$

therefore $\bar{k}_f = \bar{k}_i + \bar{q}.$

Hence $k_f \neq k_i$ (2.3.6)

This process is shown in figure (2.3.2). This means the transition is not vertical in the reduced zone scheme.

2.4 BASIC FORMALISM FOR OPTICAL CONDUCTIVITY :

The fundamental expression for optical conductivity can be derived simply from first order time dependent perturbation theory. The crystal Hamiltonian is treated as the unperturbed Hamiltonian and the eigenfunctions of this Hamiltonian as the unperturbed eigenfunctions. The one electron Schrödinger equation for such unperturbed system is then given by

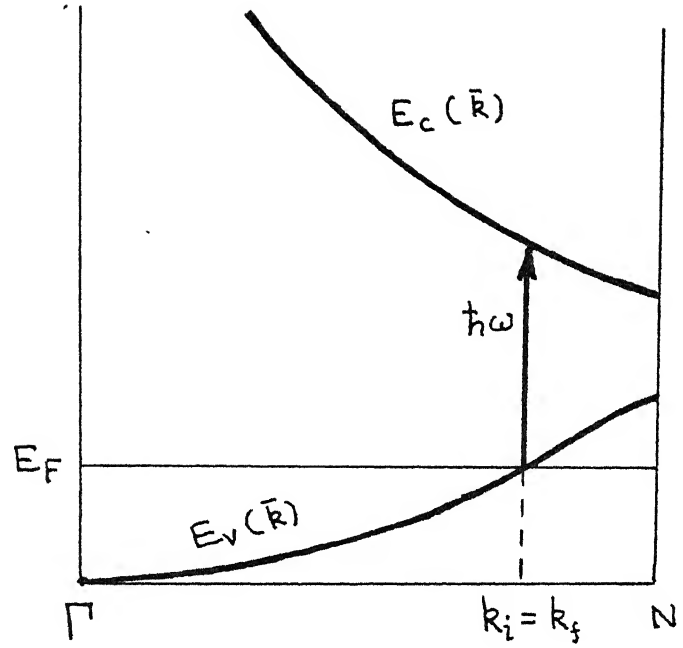

Figure 2.3.1 Interband : Direct Transition

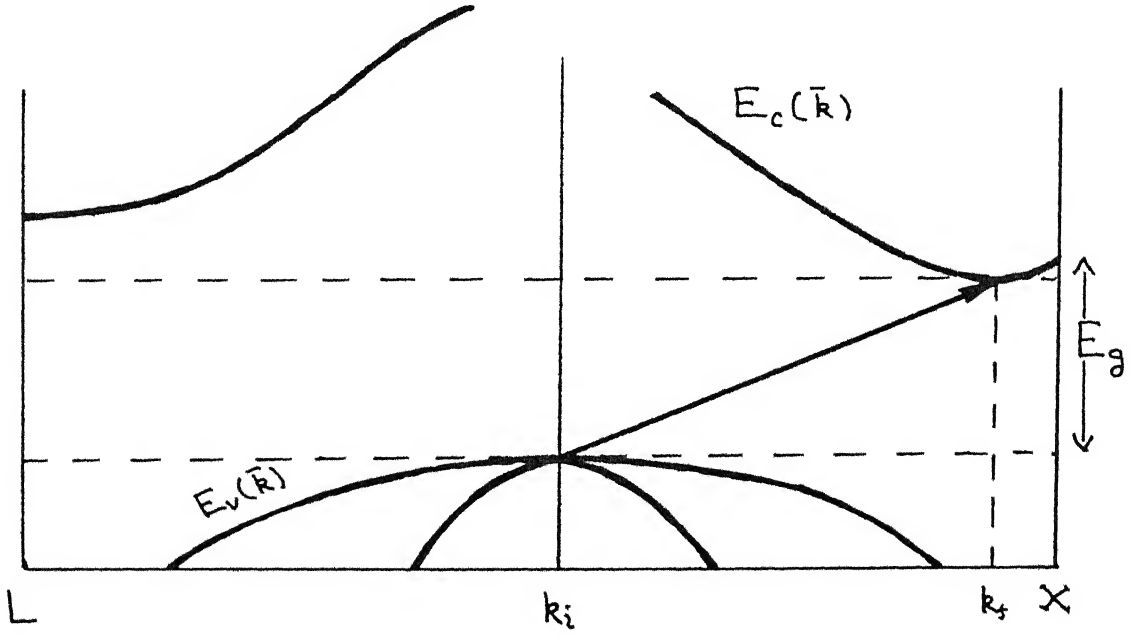

Figure 2.3.2 Interband: Indirect Transition

$$\underline{H}\,\psi^{o}_{\bar{k}} \equiv \left[-\frac{\hbar^2}{2m^*}\nabla^2 + V(\bar{r})\right]\psi^{o}_{\bar{k}} = E_{\bar{k}}\,\psi^{o}_{\bar{k}} \qquad (2.4.1)$$

where $\underline{H}_o$: crystal Hamiltonian

$V(\bar{r})$: crystal potential

$\psi^{o}_{\bar{k}}(\bar{r})$: eigen functions of $\underline{H}_o$

m^* : the effective mass of the electron in the solid

When electromagnetic radiation falls on the material, the photons interact with the electrons in the solid. This electromagnetic wave carries a usually weak electromagnetic field. The electromagnetic radiation adds an extra potential to the crystal Hamiltonian during interaction. This weak, time dependent potential is treated as the perturbation. The full Hamiltonian is then given by

$$\underline{H} = \underline{H}_o + \underline{H}_1 \qquad (2.4.2)$$

In general the Hamiltonian associated with an electron in a electromagnetic field is

$$\underline{H}' = \frac{1}{2m^*}\left(\bar{p} - \frac{e}{c}\bar{A}\right)^2 + e\phi \qquad (2.4.3)$$

where $\bar{p} = \frac{\hbar}{i}\bar{\nabla}$ is the momentum operator

$\bar{A}(\bar{r},t)$: Vector potential associated with the electromagnetic field

$\phi(\bar{r},t)$: Scalar potential associated with the electromagnetic field.

In the absence of free charges we may choose

$$\phi(\bar{r},t) = 0 \qquad (2.4.4)$$

Thus $\underline{H}'$ reduces to

$$\underline{H}' = \frac{1}{2m^*}(\bar{p} - \frac{e}{c}\bar{A}(\bar{r},t))^2 \qquad (2.4.5)$$

or $$\underline{H}' = \frac{1}{2m^*}(\bar{p}.\bar{p} + \frac{e^2}{c^2}\bar{A}.\bar{A} - \frac{e}{c}\bar{p}.\bar{A} - \frac{e}{c}\bar{A}.\bar{p}) \qquad (2.4.6)$$

If $\bar{A}(\bar{r},t)$ is a weak potential, to the first approximation the second term in the equation (2.4.6) may be neglected, leading to

$$\underline{H}' \simeq \frac{\bar{p}.\bar{p}}{2m^*} - \frac{e}{2m^*c}(\bar{p}.\bar{A} + \bar{A}.\bar{p}) \qquad (2.4.7)$$

Therefore $\underline{H}_1$ is now given by

$$\underline{H}_1 = -\frac{e}{2m^*c}(\bar{p}.\bar{A} + \bar{A}.\bar{p}) \qquad (2.4.8)$$

Absence of free charges leads to

$$\bar{\nabla}.\bar{A} = 0 \qquad (2.4.9)$$

Since $[\bar{A}, \bar{p}] = i\hbar\bar{\nabla}.\bar{A}$, therefore, $\bar{p}.\bar{A} = \bar{A}.\bar{p}$

Putting back $\bar{A}.\bar{p}$ in place of $\bar{p}.\bar{A}$ in the equation (2.4.8), we get

$$\underline{H}_1 = -\frac{e}{m^*c}\bar{A}.\bar{p} \qquad (2.4.10)$$

This extra term is responsible for excitations. Electrons in an unperturbed state $\psi_i^o(\bar{r})$ at a time $t = 0$ will subsequently have a wave function $\psi_f(\bar{r},t)$ which can be linearly decomposed into the

complete set of eigenstates, $\{\psi_i^o(\bar{r})\}$ of $\underline{H}_o$. Here $\psi_i^o(\bar{r})$ denotes the state before the transition or initial state and $\psi_f(\bar{r})$ is the state after the transition, i.e., final state.

The transition rate between an occupied state ψ_i and unoccupied state ψ_f may be calculated by solving the equation for $\psi(\bar{r},t)$ by the standard first order time dependent perturbation theory. For a monochromatic vector potential.

$$\bar{A} = \bar{A}_o \exp [i(\omega t)] \qquad (2.4.11)$$

the rate of transition accompanied by the absorption of a photon of frequency ω from the radiation field is

$$Q_{\bar{k}_f \bar{k}_i} = \frac{2\pi}{\hbar} |\langle \psi_f | \underline{H}_1 | \psi_i \rangle|^2 \delta(E_f - E_i - \hbar\omega) \qquad (2.4.12)$$

The energy absorbed per unit volume per unit time as result of this transition is $\frac{(\hbar\omega)}{\Omega} Q_{\bar{k}_f \cdot \bar{k}_i}$, where Ω is the volume of the sample. The total rate of energy loss is obtained by summing this over the initial and final states of the electrons in the system. Introducing a factor $f_i(1-f_f)$ for this purpose in equation (2.4.12), where f_i is the probability of occupation of the state $\psi_i(\bar{r})$ and f_f is the probability of occupation of the state $\psi_f(\bar{r},t)$ we find that the total rate of energy loss is

$$\frac{1}{\Omega} \sum_i \sum_f f_i(1-f_f) \hbar\omega Q_{\bar{k}_f \bar{k}_i}$$

$$= \frac{1}{\Omega} \sum_{i}\sum_{f} f_i(1-f_f)\, \hbar\omega\, \frac{2\pi}{\hbar}\, |\langle \psi_f | \underline{H}_{-1} | \psi_i \rangle|^2\, \delta(E_f - E_i - \hbar\omega)$$

$$= \frac{2\pi\omega}{\Omega} \sum_{i}\sum_{f} f_i(1-f_f)\, |\langle \psi_f | (-\frac{e}{m^* c} \bar{A}.\bar{p}) | \psi_i \rangle|^2\, \delta(E_f - E_i - \hbar\omega)$$

$$= \frac{2\pi e^2}{m^{*2} c^2 \Omega}\, \omega \sum_{i}\sum_{f} f_i(1-f_f)\, |\langle \psi_f | \bar{A}.\bar{p} | \psi_i \rangle|^2\, \delta(E_f - E_i - \hbar\omega).$$

But this is also equal to the joule heat loss due to the mobile electrons, i.e. $\bar{J}.\bar{E}$. But $\bar{J}.\bar{E} = \sigma \bar{E}.\bar{E}$, (for linear and isotropic medium).

Since $\bar{E} = \frac{i\omega}{c} \bar{A}$, therefore

$$\bar{J}.\bar{E} = \sigma\, (i\omega/c)^2\, \bar{A}.\bar{A}$$

or
$$\bar{J}.\bar{E} \equiv - \sigma\, (\omega/c)^2\, \bar{A}.\bar{A} \qquad (2.4.13)$$

Equating these two, we find

$$- \sigma\, (\omega/c)^2\, \bar{A}.\bar{A} = \frac{2\pi e^2}{m^{*2} c^2 \Omega}\, \omega \sum_{i}\sum_{f} |\langle \psi_f | \bar{A}.\bar{p} | \psi_i \rangle|^2 f_i(1-f_f)\, \delta(E_f - E_i - \hbar\omega)$$

If $\bar{A} = A\hat{e}_\gamma$, where $\hat{e}_\gamma$ is the polarization direction of the electric field vector $\bar{E}$, the above equation becomes

$$\sigma(\omega) = - \frac{2\pi e^2}{m^{*2} \Omega}\, \frac{1}{\omega} \sum_{i}\sum_{f} |\langle \psi_f | \hat{e}_\gamma . \bar{p} | \psi_i \rangle|^2\, f_i(1-f_f)\, \delta(E_f - E_i - \hbar\omega) \qquad (2.4.14)$$

This is the basic formula for the optical conductivity of a solid

due to interband transition. This can be used for any kind of material like metals, semiconductors, or insulators and in a slightly modified form ideally suited for disordered alloy systems.

2.5 ANALYSIS OF THE CONDUCTIVITY FORMULA:

Looking at the basic formula for the optical conductivity given by the equation (2.4.14), we can have some idea about the physical behaviour of the optical conductivity for both ordered and disordered systems.

ORDERED SYSTEMS

There are two important factors in the expression (2.4.14) for the optical conductivity, $\sigma(\omega)$:

(1) Conservation of energy factor : $\delta(E_f - E_i - \hbar\omega)$

(2) Square of the optical matrix element : $|\langle\psi_f|\hat{e}_\gamma . \bar{p}|\psi_i\rangle|^2$.

Let us first denote the optical matrix element as $g_{if\gamma}$. We shall now show that the first factor is related to the joint density of states.

The one-electron density of states (number of allowed energy levels per unit energy range and per unit volume) is given by :

$$n(E) = 2\Omega^{-1} \sum_n \delta(E-E_n) \qquad (2.5.1)$$

where Ω is the volume of the specimen. The factor 2 arises because of summation over the two spin orientations. From the properties of Dirac δ- function:

$$\int \delta(E-E_i)\delta(E_f-E)\, dE = \delta(E_f-E_i) \qquad (2.5.2)$$

We have

$$\delta(E_f-E_i-\hbar\omega) = \int_0^{E_f^{max.}} \delta(E-E_f)\delta(E-E_i-\hbar\omega)\, dE \qquad (2.5.3)$$

where E_f^{max} is the upper limit of conduction band. Therefore using equation (2.5.3) we have

$$\sum_f \sum_i \delta(E_f-E_i-\hbar\omega) = \sum_f \sum_i \int_0^{E_f^{max.}} \delta(E-E_f)\, \delta(E-E_i-\hbar\omega)\, dE$$

or

$$\sum_f \sum_i \delta(E_f-E_i-\hbar\omega) = \int_0^{E_f^{max}} \Big\langle \sum_f \delta(E-E_f) \Big\rangle \Big\langle \sum_i \delta(E-E_i-\hbar\omega) \Big\rangle\, dE \qquad (2.5.4)$$

Using the definition (2.5.1), we can write the right hand side of the equation (2.5.4) in terms of the conduction band density of states, $n_f(E)$ and valence band density of states, $n_i(E)$:

$$\sum_f \sum_i \delta(E_f-E_i-\hbar\omega) = \frac{\Omega^2}{4} \int_0^{E_f^{max.}} n_f(E)\, n_i(E-\hbar\omega)\, dE.$$

But $n_f(E)n_i(E-\hbar\omega) = J_{fi}(E,\omega)$, where $J_{fi}(E,\omega)$ is the joint density of states. Therefore

$$\sum_f \sum_i \delta(E_f - E_i - \hbar\omega) = \frac{\Omega^2}{4} \int_0^{E_f^{max}} J_{fi}(E,\omega)\,dE \qquad (2.5.5)$$

For an ordered system, where crystal potential is periodic and the wave-function is described by Bloch's functions, the optical matrix element factor is usually a very slowly varying function of energy (Závětova & Velický, 1976). Therefore in the first approximation $|g_{if\gamma}|^2$ may be replaced by its $\bar{k}$-average, and takenout of the integral in the equation (2.4.14). Within this approximation this equation becomes

$$\sigma(\omega) = -\frac{2\pi e^2}{m^{*2}\Omega} \frac{1}{\omega} \overline{|g_{if\gamma}|^2} \sum_i \sum_f f_i(1-f_f)\,\delta(E_f - E_i - \hbar\omega) \qquad (2.5.6)$$

For semiconductors, at $T = 0^{\circ}K$, $f_i = 1$ and $f_f = 0$. Therefore in this case equation (2.5.6) becomes

$$\sigma(\omega) = -\frac{2\pi e^2}{m^{*2}\Omega} \frac{1}{\omega} \overline{|g_{if\gamma}|^2} \sum_i \sum_f \delta(E_f - E_i - \hbar\omega) \qquad (2.5.7)$$

Using the relation (2.5.5), the equation (2.5.7) reduces to

$$\sigma(\omega) = -\frac{2\pi e^2}{m^{*2}\Omega} \frac{1}{\omega} \overline{|g_{if\gamma}|^2} \frac{\Omega^2}{4} \int_0^{E_f^{max}} J_{fi}(E,\omega)\,d\omega \qquad (2.5.8).$$

Therefore for a fixed value of ω, we have

$$\omega\,\sigma(\omega) \propto \int J_{if}(E,\omega)\,dE \qquad (2.5.9)$$

This shows that the optical conductivity for any ordered system is directly proportional to the integrated joint density of states.

In an energy resolved photoemission experiment one essentially studies the energy distribution, $N(E,\omega)$, of photoemitted electrons for a fixed value of frequency of radiation as a function of E. This is done by introducing a filter in the detector ensuring that only those electrons will be detected which have energy within a very narrow fixed range of energy defined by the filter. Doing so one gets $N(E,\omega)$ to be directly proportional to the joint density of states, *i.e.*,

$$N(E,\omega) \propto n_f(E)n_i(E-\hbar\omega) \qquad (2.5.10)$$

provided we again neglect the energy dependence of the optical matrix element. Thus photo-emission experiment provides a very good study of the density of states or the band structure of the system.

DISORDERED SYSTEMS:

In chapter I we have already seen that an extra problem is associated with the study of disordered systems : that is configuration averaging. Therefore, to get an averaged optical conductivity, the right hand side of the equation (2.4.14) has to be averaged . This means, in general the product of square of the optical matrix element and the joint density of states has to be averaged. This averaging can be done in two different cases :

CASE I: If the optical matrix element is assumed to be slowly varying function of energy and depends weakly on randomness, it may be separately averaged. Thus the vertex correction is neglected, this factor is taken out of the summation in equation (2.4.14) and averaged using the Virtual Crystal Approximation (Pickett *et.al.* 1983) . Therefore, for semiconductors, we get

$$\langle \sigma(\omega) \rangle = - \frac{2\pi e^2}{m^{*2}\Omega} \frac{1}{\omega} \left\langle \overline{|g_{if\gamma}|^2} \right\rangle_{VCA} \int \langle J_{if}(E) \rangle \, dE$$

where < > denotes the configuration averaging. This shows that, like ordered systems, we again have

$$\omega \langle \sigma(\omega) \rangle \propto \int \langle J_{if}(E) \rangle \, dE$$

In this case photoemission experiment can again be interpreted in the same way as ordered systems.

CASE II: In many instances $|g_{if\gamma}|^2$ is neither independent of energy nor randomness and its random variation may be correlated with the delta function part. We shall see that it is fairly strongly dependent on energy in dilute alloys, where the constituent potentials are very different, because of strong scattering by impurity sites. Hence the assumption that has been made in the case I is invalid.

In general for any three physical quantities A, B and C which have a relation of the form of $A = B\,C$, we have

$$\langle A \rangle = \langle BC \rangle \neq \langle B \rangle \langle C \rangle .$$

Therefore in such situation we have to take the average of the product of the square of optical matrix element and the joint density of states in the right hand side of the equation (2.4.14) together. This means we have to include vertex correction also.

$$\langle \sigma(\omega) \rangle = - \frac{2\pi e^2}{m^{*2}\Omega} \frac{1}{\omega} \left\langle \sum_{if} |g_{if\gamma}|^2 f_i (1-f_f) \delta(E_f - E_i - \hbar\omega) \right\rangle \qquad (2.5.12)$$

Thus, in this case the energy distribution of photoelectrons $N(E,\omega)$ in the photoemission experiment does not come out to be directly proportional to the joint density of states, although very sharp features in the density of states will be reflected in $N(E,\omega)$, for example, neither weight nor the exact centroids of such structures will quantitatively match, due to the dependence of optical matrix element on energy and randomness.

This is the case which has been considered in the present work and the averaging is done using Augmented Space Formalism.

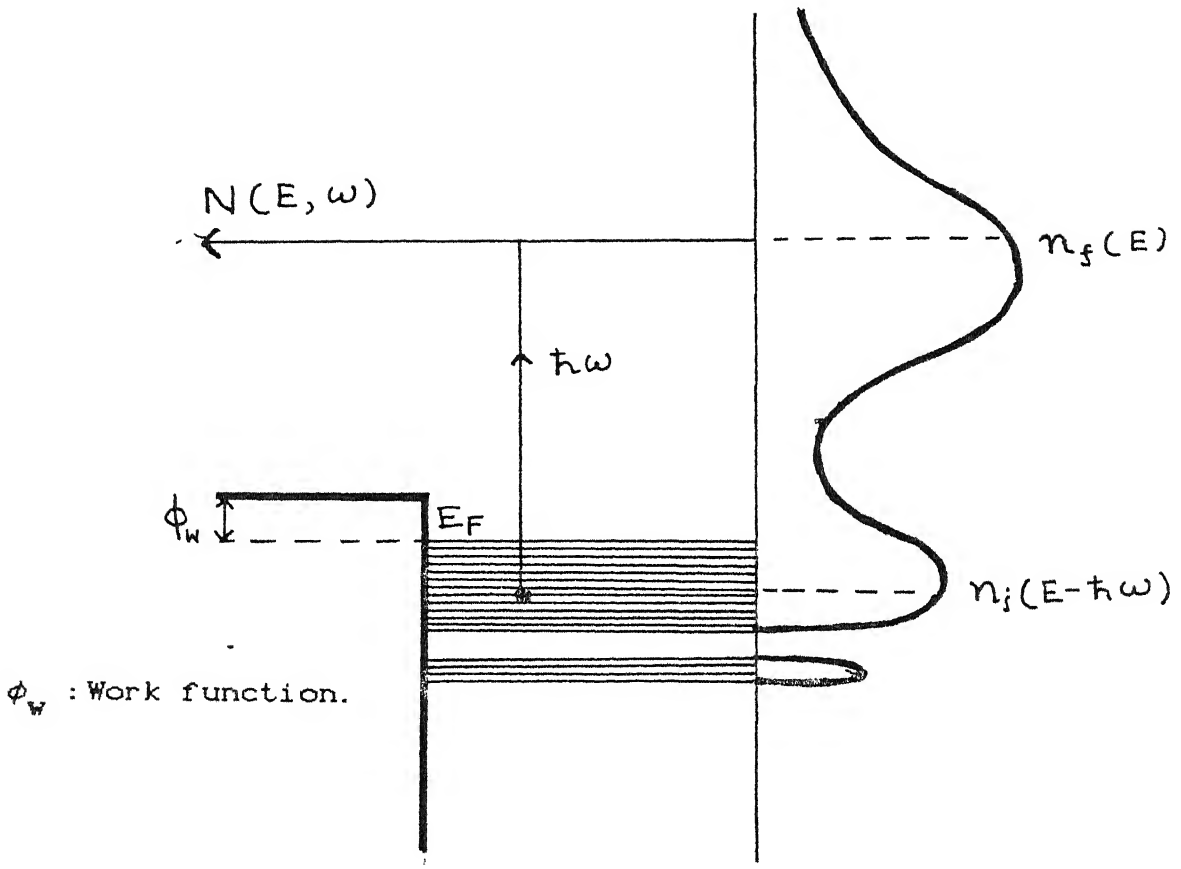

Figure 2.5.1 Photo-emission

CHAPTER III

AN AUGMENTED SPACE FORMULATION OF OPTICAL CONDUCTIVITY FOR RANDOM SEMICONDUCTING ALLOYS

3.1 INTRODUCTION :

It was shown in Chapter I that the configuration averaging is central to the problem of the study of any disordered system. This is because the system has a statistical behaviour due to random potentials. It is also seen that it is the configuration average of physical observables which reflects the macroscopic measured properties of the disordered system. As we have already seen in the case of optical properties of such systems that, to study the averaged conductivity, we have to take the average of the product $|g_{if\gamma}|^2\delta(E_f-E_i-\hbar\omega)$, where $g_{if\gamma}$ is the optical matrix element, i and f refers to initial and final states respectively and γ refers to the direction of polarization of the electromagnetic wave.

The Coherent Potential Approximation (CPA) introduced by Soven (1967) and later developed by Kirkpatrick et.al. (1970), Stocks et.al. (1971) etc. provides a very good study of averaged density of states. Soven introduced the idea of a complex site energy (or potential) which characterizes the effect of the random environment within a meaningful picture. This potential (called the coherent potential) was determined self-consistently from the

requirement that a particular configuration immersed in the effective medium (the mean field) yields no extra scattering on the average. Thus all scattering from single potentials, and uncorrelated multiple scattering from potentials are taken into account in CPA. But this approximation fails to provide the study of the average of a quantity such as $|g_{if\gamma}|^2\delta(E_f-E_i-\hbar\omega)$. Thus one needs to resort to a direct way of carrying out the averaging.

The Augmented Space Formalism provides the best way for this propose.It is a general method for the configuration averaging of any general function based on the direct way of averaging. Thus, it enables us to get an expression for the optical conductivity without making further approximation while doing the averaging i.e., it includes the vertex correction.

3.2 COHERENT POTENTIAL APPROXIMATION :

The electronic density of states per atom for any system is directly related to the single particle Green function for that system as follows

$$n(E) = -\frac{1}{\pi}\frac{1}{N}\,\mathrm{Im}\,\mathrm{Tr}\,\underline{G}(E+i0) \qquad (3.2.1)$$

where N is the total number of atoms in the system. The Green operator (or resolvent) $\underline{G}$ is given by the Hamiltonian $\underline{H}$ of the system :

$$\underline{G}(z) = (z\underline{I} - \underline{H})^{-1} \qquad (3.2.2)$$

where z is a complex variable.

Therefore, for any disordered system the electronic density of states will be given by the configuration averaged single particle Green function. In case the disordered itself is 'homogeneous' - that is, the variation of the potential is similar throughout the system then the electronic density of states will be:

$$n(E) = -\frac{1}{\pi}\frac{1}{N} \text{Im Tr} \langle \underline{G}(\bar{r}, E+i0) \rangle \qquad (3.2.3)$$

where $\bar{r}$ is any site in the system.

One of the main problems involved in the study of electrons in disordered systems is the study of configuration averaged single particle Green functions. One of the most powerful mean field or effective medium like approximation for the calculation of the averaged Green function is the self-consistent Coherent Potential Approximation (CPA). The single site CPA had remained till late the main theoretical development in the study of electronic structure of random systems. It maintains the analytic features of the exact Green function and interpolates correctly between several individual limiting cases, e.g., Virtual crystal approximation, atomic and dilute limits, in the case of binary alloys.

If we classify various literature on the single site CPA we find that these belong to three different (eventually equivalent) approaches:

(1) Diagrammatic approaches using propagator or locator formalism introduced by Yonezawa and Matsubara (1966), Yonezawa (1968) and Leath (1968, 1970).

(2) The effective medium approach introduced by Soven (1967)

(3) Multiple Scattering ideas first introduced by Anderson and M^{c}Millan (1967).

All the different approaches yield the same final result within this approximation. This indicates that single site coherent potential is unique. Here only the second approach, *i.e.* the mean field approach will be discribed as it gives a very simple and a clear physical picture of the model and will form a basis of subsequent generalization of the CPA.

The concept of a mean field or an effective medium in a disordered system was first clearly stated by Soven (1967). Seeds of the idea already existed in several problems on emulsions stated by Landau and Lifshitz. The idea of making it self-consistent apparently was Soven's. The trick is to replace the actual random potentials at different sites by an effective non-random potential in such a way that the Green function corresponding to this constructed homogeneous potential gives the averaged Green function of the actual random system. Thus if $\underline{H}$ denotes the Hamiltonian of the actual random system, the configuration averaged single particle density of states will be given by

$$\langle n(E)\rangle = -\frac{1}{\pi}\frac{1}{N}\,\mathcal{Im}\,\mathrm{Tr}\,\langle \underline{G}\rangle \qquad (3.2.4)$$

where $$\langle \underline{G}\rangle = \langle (z\underline{I} - \underline{H})^{-1}\rangle \qquad (3.2.5)$$

If $\underline{H}_{eff}$ denotes the effective Hamiltonian of the effective medium then by the definition of effective medium we have

$$\langle \underline{G}\rangle = (z\underline{I} - H_{eff})^{-1} \qquad (3.2.6)$$

From the equations (3.2.5) and (3.2.6) it is clear that $\underline{H}_{eff}$ may not necessarily be Hermitian. This means the constructed effective medium is defined by complex potentials sitting at various sites (or the complex site energies). Though the effective medium does not correspond to a real system, its Green function is related to the configurational averaged properties of the random system.

Let us illustrate the procedure in a single band tight binding model. Our actual Hamiltonian in the tight-binding basis

$$\underline{H} = \sum_i \epsilon_i \underline{P}_i + \sum_{i,j} V_{ij}\,\underline{T}_{ij} \qquad (3.2.7)$$

Here i is an index indicating position or a site, say at $\bar{r}_i$. $\underline{P}_i$ and $\underline{T}_{ij}$ are projection and transfer operators respectively, $|i\rangle\langle i|$ and $|i\rangle\langle j|$. ϵ_i's, the diagonal or 'site' energies and V_{ij}'s, the overlap integrals may be random. Within a single site CPA it is not very profitable to include effects of off-diagonal disorder, i.e., disorder in the V_{ij}'s. Therefore we set $V_{ij} = \langle V_{ij}\rangle$, where $\langle V_{ij}\rangle$ is

some mean potential. Thus the equation (3.2.7) reduces to

$$\underline{H} = \sum_i \varepsilon_i \underline{P}_i + \sum_{ij} \underline{T}_{ij} \langle V_{ij} \rangle \qquad (3.2.8)$$

Now we define our effective Hamiltonian in the same tight-binding basis as :

$$\underline{H}_{eff} = \sum_i \Sigma_o(E) \underline{P}_i + \sum_{ij} \underline{T}_{ij} \langle V_{ij} \rangle \qquad (3.2.9)$$

where site energies, Σ_o are in general complex and energy dependent, but non-random and independent of i.

The problem is now to find out $\Sigma_o(E)$, which will then yield

$$\underline{G}_{eff}(z) = \langle \underline{G}(z) \rangle \qquad (3.2.10)$$

where $\underline{G}_{eff}(z)$ is given by

$$\underline{G}_{eff}(z) = (z\underline{I} - \underline{H}_{eff})^{-1} \qquad (3.2.11)$$

and

$$\langle \underline{G}(z) \rangle = \langle (z\underline{I} - \underline{H})^{-1} \rangle_{av} \qquad (3.2.12)$$

$\Sigma_o(E)$ is determined self-consistently. In the single site CPA we do this as follows: We embed an exact site energy ε_i at a site i

within the effective medium ,as shown in the figure (3.2.1), in such a way that in doing so we do not produce any extra scattering on the average. This condition can be written mathematically as :

$$\langle \underline{G}^{(i)} \rangle = \underline{G}_{eff} = \langle \underline{G} \rangle \qquad (3.2.13)$$

where $\underline{G}^{(i)}$ is the Green function for the medium in which all the sites are occupied by $\Sigma_o(E)$ except the site i which is occupied by ε_i. The corresponding Hamiltonian of this medium is :

$$\underline{H}_{eff}^{(i)} = \underline{H}_{eff} + (\varepsilon_i - \Sigma_o)\underline{P}_i \qquad (3.2.14)$$

Therefore

$$\underline{G}^{(i)} = (z\underline{I} - \underline{H}_{eff}^{(i)})^{-1}$$

$$= \left[z\underline{I} - \underline{H}_{eff} - (\varepsilon_i - \Sigma_o)\,\underline{P}_i\right]^{-1}$$

$$= (z\underline{I} - \underline{H}_{eff})^{-1}\left[1 - \frac{(\varepsilon_i - \Sigma_o)\underline{P}_i}{z\underline{I} - \underline{H}_{eff}}\right]^{-1}$$

or

$$\underline{G}^{(i)} = \underline{G}_{eff}\left[1 - \underline{G}_{eff}(\varepsilon_i - \Sigma_o)\,\underline{P}_i\right]^{-1} \qquad (3.2.15)$$

If we expand the right hand side of the equation (3.2.15), we get

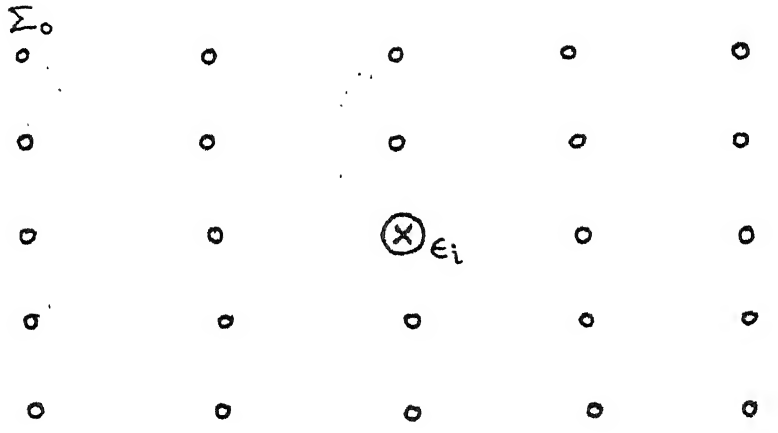

Figure 3.2.1 Single potential embeded in an effective medium

$$\underline{G}^{(i)} = \underline{G}_{eff} + \underline{G}_{eff}\left[(\varepsilon_i - \Sigma_o)\underline{P}_i\right]\underline{G}_i \qquad (3.2.16)$$

$$= \underline{G}_{eff} + \underline{G}_{eff}\left[(\varepsilon_i - \Sigma_o)\underline{P}_i\right]\underline{G}_{eff}\left[1 - \underline{G}_{eff}\left[(\varepsilon_i - \Sigma_o)\underline{P}_i\right]\right]^{-1}$$

or

$$\underline{G}^{(i)} = \underline{G}_{eff} + \underline{G}_{eff}\,\frac{(\varepsilon_i - \Sigma_o)\underline{P}_i}{1 - \underline{G}_{eff}((\varepsilon_i - \Sigma_o)\underline{P}_i)}\,\underline{G}_{eff} \qquad (3.2.17)$$

Define

$$\frac{(\varepsilon_i - \Sigma_o)\underline{P}_i}{1 - \underline{G}_{eff}((\varepsilon_i - \Sigma_o)\underline{P}_i)} = \underline{t}_i \qquad (3.2.18)$$

Then,

$$\underline{G}^{(i)} = \underline{G}_{eff} + \underline{G}_{eff}\;\underline{t}_i\;\underline{G}_{eff}$$

Therefore

$$\langle \underline{G}^{(i)} \rangle = \underline{G}_{eff} + \underline{G}_{eff}\,\langle \underline{t}_i \rangle \underline{G}_{eff} \qquad (3.2.19)$$

Condition (3.2.13) restricts ourselves to :

$$\langle \underline{t}_i \rangle = 0 \qquad (3.2.20)$$

i.e.,

$$\left\langle \frac{(\varepsilon_i - \Sigma_o)\underline{P}_i}{1 - \langle \underline{G} \rangle ((\varepsilon_i - \Sigma_o)\underline{P}_i)} \right\rangle = 0 \qquad (3.2.21)$$

This condition in the final form gives us an equation for Σ_o in the single site CPA.

For random binary alloy, the i^{th} site either can be occupied by A atom or B. Therefore, for a binary alloy without short ranged order, equation (3.2.21) reduces to :

$$c\,\frac{\varepsilon_A-\Sigma_o}{1-\langle G\rangle(\varepsilon_A-\Sigma_o)}+(1-c)\,\frac{\varepsilon_B-\Sigma_o}{1-\langle G\rangle(\varepsilon_B-\Sigma_o)}=0 \qquad (3.2.22)$$

where, c is the concentration of A atoms. This is the CPA equation for a random binary alloy. To solve this equation self-consistently a suitable initial choice $\underline{G}_o(z)$ is made for $\langle G\rangle$ to start with. We then calculate Σ_o from the equation (3.2.22) and then from Σ_o we calculate a new $\underline{G}_o(z)$. We keep on doing this until Σ_o converges. A careful choice of the initial $\underline{G}_o$ usually leads to a rapid convergence. Care must also be taken to preserve the *herglotz* analytic properties (Mookerjee, 1973) related to the physical necessity that the energy spectrum be real and the density of states be positive, this must be preserved at all levels of iteration.

3.3 AUGMENTED SPACE FORMALISM :

The Augmented Space Formalism (ASF) is a technique of configuration averaging where configuration fluctuations are

systematically taken into account. In the effective medium approaches the quantum dynamical behaviour of the system is described by a Hamiltonian suitably set up, whereas the statistical behaviour is, as it were, imposed from the outside by allowing the potentials involved in the Hamiltonian to vary randomly according to some prescription. The Hamiltonian, in itself, does not describe the full behaviour of the system and has to be augmented with the distribution of the set of random potentials. In the Augmented Space method, the Hamiltonian, expanded to include the description of possible configurations of the system ,completely describes the disordered system. It is not necessary to put in the statistical description by hand. In this sense, this alternative description is by far the most satisfying one. Since the statistical description is incorporated within the Hamiltonian, the configuration averaging is not an extra process, as in the effective medium approaches. The formalism is *formally exact* but, for practical calculations, approximations preserving constraints of physical origin may be generated.

The ASF was first introduced by Mookerjee (1973a, 1973b) and later on, Kaplan and Gray (1976, 1977) provided a detailed exposition. It has been successfully utilized for averaging quantities like one particle Green functions, particularly when one has to go beyond the single site approximations (i.e., beyond the CPA) and has to include clustering effects, large off-diagonal disorder, short ranged order, etc.

In a substitutionally disordered system the lattice sites are randomnly occupied by the atoms of the type A, B, C, ...etc. So the site energy ε_i is a random variable. For ε_A or ε_B depending upon whether the site is occupied by an A atom or a B atom respectively. The Hamiltonian for such binary alloy acts on the Hilbert space $\mathscr{H}$ spanned by a tight-binding basis. It involves random occupation variables $\{N_i\}$ defined as :

$$N_i = 0 \quad ; \quad \text{if } i^{th} \text{site is occupied by an A atom}$$
$$= 1 \quad ; \quad \text{if } i^{th} \text{ site is occupied by a B atom}$$

A set of values taken up by the random ocupation variable $\{N_i\}$ is called a configuration. A certain probability density $P(\{N_i\})$ is associated with various values of the configuration. We assume that the various N_i's are statistically independent, i.e., there is no short ranged order. In this case we have :

$$P(\{N_i\}) = \prod_i p_i(N_i) \qquad (3.3.1)$$

where $p_i(N_i)$ is the probability density of the individual variables N_i. Kaplan and Gray (1977) have generalized this to the case where various N_i's are statistically dependent within a Markovian short ranged order model.

Haydock (1972) first noted that $p_i(N_i)$ has the same properties of positive definiteness and integrability as the density

of states have, i.e., $p_i(N_i) \geq 0$

$$\int p_i(N_i)\,dN_i = 1 \qquad (3.3.2)$$

Mookerjee (1973) used this equivalence properties of $p_i(N_i)$ and density of states, n(E) and suggested that similar to density of states, $p_i(N_i)$ can also be related to some operator $\underline{M}^{(i)}$ in a hypothetical space ϕ_i, corresponding to the random variable N_i, and spanned by a basis set $\{|f_n^i\rangle\}$, through the relation :

$$p_i(N_i) = -\frac{1}{\pi} \operatorname{Im} \langle f_o^i | [(N+i\delta)\underline{I} - \underline{M}^{(i)}]^{-1} | f_o^i \rangle \qquad (3.3.3)$$

Thus the quantities $|f_n^i\rangle$, $\underline{M}^{(i)}$ and $p_i(N_i)$ are respectively analogous to the eigenvectors, the Hamiltonian and the density of states. Subsequently Mookerjee (1975) described the disorder field in analogy with a fermion/boson field and was able to give a diagrammatic representation of it in a way similar to Feynman diagrams for fermions/bosons. The disorder field contains within itself a full description of fluctuations due to disorder. Now here the problem is to find out an operator $M^{(i)}$ in some basis $\{|f_n^i\rangle\}$ corresponding to a probability distribution $p_i(N_i)$ so that equation (3.3.3) is satisfied. This is just a ineverse problem of density of states where an operator (Hamiltonian) $\underline{H}$ is given and the density of states is found from a similar relation:

$$n_i(E) = -\frac{1}{\pi}\frac{1}{N} \operatorname{Im} \langle i | (z\underline{I} - \underline{H})^{-1} | i \rangle \qquad (3.3.4)$$

where $n_i(E)$ is local density of states.

The problem can be handled in a way analogous to the continued fraction expansion of the Green function (Haydock, 1972)

$$G_{ii}(z) = \langle i | (z\underline{I} - \underline{H})^{-1} | i \rangle \qquad (3.3.5)$$

In order to find a representation of $M^{(i)}$, given the probability density $p_i(N_i)$, one has to try to write it in the form of a convergent continued fraction (the path shown in the figure (3.3.1) by full lines) of the form as shown below :

$$p_i(\varepsilon+i\eta) = -\,\mathcal{I}m \cfrac{1/\pi}{\varepsilon+i\eta-a_1-\cfrac{b_1^2}{\varepsilon+i\eta-a_2-\cfrac{b_2^2}{\ddots}}} \qquad (3.3.6)$$

Such an expansion is convergent only if all the moments of $p_i(\varepsilon)$ are finite.

Having written the probability density in the above form, the operator $\underline{M}^{(i)}$ can then be represented in some basis $\{|f_n^{(i)}\rangle\}$ as a tridiagonal matrix :

$$\underline{M}^{(i)} = \begin{bmatrix} a_1 & b_1 & 0 & 0 & \cdots \\ b_1 & a_2 & b_2 & 0 & \cdots \\ 0 & b_2 & a_3 & b_3 & 0 \cdots \\ 0 & 0 & b_3 & a_4 & b_4 \cdots \end{bmatrix} \qquad (3.3.7)$$

Let us solve the problem for a random binary alloy A_cB_{1-c}. We consider only the diagonal disorder and nearest neighbour overlap. Then the Hamiltonian $\underline{H}$ for such a system in tight-binding basis is given by :

$$\underline{H} = \sum_i \varepsilon_i \underline{P}_i + V \sum_{i,j} \sum_{\in n_i} \underline{T}_{ij} \qquad (3.3.8)$$

where

$\underline{P}_i = |i\rangle\langle i|$ is the projection operator

and $\underline{T}_{ij} = |i\rangle\langle j|$ is the transfer operator

defined in the Hilbert space $\mathcal{H}$ spanned by tight-binding basis $\{|i\rangle\}$ and n_i are the nearest neighbours of i. Here ε_i's form a set of random variables. Neglecting short ranged order, the probability density for the $\{N_i\}$ can be written as

$$p_i(N_i) = c\delta(N_i - 1) + (1-c)\delta(N_i) \qquad (3.3.9)$$

$$= -\frac{1}{\pi}\, \mathcal{I}m \left[\frac{c}{N_i + i\eta - 1} + \frac{1-c}{N_i + i\eta}\right] \; ; \; \eta \to o^+$$

$$= -\frac{1}{\pi}\, \mathcal{I}m \, \frac{1}{N_i + i\eta - c - \dfrac{c(1-c)}{N_i + i\eta - (1-c)}}$$

or,

$$p_i(N_i) = (-1/\pi)\, \mathcal{I}m \lim_{\eta \to 0^+} \frac{1}{N_i + i\eta - a_1 - \dfrac{b_1^2}{N_i i\eta - a_2}} \qquad (3.3.10)$$

where $a_1 = c$, $a_2 = (1-c)$ and $b_1^2 = c(1-c)$.

Thus the above continued fraction expansion of $p_i(N_i)$ shows that corresponding operator $M^{(i)}$ has rank 2 and has a 2x2 tridiagonal matrix representation given by :

$$M^{(i)} = \begin{bmatrix} c & \sqrt{c(1-c)} \\ \sqrt{c(1-c)} & 1-c \end{bmatrix} \qquad (3.3.11)$$

in a basis $\{|f_o^i\rangle, |f_i^i\rangle\}$ spanning the configuration space.

Let us now consider the configuration averaging. The average of any function $f(N_i)$, function of a single variable N_i, can be written as :

$$\bar{f} = \int_{-\infty}^{\infty} f(N_i) p_i(N_i)\, dN_i \qquad (3.3.12)$$

or,

$$\bar{f} = -(1/\pi) \int_{-\infty}^{\infty} f(N_i + i0^+)\, \mathcal{I}m\, g_{oo}^{M^{(i)}}(N_i + i0^+)\, dN_i \qquad (3.3.13)$$

where,

$$g_{oo}^{M^{(i)}} = \left[(N_i + i0^+)\underline{I} - \underline{M}^{(i)}\right]^{-1} \qquad (3.3.14)$$

Let us further make the assumption that $f(z)$ as a function of a complex variable z has no singularities on that part of a real axis which forms a branch cut of the function $g_{oo}(z)$, or in a neighbourhood of the branch cut. In that case we may write :

$$\bar{f} = -\frac{1}{2\pi i} \oint f(z)\, g_{oo}^{M^{(i)}}(z)\, dz \qquad (3.3.15)$$

The contour is taken around the branch cut of $g_{oo}(z)$ along the real axis and not including any singularities of $f(z)$ (see figure (3.3.2)).

Since $\underline{M}^{(i)}$ is a self-adjoint operator on $\phi^{(i)}$, therefore equation (3.3.15) can be written as

$$\bar{f} = -(1/2\pi i) \oint f(z) \langle f_o | \int_{-\infty}^{\infty} (z-h)^{-1}\, dp(h)\, | f_o \rangle\, dz \qquad (3.3.16)$$

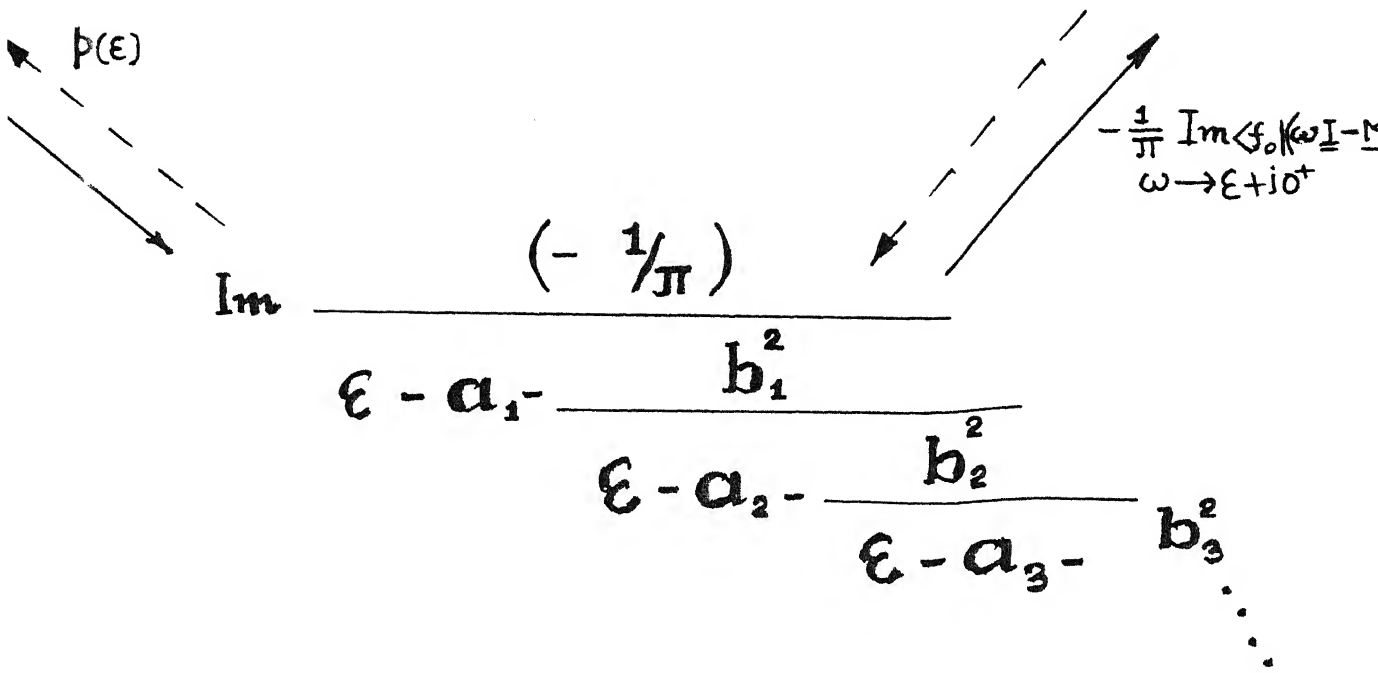

Figure 3.3.1 Representation of three mathematical form of a positive, definite, integrable density function with finite moment.

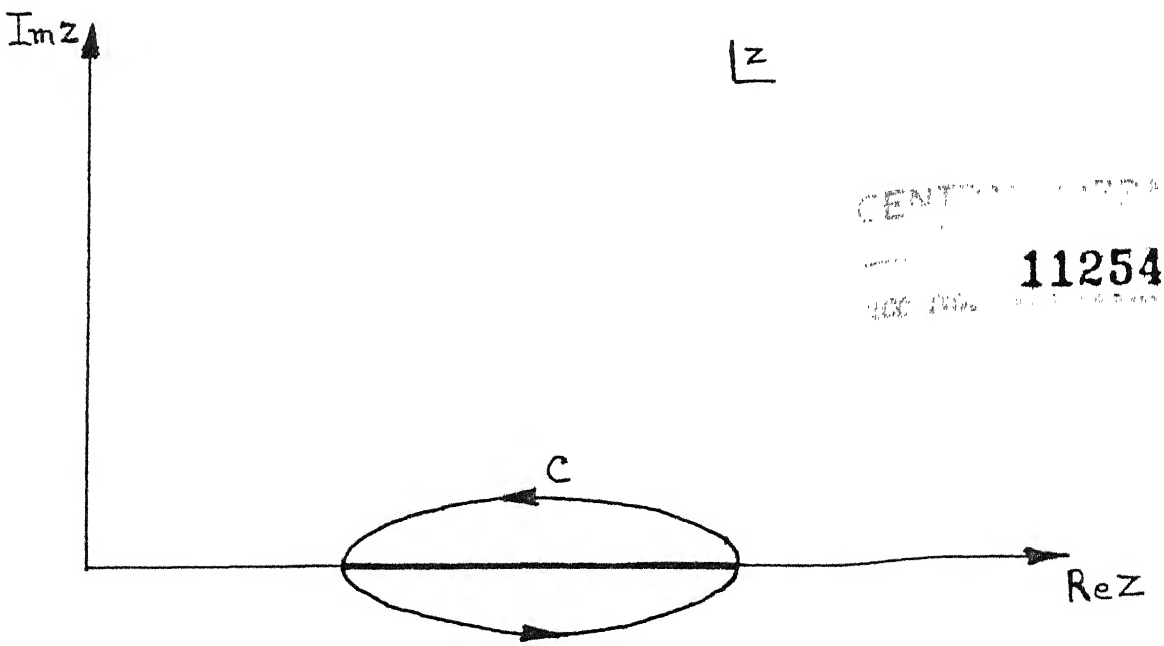

Figure 3.3.2 The contour in complex energy plane around the branch cut of the resolvent.

where,

$$g_{oo}^{M^{(i)}}(z) = \int_{-\infty}^{\infty} \frac{dp(h)}{z-h} \qquad (3.3.17)$$

and p(h) is the spectral projection operator of $\underline{M}^{(i)}$. Thus

$$\bar{f} = \langle f_o^i | \int f(h)\, dp(h) \, | f_o^i \rangle$$

or,

$$\bar{f} = \langle f_o^i | \; \underline{f}[\underline{M}^{(i)}] \; | f_o^i \rangle \qquad (3.3.18)$$

where the operator $\underline{f}(\underline{M}^i)$ has the same functional form of $\underline{M}^{(i)}$ as f(z) is of z. Thus it is found that the configuration average can be expressed as a representation of a suitably constructed operator related to the probability distribution. The entire process can be generalized for the average of a function of several random independent variables. For such statistically independent random variables N_i's we have

$$P(\langle N_i \rangle) = \prod_i p(N_i)$$

and so the entire configuration space is defined by

$$\Phi = \prod_i^{\otimes} \phi^{(i)} \qquad (3.3.19)$$

Where $\phi^{(i)}$ is the space associated to a single random variable N_i and the full Green function is then given by

$$G\left(\langle M^{(i)} \rangle\right) = \prod_i^{\otimes} g^{M^{(i)}} \qquad (3.3.20)$$

Then the average of the function $F\left(\langle N_i \rangle\right)$ is given by :

$$\bar{F} = \int_{-\infty}^{\infty} \langle \prod_i^{\otimes} dN_i \rangle \; F\left(\langle N_i \rangle\right) \; P\left(\langle N_i \rangle\right) \qquad (3.3.21)$$

or,

$$\bar{F} = \langle f_o | F\left(\langle \underline{M}^{(i)} \rangle\right) | f_o \rangle \qquad (3.3.22)$$

where

$$|f_o\rangle = \prod_i^{\otimes} \; |f_o^i\rangle \qquad (3.3.23)$$

The configuration space Φ is spanned by the basis set

$$|f_{s_1}\rangle \otimes |f_{s_2}\rangle \otimes |f_{s_3}\rangle \ldots \qquad (3.3.24)$$

where $\{|f_{s_i}\rangle\}$ spans the space $\phi^{(i)}$.

As we know that each space $\phi^{(i)}$ (for random binary alloys) is spanned by two basis vectors, $|f_o^i\rangle$ and $|f_1^i\rangle$,the space Φ will be spanned by 2^N basis vectors. $F(\langle \underline{M}^i \rangle)$ has the same operator function of $\langle \underline{M}^i \rangle$ as $F(\langle N_i \rangle)$ is a function of $\langle N_i \rangle$. Finally we define

$$\psi = \prod \mathscr{R} \otimes \prod_i^{\otimes} \phi^{(i)} \qquad (3.3.25)$$

This space is called the *Augmented space*. For a binary alloy,

consisting of N atoms, the Augmented space is spanned by $N \times 2^N$ basis vectors.

Now we are in a position to write the Hamiltonian of any disorder system in Augmented Space. Let us considder a general situation where both the diagonal and off-diagonal disorder are present. The multiband Anderson Hamiltonian in the Tight-Binding basis in the space $\mathscr{H}$, for binary alloy, is given by:

$$\underline{H} = \sum_i \sum_n \varepsilon_{in} \underline{P}_{in} + \sum_{i \neq j} \sum_{n,m} V_{in,jm} \underline{T}_{in,jm} \qquad (3.3.26)$$

where

$$\varepsilon_{in} = \varepsilon_{in}^{A} N_i + \varepsilon_{in}^{B} (1-N_i) \qquad (3.3.27)$$

and

$$V_{in,jm} = V_{nm}^{AA} N_i N_j + V_{nm}^{BB} (1-N_i)(1-N_j) \qquad (3.3.28)$$

$$+ V_{nm}^{AB} \langle N_i (1-N_j) + N_j (1-N_i) \rangle$$

i,j are the site indices and m,n are the band indices.

Here the only statistically independent random variables are N_i's. N_i can take the values either 0 or 1. Thus, the probability density associated with each N_i is given by :

$$P_i(N_i) = c\,\delta(N_i - 1) + (1-c)\,\delta(N_i) \qquad (3.3.29)$$

where c is the concentration of A atoms. Equation (3.3.26) can be rearranged as follows :

$$\underline{H} = \underline{H}_B + \sum_i \sum_n \delta\varepsilon_n N_i \underline{P}_{in} + \sum_{i\neq j} \sum_{n,m} V^{(1)}_{nm} N_i N_j \underline{T}_{in,jm}$$

$$+ \sum_{i\neq j} \sum_{n,m} V^{(2)}_{nm} (N_i + N_j) \underline{T}_{in,jm} \qquad (3.3.30)$$

where

$$\delta\varepsilon_n = (\varepsilon^A_n - \varepsilon^B_n)$$

$$V^{(1)}_{nm} = V^{AA}_{nm} + V^{BB}_{nm} + -2V^{AB}_{nm}$$

$$V^{(2)}_{nm} = V^{AB}_{nm} - V^{BB}_{nm} \quad \text{and} \qquad (3.3.31)$$

$$\underline{H}_B = \sum_i \sum_n \varepsilon^B_n \underline{P}_{in} + \sum_i \sum_n \sum_j \sum_m V^{BB}_{nm} \underline{T}_{ij}$$

The $\underline{M}^{(i)}$ for each value of N_i's has representation :

$$\underline{M}^{(i)} = \begin{bmatrix} c & \sqrt{c(1-c)} \\ \sqrt{c(1-c)} & 1-c \end{bmatrix} \qquad (3.3.32)$$

in the basis $|f^i_o\rangle$, $|f^i_1\rangle$ spanning $\phi^{(i)}$. The Augmented Space method then yields the Hamiltonian $\underline{H}$ in the Augmented Space as :

$$\tilde{\underline{H}} = \underline{H}_B \otimes \underline{I} + \sum_{i,n} \varepsilon_n \underline{P}_{in} \otimes \underline{M}^{(i)} \otimes \underline{I}^{(i)}$$

$$+ \sum_{m,n} \sum_{i,j} V^{(1)}_{nm} \underline{T}_{in,jm} \otimes \underline{M}^{(i)} \otimes \underline{M}^{(j)} \otimes \underline{I}^{(i,j)}$$

$$+ \sum_{n,m} V^{(2)}_{nm} \sum_{i \neq j} \underline{T}_{in,jm} \otimes (\underline{M}^{(i)} \otimes \underline{I}^{(i)} + \underline{M}^{(j)} \otimes \underline{I}^{(j)})$$

(3.3.33)

$$\tilde{\underline{H}} \in \mathscr{H} \otimes \prod_i^{\otimes} \phi^{(i)}$$

$\underline{I}^{(i)}$, $\underline{I}^{(i,j)}$ in the above equation indicate identity operators in all subspaces $\phi^{(k)}$ except those superscripted.

3.4 CPA THROUGH AUGMENTED SPACE FORMALISM USING GRAPHICAL METHOD

Having described the Augmented Space formalism we are now in a position to describe CPA in the Augmented space. We shall describe it with the use of the graphical technique (Haydock 1972, Thesis) because it provides a clear visual illustration, particularly when we generalize to the cluster CPA's. The standard algebraic formulation may often hide essentials of the approximation in the complexities of the algebraic equations.

Let us first describe the graphical method. By a graph we shall mean a set of 'Vertices' connected by 'links'. These vertices

and links have one to one correspondence with a countable basis of representation of an operator. If $\underline{M}$ is any operator represented the basis $\{|i\rangle\}$ then to each element in the basis $\{|i\rangle\}$ the corresponds a vertex v_i. Associated with each vertex v_i is t contribution $[\ 1/\langle i|\underline{M}|i\rangle\ ]$ to the inverse of $\underline{M}$. With each pair $|i\rangle$, $|j\rangle$ is associated a link l_{ij} and a contribution $\langle i|\underline{M}|j\rangle$ to t inverse of $\underline{M}$. The link l_{ij} may be directional meaning M_{ij} may n be equal to M_{ji} (shown in the figure (3.4.1). We shall define path in a graph of length n as a sequence of n+1 vertices connecte by n links. It is denoted by $P_n(i,j,k,\ldots,m)$ where i,j,k,...,m ar vertices. The contribution of a path of length n is given by

$$k[P_n(i,j,k,\ldots,m)] = \prod_{i=1}^{n+1} \frac{1}{\underline{M}_{ii}} \prod_{i\neq j=1}^{n+1} \underline{M}_{ij} \qquad (3.4.1$$

Now we can associate the representation of the Gree operator $\underline{G}$ in the basis $\{|i\rangle\}$ to the corresponding graph. The Gree operator or the resolvent defined as

$$\underline{G} = (z\underline{I} - \underline{H})^{-1} \qquad (3.4.2$$

then the representation of $\underline{G}$ is given by

$$\underline{G}_{ij}(z) = \sum_{n=0}^{\infty} \sum_{P_n \in S_n} k(P_n) \qquad (3.4.3$$

where S_n is the set of all the paths connecting the vertices v_i

and v_j.

It is clear that for a general infinite lattice the number of paths between two vertices is too large. Any indiscriminate approximation to equation (3.4.3) may seriously violate the analytic properties of the resolvent. The enumeration or even statistical estimation of all paths is not a tractable problem. In order to evaluate the Green function we go through the Feenberg renormalization procedure. For this purpose we introduce the definition of a *non-intersecting* path P'_n. A path $P'_n = (v_o l_{o1} v_1 l_{12} \ldots v_n)$ is defined to be *non-intersecting* if none of the internal vertices $v_1 \ldots v_{n-1}$ are the same. If $v_o = v_n$ then the path is called a *closed*, or *polygonal non-intersecting path*.

We now gather together all paths starting from v_o, going through v_1 to v_2 either directly or via other vertices. This renormalizes the vertex v_1 (see figure (3.4.2)). The contribution at v_1 are all paths going from v_1 to v_1 but not touching v_o. This is just $G^{(o)}_{11}$, the Green function calculated on a graph with the vertex v_o missing. If we do this for every vertex, we obtain at the end only non-interacting paths but the contribution $k(v_n)$ is renormalized to (Haydock 1972, Mookerjee 1979)

$$k'(v_n) = G^{(o,1,2,\ldots,n-1)}_{nm} \qquad (3.4.4)$$

The superscripts denote that the Green function is calculated on a graph in which the superscripted vertices are absent and

$$v_i = \frac{1}{\langle i|\underline{m}|i\rangle}$$

$$l_{ij} = \langle i|m|j\rangle$$

Figure 3.4.1 Graphical representation of vertices and links associated with an operator $\underline{M}$

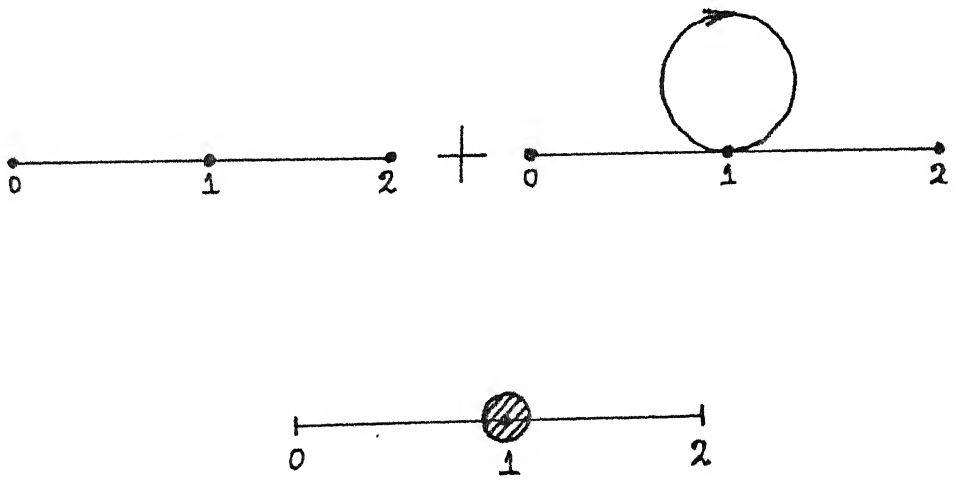

Figure 3.4.2 Representation of renormalized Vertices

$$\underline{G}_{ij}(z) = \sum_{n=0}^{\infty} \sum_{P \in S'_n} k'(P_n) \qquad (3.4.$$

where S'_n includes all the non-intersecting paths of length n from to v_j on the lattice. This expression is identical to Feenbu renormalized perturbation expansion. Statistical estimation of t non-intersecting paths is a more tractable geometrical problem.

Now we shall describe CPA through Augmented spac formalism. The Hamiltonian defined in the Hilbert space $\mathscr{H}$, can b written in the site representation $|n\rangle$ as

$$H_{nm} = \varepsilon_n \delta_{nm} + \underline{V}_{nm} \qquad (3.4.6$$

The Hamiltonian defined in the Augmented Space $\psi = \mathscr{H} \otimes \Phi$, can b written in the site-configuration state representation $|nf\rangle$ as

$$\tilde{\underline{H}}_{nf,mf'} = \underline{M}^n_{ff'} \delta_{nm} + \underline{V}_{nm} \delta_{ff'} \qquad (3.4.7$$

where, $\underline{M}^n$ is the operator in the space Φ associated with th probability distribution and $\underline{V}$ is the operator in $\mathscr{H}$. For a bimoda distribution of ε_n's the $\underline{M}^n$ for each n is given by the equatio (3.3.32) and the graph is a single link chain like figure (3.4.3 where $a_1 = 1-c$, $a_2 = c$, $b = \sqrt{c(1-c)}$. The configuration average Green function for this model is then given by the resolvent corresponding to the Hamiltonian $\tilde{H}$, i.e.

$$\langle G_{nm}(z)\rangle = \langle nf_o|(z\underline{I}-\underline{\tilde{H}})^{-1}|mf_o\rangle \qquad (3.4.8)$$

here, the problem is reduced to that of an ordered system with a much amplified set of eigenfunctions.

Until now all equations are *exact*. Approximations are made while employing the graphical technique. Haydock (Thesis, 1972) showed that geometrical approximations on graphs involving delinking do not violate Herglotz analytic properties of the corresponding approximate Green functions. The configurationally averaged Green function $\langle G(z)\rangle$ can be determined by considering self-avoiding paths between $|nf_o\rangle$ and $|mf_o\rangle$ in the full Augmented space ψ. Walks in the Augmented space imply that an electron at a site labelled by n and configuration state $|f_o\rangle = |f_1^o\rangle \otimes |f_j^o\rangle \cdots\cdots$ can be induced by $\underline{\tilde{H}}$ either to make spatial hops to one of the neighbours of n with the matrix element V, keeping the configuration state same, or it can remain on the spatial site while the configuration state at the site n changes according to $\underline{M}^n$, the configuration state at all other sites remaining same.

Starting from the vertex |of> thefirst steps possible are to the near neighbours l_i in the Hilbert space $\mathcal{H}$ as shown by single lines in figure (3.4.4) or to a different configuration state of the site 'o' labelled by, say, (of_o) by a hop shown by double lines.

If $R_o(z)$ is the contribution of all self-avoiding non-intersecting paths from vertex 0 and back in the space $\mathcal{H}$, the

Green function in an ordered system would be

$$g_{oo}(z) = \frac{1}{z-R_o(z)} \qquad (3.4.9)$$

In three dimensions, $R_o(z)$ will include the contribution $\sum_i V_i^2 g_{oo}(z)$, where i are various neighbours of 'o' and $g_{ii}^{(o)}$ corresponds to the Green function calculated from a sub-graph in which the vertex 'o' is missing as well as the contributions of all closed self-avoiding loops in $\mathscr{R}$. In the Augmented space the configuration averaged Green function can be written as

$$\langle G(z)\rangle = \frac{1}{z-R(z)-T(z)} \qquad (3.4.10)$$

where R(z) is the contribution of all self-avoiding paths from the vertex 'of' and back that are either (a) entirely in the spatial part of the Augmented space or (b) self-avoiding paths in the Augmented space which includes configuration state-hops but do not form closed loops. T(z) is the contribution of all the closed non-interacting loops from 'of' in the Augmented space. Figure (3.4.5) shows a self-avoiding closed loops involving both spatial and configuration state-hops.

There are numerous loops like this and it is almost impossible to account for all of them. Therefore the essential approximation is now made here to avoid this difficulty. Our approximation is to delink all those closed paths having both spatial and configuration state hops, i.e,

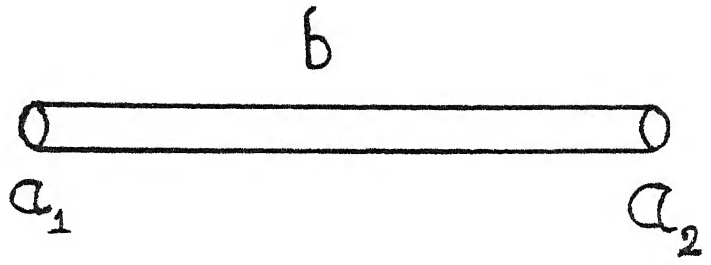

Figure 3.4.3 Representation of a single link chain

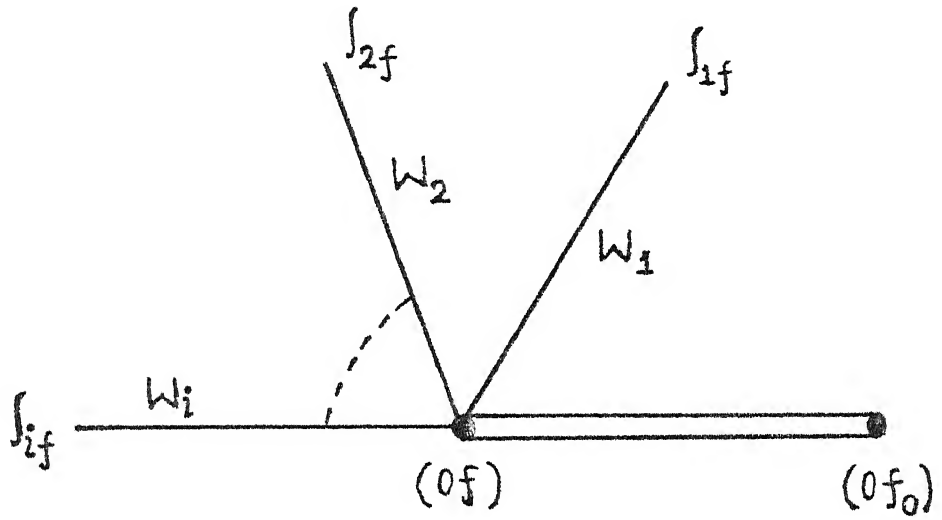

Figure 3.4.4 CPA graph in Augmented Space

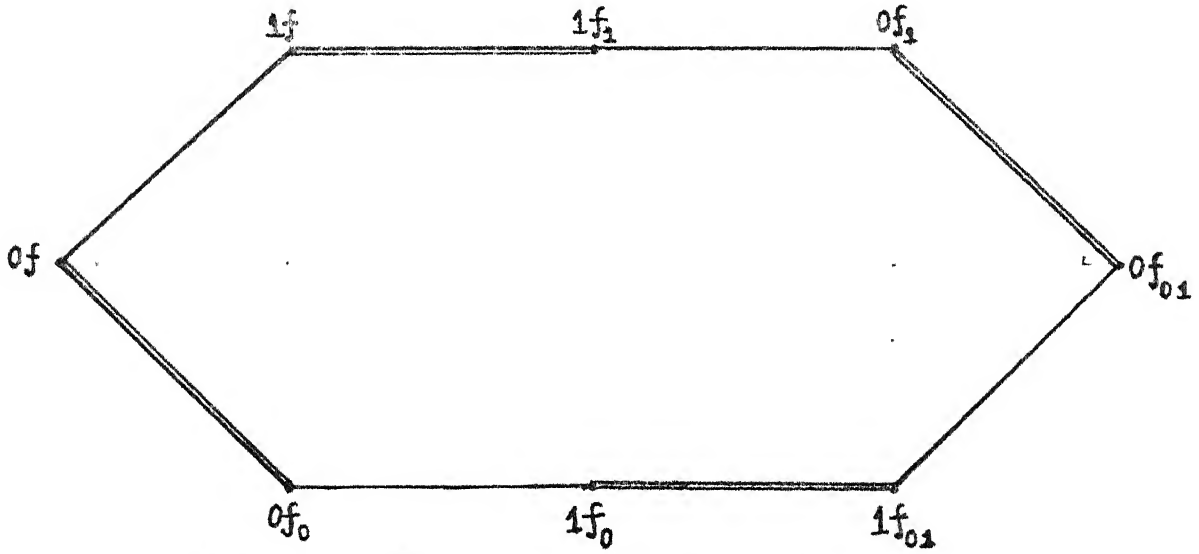

Figure 3.4.5 Shortest self-avoiding, closed loop in the Augmented Space involving both Spatial and configuration state hops

$$T(z) = 0 \qquad (3.4.11)$$

Once we have made this approximation our approximate delinked graph consists of essentially that in the ordered system together with an extra configuration state hop with the off-diagonal element of $\underline{M}^{(n)}$ in the tridiagonal representation ($b = \sqrt{c(1-c)}$ in the case of binary alloys) as the link contribution. If starting from a vertex 'nf' we hop to a vetex 'nf_n' then the sub graph with the vertex 'nf' missing is an infinite graph which is exactly similar to the original one. A direct consequence of this property is :

$$G^{(of)}_{of,of} = G_{of,of} = \langle G_{oo} \rangle \qquad (3.4.12)$$

This will not hold in the absence of the type of delinking adopted above.

This approximation gives exactly the 1CPA result. We can show this as follows :

Let $G^{DL}(z)$ be the Green function corresponding to the delinked graph in the Augmented space and let

$$\underline{M}_{ij} = W_i \delta_{j,i+1} \qquad (3.4.13)$$

be the tridiagonal representation of the operator $\underline{M}^{(n)}$ in each subspace ϕ^n of Φ, then

$$G^{DL}(z) = \frac{1}{z - R_o(z - W_1^2 G_1(z)) - W_1^2 G_1(z)}$$

$$= g_{oo}[z - W_1^2 G_1(z)] \qquad (3.4.14)$$

where

$$G_i(z) = \frac{1}{z - R_o(z - W_1^2 G_1(z)) - W_{i+1}^2 G_{i+1}(z)} \qquad (3.4.15)$$

In the conventional 1CPA formalism the self energy $\Sigma_o(z)$ is defined by

$$G^{CP}(z) = \frac{1}{z - \Sigma_o(z) - R_o(z - \Sigma_o)}$$

$$= g_{oo}\,[z - \Sigma_o(z)] \qquad (3.4.16)$$

$$\Sigma_o(z) = W_1^2\, G_1(z) \qquad (3.4.17)$$

$W_1 = \delta\varepsilon\ \sqrt{c(1-c)}$ for binary alloy

Thus equations (3.4.14) and (3.4.16) are equivalent. This equivalence has been discussed in detail by Bishop and Mookerjee (1974).

3.5 CCPA THROUGH AUGMENTED SPACE FORMALISM

The generalization of CPA to CCPA involves a cluster of finite sites embeded in an effective medium, thus including the effects of correlated scattering from a cluster. This

approximation, apart from retaining contribution of all paths described in CPA, also includes the self-avoiding, non-intersecting paths which involve hops that change the configurations over the n-sites of the cluster. Such polygonal self-avoiding paths take into account of the multiple scattering by the cluster.

The vertices and links (bonds) have to be renormalized accordingly. To illustrate the procedure we shall, as an example, examine the case of a 2CPA: a 2-sites cluster is immersed in a self consistent medium. If we delink all polygonal paths linking configuration changes of more than two chosen sites, we have an octagonal decoration of self-avoiding polygonal paths in the Augmented space, graph shown in figure (3.5.1). The eight vertices of the octagon correspond to the two sites and their four different configurations ($2x2^2$). This is the rank of the subspace in Augmented space spanned by the cluster and its configurations. The octagon belonging to a bond has no connection to that of another bond through links in the Augmented space, which effectively ensures that the correlated scattering from three or more sites belonging to different bonds is ignored. The final effect is that each bond is renormalized as shown in figure (3.5.3). This gives rise to a matrix self-energy :

$$\underline{\Sigma} = \begin{bmatrix} \Sigma_o & \Sigma_1 \\ \Sigma_1 & \Sigma_o \end{bmatrix} \qquad (3.5.1)$$

The aim is to calculate $\underline{\Sigma}$ self-consistently. It fully describes the self-consistent medium in the 2CPA.

The bond renormalization procedure follows in two steps :

Step 1 :

The decorating octagon is not an isolated octagon involving only the two spatial sites (0 and 1). Let us take the vertex A ,*i.e.*, $1f_1$ in the notation of Mookerjee (1973). The bond AE ($1f_1$ to $0f_1$) belonging to the octagon is only one of the z bonds emanating from A to the z nearest neighbours of 1. The other remaining (z-1) bonds ($1f_1$ to $2f_1$, $3f_1$,....) also hang on to the site A. These bonds themselves in turn have their own octagons decorating them (figure (3.5.2)). Thus the bond AE is itself immersed in a self-consistent medium. The same is true for the bonds FG and HK of the octagon. We may take this into account by saying that the medium renormalizes the bonds AE, FG and HK. Once the renormalization is accounted for, the octagon is effecively isolated.

The renormalized vertices $\sigma_0(z)$ and links $\sigma_1(z)$ are found as follows : We first divide the whole lattice into two sublattices, namely (1) and (2). (1) is an unrenormalized bond AE. It has a Hamiltonian :

$$\underline{H}^{(1)} = V_2(\underline{T}_{AE} + \underline{T}_{EA}) \qquad (3.5.2)$$

(2) is a lattice $\mathcal{L}$ which is the original lattice *minus* the link AE and in which all bonds and sites are renormalized by Σ. It has a Hamiltonian

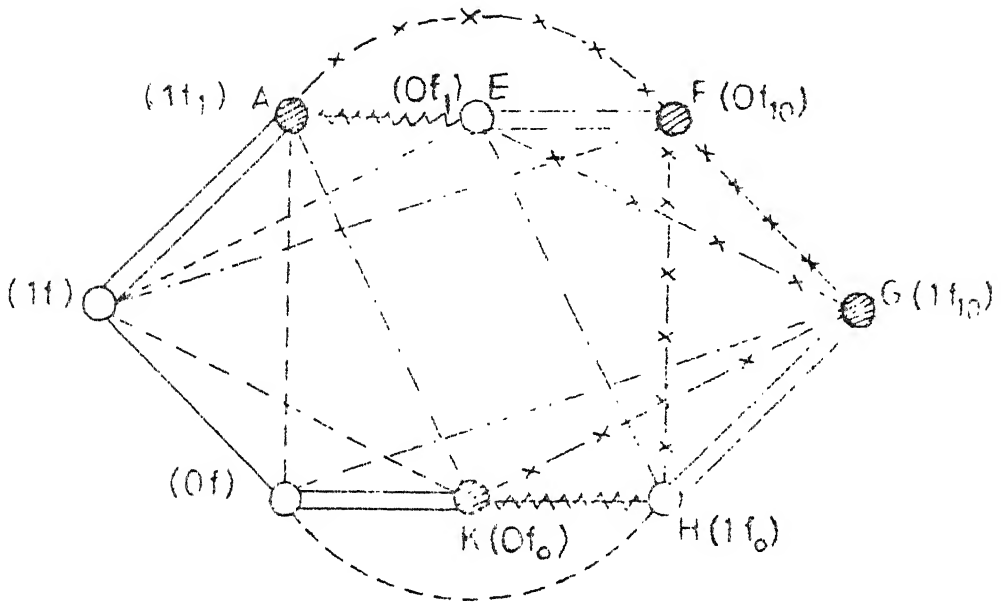

$V_1 = 2CV^{(2)} + C^2V^{(1)} + V_{BB}$

$V_2 = V^{(2)} + C(1-C)V^{(1)} + V_{BB}$

$V_3 = 2(1-C)V^{(2)} + (1-C)^2V^{(1)} + V_{BB}$

$\sqrt{C(1-C)}\left[V^{(2)} + (1-C)V^{(1)}\right]$

$\sqrt{C(1-C)}\left[V^{(2)} + CV^{(1)}\right]$

$C(1-C)V^{(1)}$

$\sqrt{C(1-C)}\,e$

$\equiv e_B + Ce$

$\equiv e_B + (1-C)e$

Figure 3.5.1 Octagonal decoration corresponding to 2CPA in Augmented Space

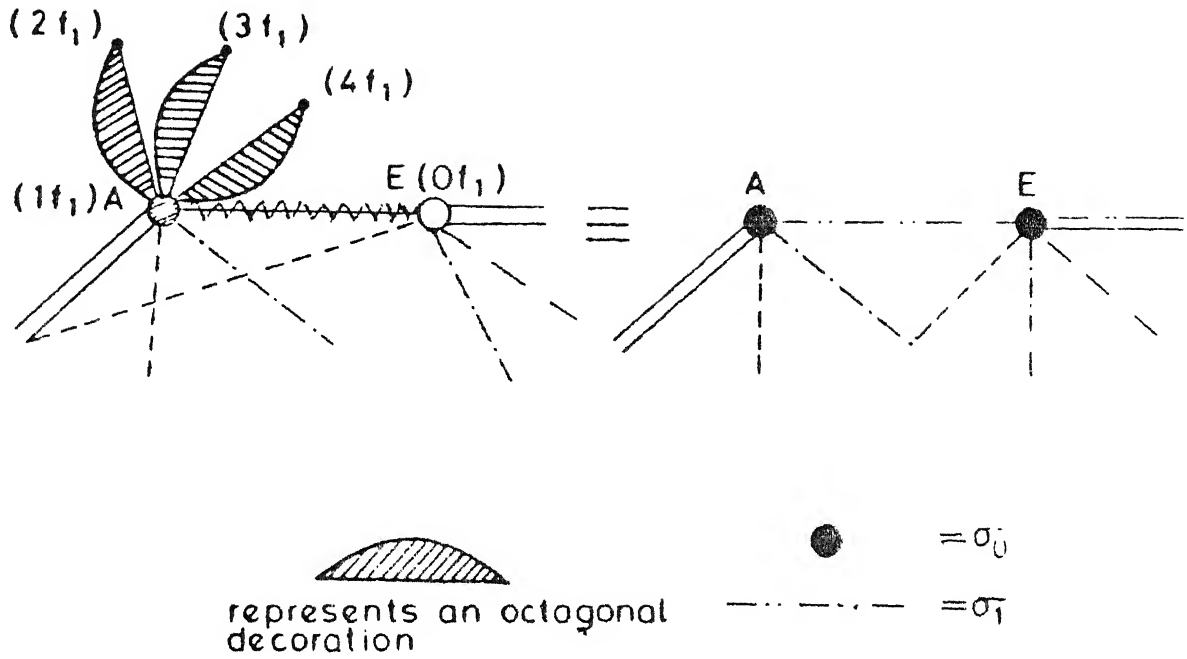

Figure 3.5.2 Renormalization of site and bond of the octagon in ASF due to infinite medium

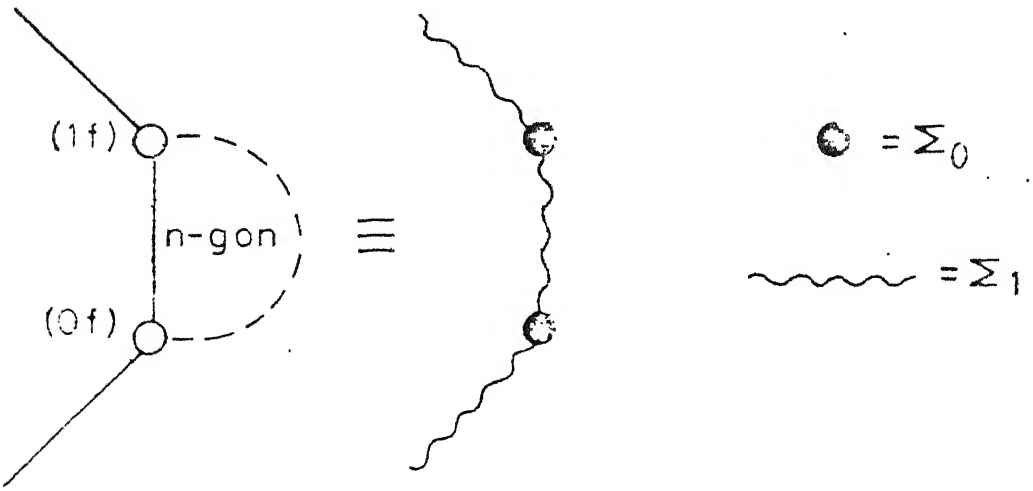

Figure 3.5.3 Final renormalized site and bond in 2CPA for the octagon in Figure (3.5.1.).

$$\underline{H}^{(2)} = \Sigma_o(z) \sum_{i \neq A,E} \underline{P}_i + \Sigma_1(z) \sum_{i,j \neq A,E} \underline{T}_{ij} \qquad (3.5.3)$$

$\underline{H}^{(1)}$, $\underline{H}^{(2)}$ represents the diagonal blocks in the partition of the Augmented space into a subspace $\mathbb{D}$ spanned by the cluster and its configurations and its complement $\mathbb{D}'$. The off-diagonal blocks $\underline{H}^{(1,2)}$ and $\underline{H}^{(2,1)} = H^{(1,2)\dagger}$ are given by

$$\underline{H}^{(1,2)} = \Sigma_1(z) \sum_{i \neq A,E} (\underline{T}_{iA} + \underline{T}_{Ai} + \underline{T}_{iE} + \underline{T}_{Ei}) \qquad (3.5.4)$$

The Green operator, $\underline{G}^{(1)}$, corresponding to the subspace (1) is then given by projection of the full Green Operator, $\underline{G}$, onto the subspace (1), i.e.,

$$\underline{G}_1^{(1)} = \underline{P}_1 \underline{G} \underline{P}_1$$

$$= \left[z\underline{I} - \underline{H}^{(1)} - \underline{H}^{(1,2)\dagger} \underline{G}^{(2)} H^{(2,1)} \right]^{-\underline{P}_1} \qquad (3.5.5)$$

where

$$\underline{G}^{(2)} = \left[z\underline{I} - \underline{H}^{(2)} \right]^{-\underline{P}_2} \qquad (3.5.6)$$

with $\underline{P}_1 + \underline{P}_2 = \underline{I}$ (3.5.7)

Here we have used the notation $\underline{X}^{-Py}$ to denote the inverse of the operator $\underline{X}$ on the subspace y.

It is clear from the above equation that the effect of the rest of the lattice hanging on to the bond AE is to renormalize the Hamiltonian $\underline{H}^{(1)}$ to $\underline{H}^{(1)} + \underline{\sigma}$ where the self-energies

$$\underline{\sigma} = \begin{bmatrix} \sigma_o & \sigma_1 \\ \sigma_1 & \sigma_o \end{bmatrix} \qquad (3.5.8)$$

are given by

$$\sigma_{AA} = \sigma_{EE} = \sigma_o(z) = \Sigma_1^2(z) \sum_{k,m\in\eta_A} G_{km}^{(z)} \qquad (3.5.9)$$

$$\sigma_{AE} = \sigma_{EA} = \sigma_1(z) = \Sigma_1^2(z) \sum_{k\in\eta_A} \sum_{m\in\eta_E} G_{km}^{(z)} \qquad (3.5.10)$$

Step 2 :

The next step is to work with the isolated renormalized octagon. This octagon is to be renormalized again because each of the vertices such as A,E etc. are connected to other vertices through either a hop that changes the site labelling or a hop that changes the configuration. For carrying out this final renormalization we again divide the octagon into two subspaces :

(1) a bond B (0f, 1f) and

(2) the rest of the octagon M

The corresponding Hamiltonians are given by :

$$\underline{\tilde{H}}^B = \sum_{i,j\in 0f,1f} \underline{\tilde{H}}_{ij} \qquad (3.5.11)$$

$$\underline{\tilde{H}}^M = \sum_{i,j\neq 0f,1f} \underline{\tilde{H}}_{ij} \qquad (3.5.12)$$

and the interaction Hamiltonian is given by :

$$\underline{\tilde{H}}^{BM} = \sum_{i\in B} \sum_{j\in M} (\underline{\tilde{H}}_{ij} + \underline{\tilde{H}}_{ji}) = \underline{\tilde{H}}^{MB\dagger}. \qquad (3.5.13)$$

The Hamiltonian $\underline{\tilde{H}}$ is given by the equation (3.3.33). As before, we have

$$\underline{G}^{B} = \underline{P}_B \, \underline{G} \, \underline{P}_B$$

$$= \left[z\underline{I} - \underline{\tilde{H}}^{B} - \underline{\tilde{H}}^{BM\dagger} \, \underline{G}^{M} \, \underline{\tilde{H}}^{MB} \right]^{-\underline{P}_B} \qquad (3.5.14)$$

$$\underline{G}^{M} = \left[z\underline{I} - \underline{\tilde{H}}^{M} \right]^{-\underline{P}_M} \qquad (3.5.15)$$

and $$\underline{P}_B + \underline{P}_M = \underline{I} \qquad (3.5.16)$$

Finally we obtain the renormalized site self-energy $\Sigma_o(z)$ and bond self-energy $\Sigma_1(z)$ as

$$\Sigma_o(z) = \underline{\tilde{H}}^{B}_{oo} + \sum_{j\neq o} \sum_{k\neq o} \underline{\tilde{H}}^{BM}_{oj} \, \underline{G}^{M}_{jk} \, \underline{\tilde{H}}^{BM}_{ko} \qquad (3.5.17)$$

$$\Sigma_1(z) = \underline{\tilde{H}}^{B}_{o1} + \sum_{j\neq o} \sum_{k\neq 1} \underline{\tilde{H}}^{BM}_{oj} \, \underline{G}^{M}_{jk} \underline{\tilde{H}}^{BM}_{k1} \qquad (3.5.18)$$

Equations (3.5.9), (3.5.10), (3.5.17) and (3.5.18) together provide a sel-consistent set of equations for the calculations of the self-energy operator $\underline{\Sigma}$ which defines the effective medium.

The Green operator may now be calculated

$$\underline{H}_{eff} = \sum_i \Sigma_o \, \underline{P}_i + \sum_{i,j} \Sigma_1 \, \underline{T}_{ij}$$

$$= \Sigma_o \underline{I} + (\Sigma_1/V) \sum_{i,j} \underline{V}_{ij} \underline{I}$$

$$= \Sigma_o \underline{I} + (\Sigma_1/V) \underline{h}_o \qquad (3.5.19)$$

where

$$\underline{h}_o = \sum_{i,j} V \underline{I}_{ij} \qquad (3.5.20)$$

$$\langle \underline{G}(z) \rangle = (z\underline{I} - \underline{H}_{eff})^{-1} = \left[(z-\Sigma_o)\underline{I} - (\Sigma_1/V)\underline{h}_o\right]^{-1}$$

$$= \left(\frac{V}{\Sigma_1}\right) \left[\left((z-\Sigma_o)\frac{V}{\Sigma_1}\right)\underline{I} - \underline{h}_o\right]^{-1}$$

$$= \left(\frac{V}{\Sigma_1}\right) g(\xi) \qquad (3.5.21)$$

where

$$\xi = \left(\frac{z-\Sigma_o}{\Sigma_1}\right) V \quad \text{and} \quad g(\xi) = (\xi\underline{I} - \underline{h}_o)^{-1} \qquad (3.5.22)$$

Once we calculate $g(\xi)$ by methods available for translationally symmetric Hamiltonians, the equations (3.5.9) to (3.5.22) are the basic equations governing the 2CPA.

For the full cluster CPA, we first partition the Augmented space ψ into a $\mathbb{D}$ which is spanned by all sites in the cluster and their configurations and its complement $\mathbb{D}' = \psi \setminus \mathbb{D}$. The rank of $\mathbb{D}$ is $nx2^n$, where n is the size of the cluster and the system is a binary alloy. We now replace by Hamiltonian $\underline{H}' = P_{\mathbb{D}} \cdot \tilde{\underline{H}} P_{\mathbb{D}}$, by an effective $\underline{H}'_{eff}$ which is translationally symmetric and has to be self-consistently calculated.

Using the partition theorem

$$G_{\mathbb{D}} = (z\tilde{\underline{I}} - \tilde{\underline{H}})^{-P_{\mathbb{D}}}$$

$$= (z\underline{I} - \underline{H}_{\mathbb{D}} - \underline{H}_{\mathbb{D}\mathbb{D}'}\, \underline{G}^{(\mathbb{D})}\, \underline{H}_{\mathbb{D}',\mathbb{D}})^{-1} \qquad (3.5.23)$$

$$= (z\underline{I} - \underline{H}_{\mathbb{D}} - \underline{\sigma}\,(H_{eff}))^{-1}$$

Here

$$\underline{H}_{\mathbb{D}} = \underline{P}_{\mathbb{D}}\, \tilde{\underline{H}}\, P_{\mathbb{D}}$$

$$\underline{H}_{\mathbb{D}\mathbb{D}'} = \underline{P}_{\mathbb{D}}\, \tilde{\underline{H}}\, \underline{P}_{\mathbb{D}'} = \underline{H}^{\dagger}_{\mathbb{D}'\mathbb{D}}$$

$$\underline{G}^{\mathbb{D}} = (z\tilde{\underline{I}} - \underline{H}_{eff})^{-P_{\mathbb{D}'}}$$

$$\underline{\sigma}(H_{eff}) = \underline{H}_{\mathbb{D}\mathbb{D}'}\, \underline{G}^{(\mathbb{D})}(H_{eff})\, \underline{H}_{\mathbb{D}',\mathbb{D}} \qquad (3.5.24)$$

We now partition the space $\mathbb{D}$ on which $\hat{\underline{H}} = \underline{H}_{\mathbb{D}} + \underline{\sigma}$ acts into one $\mathbb{c}$ which is spanned by (nf) and its complement $\mathbb{c}'$. Again using the partition theorem

$$G_{\mathbb{c}} = (z\tilde{\underline{I}} - \underline{H}_{\mathbb{D}})^{-P_{\mathbb{c}}}$$

$$= z\underline{I} - \underline{H}_{\mathbb{c}} - \underline{H}_{\mathbb{c}\mathbb{c}'}\, G^{\mathbb{c}'}(\underline{H}_{eff})\, \underline{H}_{\mathbb{c}',\mathbb{c}}\,(\underline{H}_{eff}) \qquad (3.5.25)$$

But the Augmented Space theorem states

$$\underline{G}_{\mathbb{c}} = \langle \underline{G} \rangle_{av.} = (z\tilde{\underline{I}} - \tilde{\underline{H}}_{eff})^{-1}$$

$$\underline{\underline{H}}_{eff} = z\underline{I} - \underline{H}_{c} - \underline{H}_{cc'}[\underline{\sigma}]\ \underline{G}^{(c')}[\underline{\sigma}]\ \underline{H}_{c'c}[\underline{\sigma}] \qquad (3.5.26)$$

Equations (3.5.24) and (3.5.26) are the self-consistent equations for $\underline{H}_{eff}$

$$\langle G \rangle = (z\underline{A} - \underline{h}_{o})^{-1}\ \underline{A} = \underline{\Gamma}\ \underline{A} \qquad (3.5.27)$$

where $$\underline{A} = \underline{h}_{o} H^{-1}_{eff} \qquad (3.5.28)$$

Γ_{ij} may be easily calculated, even if $\underline{A}$ is not diagonal by using the modified version of the Recursion method with $\underline{A}$ taking the place of the overlap matrix.

3.6 OPTICAL CONDUCTIVITY FOR RANDOM SEMICONDUCTING ALLOYS IN AUGMENTED SPACE

We have already discussed the general formultation for optical conductivity for any crystalline solid in § 2.4.In this section we shall now use the basic formula for optical conductivity and generalize it for random semiconducting alloys within the Augmented space formalism.

The basic formula for optical conductivity is given by :

$$\alpha(\omega) = - \frac{2\pi e^2}{m^{*2}\Omega} \frac{1}{\omega} \sum_{if\gamma} |\langle \psi_f | \hat{e}_\gamma . \bar{p} | \psi_i \rangle|^2 f_i (1-f_f)\ \delta(E_f - E_i - \hbar\omega) \qquad (3.6.1)$$

where

m^*	:	effective mass of electron
Ω	:	volume of the specimen
ω	:	frequency of incident photon
i	:	refers to the initial state (valence band)
f	:	refers to the final state (conduction band)
γ	:	refers to direction of polarization of the incoming photon
$\bar{p}$	:	momentum of the electron
$f_{i,f}$	:	occupation probability of initial or final states

For semiconductors, at $T = 0^{\circ}K$, we have

$$f_i = 1 \text{ and } f_f = 0 \qquad (3.6.2)$$

Thus, the equation (3.6.1) reduces to

$$\alpha(\omega) = - \frac{2\pi e^2}{m^{*2}\Omega} \frac{1}{\omega} \sum_{if\gamma} |\langle \psi_f | \hat{e}_\gamma . \bar{p} | \psi_i \rangle|^2\ \delta(E_f - E_i - \hbar\omega) \qquad (3.6.3)$$

As before, we use the property of Dirac δ-function and find

$$\alpha(\omega) = - \frac{2\pi e^2}{m^{*2}\Omega} \frac{1}{\omega} \sum_{if\gamma} |\langle \psi_f | \hat{e}_\gamma . \bar{p} | \psi_i \rangle|^2 \int_0^{E_{max.}} \delta(E-E_f)\ \delta(E-E_i)\ dE$$

$$= - \frac{2\pi e^2}{m^{*2}\Omega} \frac{1}{\omega} \sum_{\gamma} \int_0^{E_0} |\langle \psi_f | \hat{e}_\gamma . \bar{p} | \psi_i \rangle|^2 \sum_{if} \delta(E-E_f)\ \delta(E-E_i)\ dE \qquad (3.6.4)$$

Where the upper limit E_o is determined both by the band limits and $\hbar\omega$. But, by definition :

$$4\Omega^{-2} \sum_i \sum_f \delta(E-E_f)\ \delta(E-\hbar\omega-E_i) = n_f(E)\ n_i(E-\hbar\omega) \qquad (3.6.5)$$

where $n_f(E)$: conduction band density of states per atom or bond

$n_i(E-\hbar\omega)$: valence band density of state per atom or bond

The factor 4 appears in the equation (3.6.5) due to two possible spin orientations of the electron in the initial and final states. Therefore the equation (3.6.4) reduces to

$$\sigma(\omega) = -\frac{2\pi e^2}{m^{*2}\Omega}\frac{1}{\omega} \sum_\gamma \int_0^{E_o} |\langle\psi_f|\hat{e}_\gamma.\bar{p}|\psi_i\rangle|^2 \frac{1}{4\Omega^{-2}}\ n_f(E)\ n_i(E-\hbar\omega)\ dE$$

$$= -\frac{\pi e^2}{2\ m^{*2}}\frac{\Omega}{\omega} \sum_\gamma \int_0^{E_o} |\langle\psi_f|\hat{e}_\gamma.\bar{p}|\psi_i\rangle|^2\ n_f(E)\ n_i(E-\hbar\omega)\ dE \qquad (3.6.6)$$

We shall be dealing with disordered systems and shall interested in finding the configuration averaged $\sigma(\omega)$ by averaging the product of the square of optical matrix element and the valence band density of states. Although, in general, the product of the square of optical matrix element and joint density of states has to be averaged to include the full vertex correction, but subsequently we shall factor the initial and final densities of states. We shall

take the conduction band density of states to be free electron like in a Virtual Crystal sense. Since the conduction electrons are reasonably extended, such an averaging may not be too bad. The full calculation should include the joint two particle propagator for initial and final states. The Augmented Space formalism is capable of handling such problems (Thakur *et.al.*1987). We shall leave this development for later work. As the free-electron like density of states is randomness independent,

We have,

$$\langle \sigma(\omega) \rangle_{av} = - \frac{\pi e^2}{2m^{*2}} \frac{\Omega}{\omega} \sum_{\gamma} \int_{0}^{E_o} n_f(E) \left\langle |\langle \psi_f | \hat{e}_\gamma . \bar{p} | \psi_i \rangle|^2 n_i(E-\hbar\omega) \right\rangle_{av} dE \qquad (3.6.7)$$

We shall expand the initial states in terms of the set of Tight-binding basis $\{|n\rangle\}$. For a semiconductor the Tight-binding basis $\{|n\rangle\}$ consiting of say, bond orbitals (to be discussed in §4.2), do span the valence and subspace. Therefore equation (3.6.7) gives the averaged optical conductivity $\langle \sigma(\omega) \rangle$ to be

$$\frac{e^2}{2m^{*2}} \frac{\Omega}{\omega} \mathcal{I}m \sum_{\gamma} \sum_{m} \sum_{n} \delta_{mn} \int_{0}^{E_o} n_f(E) \left\langle \langle \psi_f | p_\gamma | m \rangle \langle m | \underline{G}(\eta^-) | n \rangle \langle n | p_\gamma | \psi_f \rangle \right\rangle dE \qquad (3.6.8)$$

Here we have replaced the valence band density of states $n_i(E-\hbar\omega)$ by the corresponding Green function.

$$n_i(E_i - \hbar\omega) = -\frac{1}{\pi} \mathrm{Im} \sum_m \sum_n \delta_{mn} \langle m|\underline{G}(\eta^-)|n\rangle$$

where $\eta^- = E - \hbar\omega - 0^+$

$$p_\gamma = \hat{e}_\gamma . \bar{p}.$$

We may expand the final state in terms of plane waves

$$\psi_f = \sum_{\bar{G}} e^{i(\bar{k}+\bar{G}).\bar{r}} \psi_{\bar{G},\bar{k}}. \qquad (3.6.9)$$

Replacement of the full sum over all reciprocal lattice vectors by only $\bar{G} = \bar{0}$ leads to the free electron case. The optical matrix element factor in equation (3.6.8) can now be evaluated as follows :

$$\langle n|p_\gamma|\psi_f\rangle = \langle n|\hat{e}_\gamma.(-i\hbar\bar{\nabla})|\psi_f\rangle$$

$$= -i\hbar\langle n|\hat{e}_\gamma.\bar{\nabla}|\psi_f\rangle \qquad (3.6.10)$$

In the $\bar{r}$ representation, $\langle|n\rangle\rangle$ are given by the centred orbitals like $\langle\phi(\bar{r} - \bar{r}_m)\rangle$. Therefore,

$$\langle n|f\rangle = \frac{1}{\sqrt{\Omega}} \int \phi^*(\bar{r} - \bar{r}_n)\, e^{i\,\bar{k}_f.\bar{r}}\, d^3\bar{r} \qquad (3.6.11)$$

Therefore equation (3.6.10) becomes :

$$\langle n|\hat{e}_\gamma.\bar{p}|\psi_f\rangle = -\frac{i\hbar}{\sqrt{\Omega}} \int \phi^*(\bar{r} - \bar{r}_n)\, \hat{e}_\gamma.\bar{\nabla}\, e^{i\,\bar{k}_f.\bar{r}}\, d^3r$$

$$= \frac{\hbar}{\sqrt{\Omega}} \hat{e}_\gamma . \bar{k}_f \int \phi^*(\bar{r} - \bar{r}_n)\, e^{i\,\bar{k}_f . \bar{r}}\, d^3r$$

$$= \frac{\hbar}{\sqrt{\Omega}} \hat{e}_\gamma . \bar{k}_f\, \phi^*(\bar{k}_f)\, e^{i\,\bar{k}_f . \bar{r}_n} \qquad (3.6.12)$$

where $\phi^*(\bar{k}_f)$ is the Fourier transform of $\phi(\bar{r})$. But for random alloys, $\phi(\bar{r})$'s are random. For a binary alloy of constituents A and B with concentration c and (1-c) respectivity, $\phi(\bar{r} - \bar{r}_n)$ is given by

$$\phi(\bar{r}-\bar{r}_n) = \phi_A(\bar{r}-\bar{r}_n)\, N_n + \phi_B(\bar{r}-\bar{r}_n)\,(1-N_n)$$

$$= \phi_B(\bar{r}-\bar{r}_n) + \delta\phi(\bar{r}-\bar{r}_n)\, N_n \qquad (3.6.13)$$

where N_n is defined as :

$N_n = 1$ if n^{th} site is occupied by A atom

$= 0$ if n^{th} site is occupied by B atom.

$\phi_A(\bar{r})$ and $\phi_B(\bar{r})$ are respectively centred orbitls associated with A and B atoms and $\delta\phi = \phi_A - \phi_B$.

The probability density is given by

$$p(N_n) = c\,\delta(N_n - 1) + (1-c)\,\delta(N_n) \qquad (3.6.14)$$

Therefore,

$$\phi^{*}(\bar{k}_f)\, e^{i\bar{k}_f\cdot\bar{r}_n} = \left[\phi_B^{*}(\bar{k}_f) + \delta\phi^{*}(\bar{k}_f)N_n\right] e^{i\bar{k}_f\cdot\bar{r}_n} \qquad (3.6.15$$

Hence for random semiconducting binary alloys, the equation (3.6.12 becomes :

$$\langle n|\hat{e}_\gamma\cdot\bar{p}|\psi_f\rangle = \frac{\hbar}{\sqrt{\Omega}}\,\hat{e}_\gamma\cdot\bar{k}_f\, e^{i\,\bar{k}_f\cdot\bar{r}_n}\left[\phi_B^{*}(\bar{k}_f) + \delta\phi^{*}(\bar{k}_f)N_n\right] \qquad (3.6.16$$

Similarly $\langle\psi_f|\hat{e}_\gamma\cdot\bar{p}|m\rangle$ is given by

$$\langle\psi_f|\hat{e}_\gamma\cdot\bar{p}|m\rangle = -\frac{\hbar}{\sqrt{\Omega}}\,\hat{e}_\gamma\cdot\bar{k}_f\, e^{-i\,\bar{k}_f\cdot\bar{r}_m}\left[\phi_B(\bar{k}_f) + \delta\phi(k_f)N_m\right]$$

(3.6.17)

Equation (3.6.8) now becomes :

$$\langle\sigma(\omega)\rangle = \frac{e^2}{2m^{*2}}\,\frac{\Omega}{\omega}\,\mathcal{I}m\sum_\gamma\sum_m\sum_n\delta_{mn}\int_0^{E_o} n_f(E)\left\langle\left[-\frac{\hbar}{\sqrt{\Omega}}\,\hat{e}_\gamma\,\bar{k}_f e^{-i\bar{k}_f\cdot\bar{r}_m}\right.\right.$$

$$\left.\left(\phi_B(\bar{k}_f) + \delta\phi(\bar{k}_f)N_m\right)\right]\langle m|\underline{G}(\eta^{-})|n\rangle\left[\frac{\hbar}{\sqrt{\Omega}}\,\hat{e}_\gamma\cdot\bar{k}_f\, e^{i\bar{k}_f\cdot\bar{r}_m}\right.$$

$$\left.\left.\left(\phi_B^{*}(\bar{k}_f) + \delta\phi^{*}(\bar{k}_f)\,N_n\right)\right]\right\rangle dE$$

$$= -\frac{e^2}{2m^{*2}}\,\frac{\Omega}{\omega}\left(\frac{\hbar}{\sqrt{\Omega}}\right)^2\mathcal{I}m\sum_\gamma\sum_m\sum_n\delta_{mn}\int_0^{E_o} n_f(E)\left\langle k_{f\gamma}^2\, e^{i\bar{k}_f\cdot(\bar{r}_n-\bar{r}_m)}\right.$$

$$\left[\phi_B(\bar{k}_f) + \delta\phi(\bar{k}_f)N_m\right]G_{mn}(\eta^-)\left[\phi_B^*(\bar{k}_f)+\delta\phi^*(\bar{k}_f)N_n\right]\Big\rangle\, dE$$

$$= -\frac{e^2\hbar^2}{2m^{*2}}\frac{1}{\omega}\,\mathcal{P}m\sum_{\gamma}\sum_{m}\sum_{n}\delta_{mn}\int_0^{E_o} n_f(E)\left\langle k_{f\gamma}^2\, e^{i\bar{k}_f.(\bar{r}_n-\bar{r}_m)}\right.$$

$$\left[|\phi_B(\bar{k}_f)|^2\, G_{mn}(\eta^-) + \phi_B^*(\bar{k}_f)\,\delta\phi(\bar{k}_f)\,N_m\,G_{mn}(\eta^-)\right.$$

$$\left.\left. + \phi_B(\bar{k}_f)\delta\phi^*(\bar{k}_f)G_{mn}(\eta^-)N_n + |\delta\phi(\bar{k}_f)|^2 N_m G_{mn}(\eta^-)N_n\right]\right\rangle dE$$

(3.6.18)

where $k_{f\gamma} = \hat{e}_\gamma.\bar{k}_f$

Equation (3.6.18) clearly shows that to average $\sigma(\omega)$ we must average the following quantities :

(1) $\quad |\phi_B(\bar{k}_f)|^2 G_{mn}(\bar{\eta})$

(2) $\quad \phi_B^*(\bar{k}_f)\delta\phi(\bar{k}_f)N_m G_{mn}(\eta^-)$

(3) $\quad \phi_B(\bar{k}_f)\delta\phi^*(\bar{k}_f)G_{mn}(\eta^-)N_n$ (3.6.19)

(4) $\quad |\delta\phi(\bar{k}_f)|^2 N_m G_{mn}(\eta^-)N_n.$

The factors $k_{f\gamma}^2$ and $e^{i\bar{k}_f.(\bar{r}_n-\bar{r}_m)}$ are randomness independent.

The averaging will be done using the Augmented Space formalism. Let us first write the averages of above quantities in the Augmented

Space with site-configuration state representation :

(1) $$\left\langle |\phi_B(\bar{k}_f)|^2 G_{mn}(\eta^-) \right\rangle = |\phi_B(\bar{k}_f)|^2 \left[G_{mn}(\eta^-)\right]_{av}$$

$$= |\phi_B(\bar{k}_f)|^2 \langle mf | \tilde{\underline{G}} | nf \rangle$$

(2) $$\left\langle \phi_B^*(\bar{k}_f)\delta\phi(\bar{k}_f) N_m G_{mn}(\eta^-) \right\rangle = \phi_B^*(\bar{k}_f)\delta\phi(\bar{k}_f) \left[N_m G_{mn}(\eta^-)\right]_{av.}$$

$$= \phi_B^*(\bar{k}_f)\delta\phi(\bar{k}_f) \langle mf | \underline{M}^m \otimes \tilde{\underline{G}} | nf \rangle \qquad (3.6.20)$$

(3) $$\left\langle \phi_B(\bar{k}_f)\delta\phi^*(\bar{k}_f) G_{mn}(\eta^-) N_n \right\rangle = \phi_B(\bar{k}_f)\delta\phi^*(\bar{k}_f) \left[G_{mn}(\eta^-) N_n\right]_{av.}$$

$$= \phi_B(\bar{k}_f)\delta\phi^*(\bar{k}_f) \langle mf | \tilde{\underline{G}} \otimes \underline{M}^n | nf \rangle$$

(4) $$\left\langle \langle |\delta\phi(\bar{k}_f)|^2 N_m G_{mn}(\eta^-) N_n \right\rangle = |\delta\phi(\bar{k}_f)|^2 \left[N_m G_{mn}(\eta^-) N_n\right]_{av.}$$

$$|\delta\phi(\bar{k}_f)|^2 \langle mf | \underline{M}^m \otimes \tilde{\underline{G}} \otimes \underline{M}^n | nf \rangle$$

We shall now evaluate the above quantities using the representation of $\underline{M}^n$ in configuration space ϕ^m, given by the relation (3.3.32). Therefore :

$$\langle mf | \underline{M}^m \otimes \tilde{\underline{G}} | nf \rangle =$$

$$\langle mf | \left[c\, P^m_{\gamma_o} + (1-c)\, P^m_{\gamma_1} + \sqrt{c(1-c)} \left[T^m_{\gamma_o \gamma_1} + T^m_{\gamma_1 \gamma_o} \right] \right] \otimes \tilde{\underline{G}} | mf \rangle .$$

Here we have used the notation γ^m_o for $|f^m_o\rangle$ and γ^m_1 for $|f^m_1\rangle$ in the configuration space ϕ^m.

$$P_{\gamma_o^m} = |f_o^m\rangle\langle f_o^m| \qquad \text{and}$$

$$T_{\gamma_o^m \gamma_1^m} = |f_o^m\rangle\langle f_1^m|. \quad \text{Therefore :}$$

$$\langle mf|\underline{M}^m \otimes \tilde{\underline{G}}|nf\rangle = c\langle mf|\tilde{\underline{G}}|nf\rangle + \sqrt{c(1-c)}\,\langle mf_m|\tilde{\underline{G}}|nf\rangle$$

$$\langle mf|\tilde{\underline{G}} \otimes \underline{M}^n|nf\rangle = \langle mf|\tilde{\underline{G}} \otimes \Big[cP_{\gamma_o^n} + (1-c)P_{\gamma_1^n} + \sqrt{c(1-c)}\,\Big[T_{\gamma_o^n\gamma_1^n} + T_{\gamma_1^n\gamma_o^n}\Big]\Big]\,|nf\rangle$$

$$= c\langle mf|\tilde{\underline{G}}|nf\rangle + \sqrt{c(1-c)}\,\langle mf|\tilde{\underline{G}}|nf_n\rangle$$

and

$$\langle mf|\underline{M}^m \otimes \tilde{\underline{G}} \otimes \underline{M}^n|nf\rangle = \langle mf|\Big[c\,P_{\gamma_o^m} + (1-c)\,P_{\gamma_1^m} + \sqrt{c(1-c)}\Big[T_{\gamma_o^m\gamma_1^m} + T_{\gamma_1^m\gamma_o^m}\Big]\Big]\,\tilde{\underline{G}} \otimes \Big[c\,P_{\gamma_o^n} + (1-c)\,P_{\gamma_1^n} + \sqrt{c(1-c)}\Big[T_{\gamma_o^n\gamma_1^n} + T_{\gamma_1^n\gamma_o^n}\Big]\Big]\,|nf\rangle$$

$$= \Big[c\,\langle mf| + \sqrt{c(1-c)}\,\langle mf_m|\Big]\,\tilde{\underline{G}}\,\Big[c|nf\rangle + \sqrt{c(1-c)}\,|nf_n\rangle\Big]$$

$$= c^2\langle mf|\tilde{\underline{G}}|nf\rangle + c\sqrt{c(1-c)}\langle mf_m|\tilde{\underline{G}}|nf\rangle + c\sqrt{c(1-c)}\langle mf|\tilde{\underline{G}}|nf_n\rangle + c(1-c)\,\langle mf_m|\tilde{\underline{G}}|nf_n\rangle.$$

Thus the expressions (3.6.20) now become :

(1) $\quad |\phi_B(\bar{k}_f)|^2\langle mf|\tilde{\underline{G}}|nf\rangle$

(2) $\quad \phi_B^*(\bar{k}_f)\delta\phi(\bar{k}_f)\Big[c\langle mf|\tilde{\underline{G}}|nf\rangle + \sqrt{c(1-c)}\langle mf_m|\tilde{\underline{G}}|nf\rangle\Big]$

(3) $\quad \phi_B(\bar{k}_f)\delta\phi^*(\bar{k}_f)\Big[c\langle mf|\tilde{\underline{G}}|nf\rangle + \sqrt{c(1-c)}\langle mf|\tilde{\underline{G}}|nf_n\rangle\Big]$ $\qquad$ (3.7.21)

(4) $$|\delta\phi(\bar{k}_f)|^2\Big[c^2\langle mf|\tilde{\underline{G}}|nf\rangle + c\sqrt{c(1-c)}\,\langle mf_m|\underline{G}|nf\rangle + c\sqrt{c(1-c)}\,\langle mf|\tilde{\underline{G}}|nf_n\rangle + c(1-c)\langle mf_m|\tilde{\underline{G}}|nf_n\rangle\Big].$$

Therefore, after taking together the above expressions(3.7.21), we get

$$\Big[|\phi_B|^2 + c\,\phi_B^*\delta\phi + c\,\phi_B\delta\phi^* + c^2|\delta\phi|^2\Big]\langle mf|\tilde{\underline{G}}|nf\rangle$$

$$+\Big[\sqrt{c(1-c)}\,\phi_B^*\delta\phi + c\sqrt{c(1-c)}\,|\delta\phi|^2\Big]\langle mf_m|\tilde{\underline{G}}||nf\rangle$$

$$+\Big[\sqrt{c(1-c)}\,\phi_B\delta\phi^* + c\sqrt{c(1-c)}\,|\delta\phi|^2\Big]\langle mf|\tilde{\underline{G}}|nf_n\rangle +$$

$$c(1-c)\,|\delta\phi|^2\,\langle mf_m|\tilde{\underline{G}}|nf_n\rangle$$

$$= \langle mf|\tilde{\underline{G}}|nf\rangle\Big[\phi_B\phi_B^* + c\phi_B^*\phi_A - c\phi_B^*\phi_B + c\phi_B\phi_A^* - c\phi_B\phi_B^* + c^2\phi_A\phi_A^* + c^2\phi_B\phi_B^* - c^2\phi_A\phi_B^* - c^2\phi_A^*\phi_B\Big]$$

$$+\langle mf_m|\tilde{\underline{G}}|nf\rangle\Big[\sqrt{c(1-c)}\,\phi_B^*\phi_A - \sqrt{c(1-c)}\,\phi_B^*\phi_B + c\sqrt{c(1-c)}\,\phi_A\phi_A^* + c\sqrt{c(1-c)}\,\phi_B\phi_B^* - c\sqrt{c(1-c)}\,\phi_A\phi_B^* - c\sqrt{c(1-c)}\,\phi_A^*\phi_B\Big]$$

$$+\langle mf|\tilde{\underline{G}}|nf_n\rangle\Big[\sqrt{c(1-c)}\,\phi_B\phi_A^* - \sqrt{c(1-c)}\,\phi_B\phi_B^* + c\sqrt{c(1-c)}\,\phi_A\phi_A^* + c\sqrt{c(1-c)}\,\phi_B\phi_B^* - c\sqrt{c(1-c)}\,\phi_A\phi_B^* - c\sqrt{c(1-c)}\,\phi_A^*\phi_B\Big]$$

$$+\langle mf_m|\tilde{\underline{G}}|mf_n\rangle\Big[c(1-c)\delta\phi\delta\phi^*\Big]$$

$$= \langle mf|\tilde{\underline{G}}|nf\rangle\Big[\phi_B\phi_B^*(1-2c+c^2) + \phi_A\phi_A^*\,c^2 + \phi_A\phi_B^*(c-c^2) + \phi_A^*\phi_B(c-c^2)\Big]$$

$$+\langle mf_m|\tilde{\underline{G}}|nf\rangle\Big[\phi_A\phi_B^*\big(\sqrt{c(1-c)} - c\sqrt{c(1-c)}\big) - \phi_B\phi_B^*\big(\sqrt{c(1-c)} -$$

$$c\sqrt{c(1-c)}\Big) + c\sqrt{c(1-c)}\phi_A\phi_A^* - c\sqrt{c(1-c)}\phi_A^*\phi_B \Big] +$$

$$+ \langle mf|\tilde{\underline{G}}|nf_n\rangle \Big[c\sqrt{c(1-c)}\phi_A\phi_A^* - \phi_B\phi_B^*\big(\sqrt{c(1-c)} - c\sqrt{c(1-c)}\big)$$

$$- c\sqrt{c(1-c)}\phi_A\phi_B^* + \phi_A^*\phi_B\big(\sqrt{c(1-c)} - c\sqrt{c(1-c)}\big) \Big]$$

$$+ \langle mf_m|\tilde{\underline{G}}|nf_n\rangle \Big[c(1-c)\delta\phi\delta\phi^*\Big]$$

$$= \langle mf|\tilde{\underline{G}}|nf\rangle \Big[\phi_B\phi_B^*(1-c)^2 + \phi_A\phi_A^*c^2 + \phi_A\phi_B^*c(1-c) + \phi_A^*\phi_B\, c(1-c)\Big]$$

$$+ \langle mf_m|\tilde{\underline{G}}|nf\rangle \Big[\sqrt{c(1-c)}\ \Big[\phi_A\phi_B^*(1-c) - \phi_B\phi_B^*(1-c) + \phi_A\phi_A^*(c) -$$

$$\phi_A^*\phi_B(c)\Big]\Big]$$

$$+ \langle mf|\tilde{\underline{G}}|nf_n\rangle \Big[\sqrt{c(1-c)}\Big[\phi_A\phi_A^*c - \phi_B\phi_B^*(1-c) - \phi_A\phi_B^*c + \phi_A^*\phi_B(1-c)\Big]\Big]$$

$$+ \langle mf_m|\tilde{\underline{G}}|nf_n\Big[c(1-c)\delta\phi\delta\phi^*\Big]$$

$$= \langle mf|\tilde{\underline{G}}|nf\rangle \Big[(1-c)\phi_B^*((1-c)\phi_B+c\phi_A) + c\,\phi_A^*(c\,\phi_A+(1-c)\phi_B)\Big]$$
$$+\langle mf_m|\tilde{\underline{G}}|nf\rangle\ (c(1-c))^{1/2}\Big[(1-c)\phi_B^*\,(\phi_A-\phi_B) + c\,\phi_A^*(\phi_A-\phi_B)\Big]$$
$$+\langle mf|\tilde{\underline{G}}|nf_n\rangle(c(1-c))^{1/2}\Big[(1-c)\phi_B(\phi_A^*-\phi_B^*) + c\phi_A(\phi_A^*-\phi_B^*)\Big]$$
$$+\langle mf_m|\tilde{\underline{G}}|nf_n\rangle c(1-c)\delta\phi\delta\phi^*$$

$$= \langle mf|\tilde{\underline{G}}|nf\rangle \Big[(c\phi_A+(1-c)\phi_B)(c\phi_A^*+(1-c)\phi_B^*)\Big]$$

$$+\langle mf_m|\tilde{\underline{G}}|nf\rangle\ (c(1-c))^{1/2}\Big[(\phi_A-\phi_B)(c\phi_A^*+(1-c)\phi_B^*)\Big]$$

$$+ \langle mf|\tilde{\underline{G}}|nf_n\rangle (c(1-c))^{1/2} \left[(\phi_A^* - \phi_B^*)\{c\phi_A + (1-c)\phi_B\}\right]$$

$$+ \langle mf_m|\tilde{\underline{G}}|nf_n\rangle c(1-c)[\delta\phi\delta\phi^*].$$

But $c\phi_A + (1-c)\phi_B = \bar{\phi}$

$c\phi_A^* + (1-c)\phi_B^* = \bar{\phi}^*$

$\phi_A - \phi_B = \delta\phi$ (3.6.22)

$\phi_A^* - \phi_B^* = \delta\phi^*$ and

$\langle mf|\tilde{\underline{G}}|nf\rangle = [G_{mn}]_{av.}$.

Thus the sum of the four quantities (3.6.19) becomes :

$$S \equiv [G_{mn}]_{av.}[\bar{\phi}.\bar{\phi}^*] + \langle mf_m|\tilde{\underline{G}}|nf\rangle (c(1-c))^{1/2}[\delta\phi\bar{\phi}^*]$$

$$+ \langle mf|\tilde{\underline{G}}|nf_n\rangle (c(1-c))^{1/2}[\delta\phi^*\bar{\phi}]$$

$$+ \langle mf_m|\tilde{\underline{G}}|nf_n\rangle c(1-c)[\delta\phi\delta\phi^*] \quad (3.6.23)$$

where the sum of the four quantities in equation (3.6.19) is denoted by S.

Since the Augmented space is homogeneous therefore by using the symmetry of the Augmented space, we have :

$$\langle mf_m|\tilde{\underline{G}}|nf\rangle = \langle mf|\tilde{\underline{G}}|nf_n\rangle \quad (3.6.24)$$

Then,

$$S = [G_{mn}]_{av.} |\bar{\phi}|^2 + \langle mf_m|\tilde{\underline{G}}|nf\rangle (c(1-c))^{1/2}[\delta\phi\bar{\phi}^* + \delta\phi^*\bar{\phi}]$$

$$+ \langle mf_m|\tilde{\underline{G}}|nf_n\rangle c(1-c)|\delta\phi|^2$$

But, $\delta\phi\bar{\phi}^* + \delta\phi^*\bar{\phi} = 2\,\mathrm{Re}\,(\bar{\phi}^*\delta\phi)$, therefore,

$$S \equiv [G_{mn}]_{av.} |\bar{\phi}|^2 + \langle mf_m|\tilde{\underline{G}}|nf\rangle (c(1-c))^{1/2}\, 2\,\mathrm{Re}(\bar{\phi}^*\delta\phi)$$

$$+ \langle mf_m|\tilde{\underline{G}}|nf_n\rangle c(1-c)|\delta\phi|^2 \qquad (3.6.25)$$

Let us now evaluate $\langle mf_m|\tilde{\underline{G}}|nf\rangle$ and $\langle mf_m|\tilde{\underline{G}}|nf_n\rangle$ using graphs. We shall use different notation now that is

$$\langle mf_m|\tilde{\underline{G}}|nf\rangle = \tilde{G}_{mf_m,nf}$$

$$\langle mf_m|\tilde{\underline{G}}|nf_n\rangle = \tilde{G}_{mf_m,nf_n}$$

In graph $\tilde{G}_{mf_m,nf}$ is given by

$$\tilde{G}_{mf_m,nf} = \sum_{P\in S_{mf_m,nf}} k(P) \qquad (3.6.26)$$

where $S_{mf_m,nf}$ denotes all the self-avoiding paths between vertices mf_m and nf. But $P_{mf_m,nf}$ can be written as (see figure 3.6.1)

$$P_{mf_m,nf} = P_{mf,nf}\, P^{mf}_{mf_m,mf_m}$$

where $\sqrt{c(1-c)}$ is the contribution associated with the link l_{mf,mf_m} and

$\delta\varepsilon = \varepsilon_A - \varepsilon_B$, ε_A and ε_B are the site energies corresponding to A and B atoms respectively.

Therefore $\tilde{G}_{mf_m,nf}$ can now be written as

$$\tilde{G}_{mf_m,nf} = \tilde{G}_{mf,nf}\, k\left(P^{mf}_{mf_m,mf_m}\right)$$

But $$k\left(P^{mf}_{mf_m,mf_m}\right) = \sqrt{c(1-c)}\ \delta\varepsilon\ \tilde{G}^{mf}_{mf_m,mf_m}.$$

Hence

$$\tilde{G}_{mf_m,nf} = \tilde{G}_{mf,nf}\ \sqrt{c(1-c)}\ \delta\varepsilon\ \tilde{G}^{mf}_{mf_m,mf_m}$$

$$= \left[G_{mn}\right]_{av.}\ \sqrt{c(1-c)}\ \delta\varepsilon\ \tilde{G}^{mf}_{mf_m,mf_m} \qquad (3.6.27).$$

Similarly, we evaluate $\tilde{G}_{mf_m,nf_n}$ (see figure (3.6.2)), i.e.,

$$\tilde{G}_{mf_m,nf_n} = \sum k(P_{mf_m,nf_n})$$

$$P_{mf_m,nf_n} = P^{mf}_{mf_m,mf_m}\ P_{mf,nf}\ P^{nf}_{nf_n,nf_n}$$

So, $$\tilde{G}_{mf_m,nf_n} = \sqrt{c(1-c)}\ \delta\varepsilon\ \tilde{G}^{mf}_{mf_m,mf_m}\ \tilde{G}_{mf,nf}\ \tilde{G}^{nf}_{nf_n,nf_n}\ \sqrt{c(1-c)}\delta\varepsilon$$

(3.6.28)

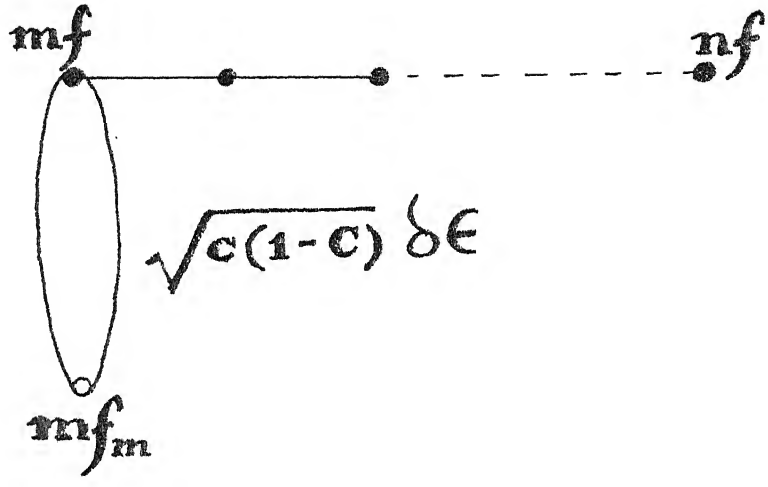

Figure 3.6.1 Graphical representation of the path $P_{mf_m,nf}$ in Augmented Space

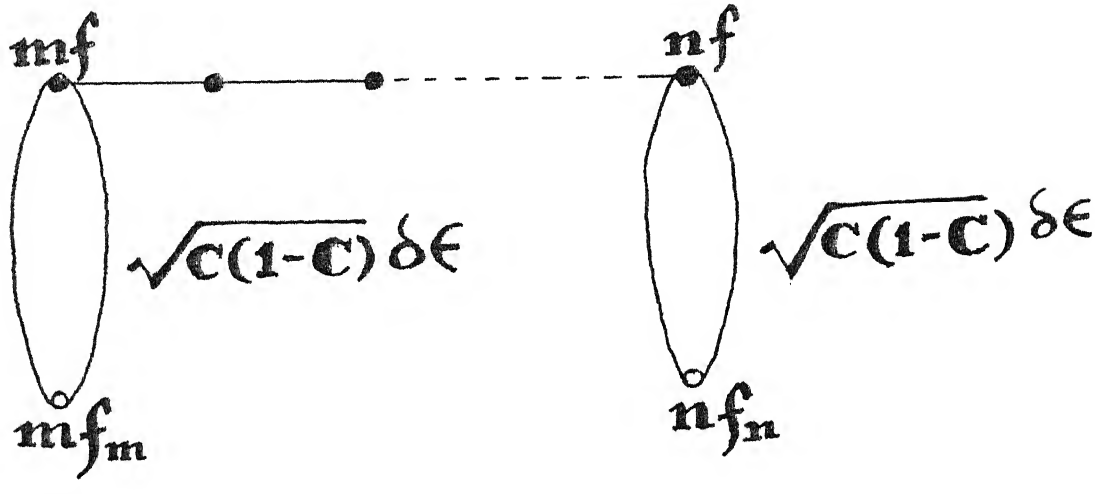

Figure 3.6.2 Graphical representation of the path P_{mf_m,nf_n} in Augmented Space

$$= [G_{mn}]_{av.} \frac{\Sigma_o}{(\delta\varepsilon\sqrt{c(1-c)})}$$

Putting these back into equation (3.6.25), we get :

$$S \equiv [G_{mn}]_{av.} |\bar{\phi}|^2 + [G_{mn}]_{av.} \frac{\Sigma_o}{\delta\varepsilon\sqrt{c(1-c)}} \sqrt{c(1-c)}$$

$$2Re\,(\bar{\phi}^* \delta\phi) + [G_{mn}]_{av.} \frac{\Sigma_o^2}{(\delta\varepsilon\sqrt{c(1-c)})^2} c(1-c)|\delta\phi|^2$$

$$= [G_{mn}]_{av.} \left[|\bar{\phi}|^2 + \frac{\Sigma_o}{\delta\varepsilon} 2Re\,(\bar{\phi}^* \delta\phi) + \frac{\Sigma_o^2}{\delta\varepsilon^2} |\delta\phi|^2 \right]$$

$$= [G_{mn}]_{av.} \left[|\bar{\phi} + \frac{\Sigma_o}{\delta\varepsilon} \delta\phi|^2 \right]$$

Calling $\bar{\phi} + \frac{\Sigma_2}{\delta\varepsilon} \delta\phi$ by ϕ_{eff}, we finally get

$$S = [G_{mn}]_{av.} |\phi_{eff}|^2 \qquad (3.6.30)$$

Therefore the configuration averaged optical conductivity for random binary semiconducting alloys is now given by :

$$\langle \sigma(\omega) \rangle = -\frac{e^2\hbar^2}{2m^{*2}} \frac{1}{\omega} \mathcal{I}m \sum\sum\sum_{\gamma mn} \delta_{mn} \int_0^{E_o} n(E_f)\, k_{f\gamma}^2\, e^{i\bar{k}_f.(\bar{r}_n - \bar{r}_m)}$$

$$[G_{mn}]_{av.} |\phi_{eff.}|^2 dE$$

$$= \frac{e^2\hbar^2\pi}{2m^{*2}} \frac{1}{\omega} \sum_{\gamma} \int_0^{E_o} n_f(E)\, k_{f\gamma}^2 |\phi_{eff}|^2 \left[-\frac{1}{\pi} \mathcal{I}m \sum_m \sum_n \delta_{mn}\, e^{i\bar{k}_f.(\bar{r}_n - \bar{r}_m)}\, [G_{mn}]_{av.} \right] dE$$

$$= \frac{\pi e^2\hbar^2}{2m^{*2}} \frac{1}{\omega} \int_0^{E_o} \left(\sum_{\gamma} k_{f\gamma}^2\right) |\phi_{eff}|^2\, n_f(E) \left[-\frac{1}{\pi} \mathcal{I}m \sum_m [G_{mm}]_{av.} \right] dE$$

Therefore

$$\langle \sigma(\omega) \rangle = \frac{\pi e^2\hbar^2}{2m^{*2}} \frac{1}{\omega} \int_0^{E_o} \left(\sum_{\gamma} k_{f\gamma}^2\right) |\phi_{eff}|^2 n_f(E) \langle n_i(E-\hbar\omega) \rangle dE$$

(3.6.31)

Let us now evaluate $\sum_{\gamma} k_{f\gamma}^2$, where $k_{f\gamma} = \bar{k}_f . \hat{e}_{\gamma}$. Choose the direction of $\bar{k}_f$ along the $\hat{z}$-direction (see figure (3.6.3)), $\hat{e}_{\gamma}$ being the direction of incoming photon. Therefore, $k_{f\gamma} = k \cos\theta$ or, $k_{f\gamma}^2 = k^2 \cos^2\theta$.

For an isotropic wave we have $\sum_{\gamma} = \int d^3\Omega_o$ where, Ω_o is the solid angle subtended at the origin. So the sum $= \int d(\cos\theta)\, d\phi$.

Therefore

$$\sum_{\gamma} k_{f\gamma}^2 = \int_{-1}^{1} \int_{0}^{2\pi} k_f^2 \cos^2\theta \, d(\cos\theta) \, d\phi$$

$$= 2\pi k_f^2 \int_{-1}^{1} \cos^2\theta \, d\cos\theta$$

$$= \frac{4\pi}{3} k_f^2.$$

Putting back this value in equation (3.6.31) we get

$$\langle \sigma(\omega) \rangle = \frac{\pi e^2 \hbar^2}{2m^{*2}} \frac{1}{\omega} \int_{0}^{E_o} \frac{4}{3} \pi k_f^2 |\phi_{eff}|^2 n_f(E) \langle n_i(E-\hbar\omega) \rangle \, dE$$

$$= \frac{2\pi^2 e^2 \hbar^2}{3m^{*2}} \frac{1}{\omega} \int_{0}^{E_o} k_f^2 |\phi_{eff}|^2 n_f(E) \langle n_i(E-\hbar\omega) \rangle dE$$

But k_f is related to E through $E(k_f) = \frac{\hbar^2 k_f^2}{2m^*}$, therefore $k_f^2 = \frac{2Em^*}{\hbar^2}$.

Thus finally we have the expression for average optical conductivity for random binary semiconducting alloys as :

$$\langle \sigma(\omega) \rangle = \frac{4\pi^2 e^2}{3m^*} \frac{1}{\omega} \int_{0}^{E_o} E |\phi_{eff}|^2 n_f(E) \langle n_i(E-\hbar\omega) \rangle dE$$

$$= \frac{4\pi^2 e^2}{3m^*} \frac{1}{\omega} \int_{0}^{E_o} |g_{eff}(E)|^2 \, n_f(E) \, \langle n_i(E-\hbar\omega) \rangle \, dE \qquad (3.6.32)$$

where the square of the optical matrix element $g_{eff}(E)$ is given by $E^{1/2}|\phi_{eff}|$

3.7 APPLICATION TO A MODEL SYSTEM :

In this section we shall apply the formulation of optical properties of random semiconducting alloys, described in § 4.6, to a model system. For our model we shall choose the following parameters :

$\varepsilon_A = -5.0$;

$\varepsilon_B = -9.5$;

$V = -1.0$ and

$c = 0.5$ and 0.2

where ε_A and ε_B are the site energies for A and B atoms respectively, V is the overlap integral (no off-diagonal disorder) and c is the concentration of A species.

The Hamiltonian for the system, in Tight-binding basis, is given by the equation (3.2.8), where $\varepsilon_i = \varepsilon_A$ or ε_B and $\langle V_{ij} \rangle = V$. The valence band density of states for the system is calculated using 1CPA and 2CPA. For our 1CPA calculation we shall choose rounded density of states (shown in figure 3.7.1):

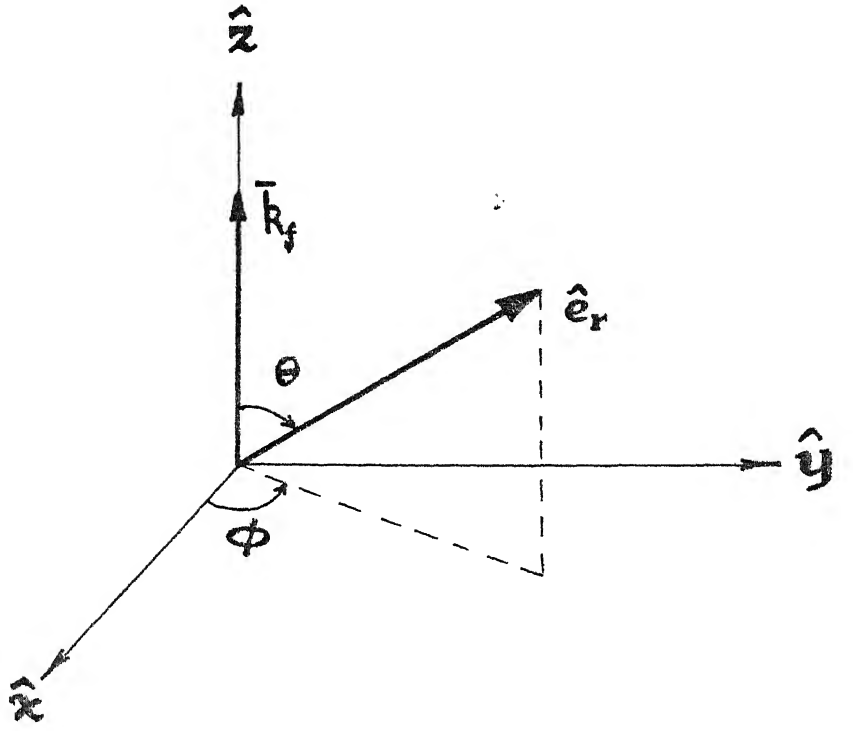

Figure 3.6.3 Direction of polarization of electric field vector, e_γ, with respect to the direction of momentum of the electron, $\bar{k}_f$.

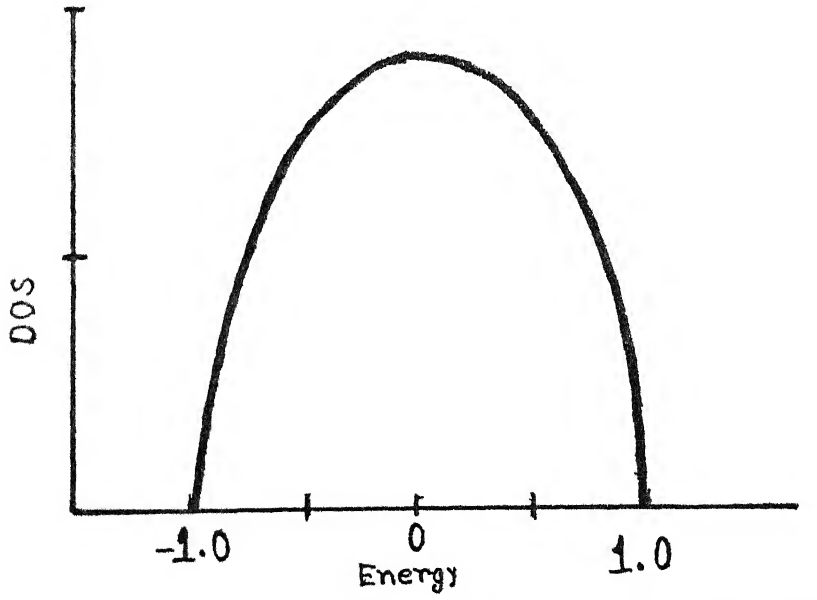

Figure 3.7.1 Model rounded Density of states

$$n_o(E_i) = \begin{cases} \frac{2}{\pi}(1-E^2)^{1/2} & \text{if } |E| < 1 \\ 0 & \text{if } |E| > 1 \end{cases} \qquad (3.7.1$$

as the initial choice for <G> appeared in the 1CPA equation (3.2.22). We then calculate self-energy $\Sigma_o(E)$ using the 1CPA equation (3.2.22) and then new <G> self consistently. The valence band density of states $\langle n_i(E_i)\rangle$ for c = 0.5 and c = 0.2 are shown in figures(3.7.2) and (3.7.3) respectively.

The 2CPA calculation of $\langle n_i(E_i)\rangle$ is done by choosing the initial choice for Σ_o as calculated within 1CPA and Σ_1 equal to $\langle V_{ij}\rangle$. We then calculate new Σ_o, Σ_1 and <G> self-consistently using equations (3.5.9), (3.5.10), (3.5.17) and (3.5.18). The averaged density of states $\langle n_i(E_i)\rangle$ as calculated within 2CPA for c = 0.5 and c = 0.2 are shown in figures (3.7.2) and (3.7.3) respectively.

There are some structures seen in the impurity band in the case of 2CPA calculations of density of states. These two peaked structures are due to bonding-antibonding states of the AB cluster. These structures were also seen and extensively discussed in the earlier works for both model calculations (Kumar et.al. 1982) and for Cu-Ni alloys (Thakur et. al. 1987).

We shall now calculate the optical conductivity, $\sigma(\omega)$, and other related response functions. The optical conductivity is given by the equation (3.6.32)

The conduction band density of states, $n_f(E)$, (for free electron like) is given by

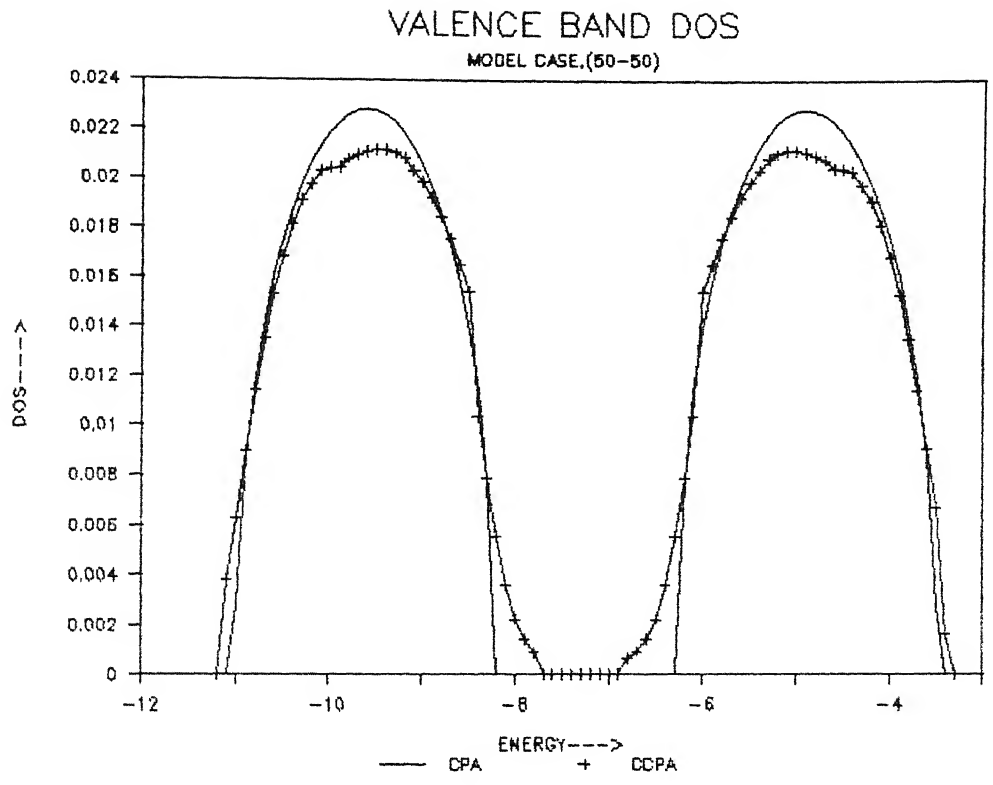

Figure 3.7.2

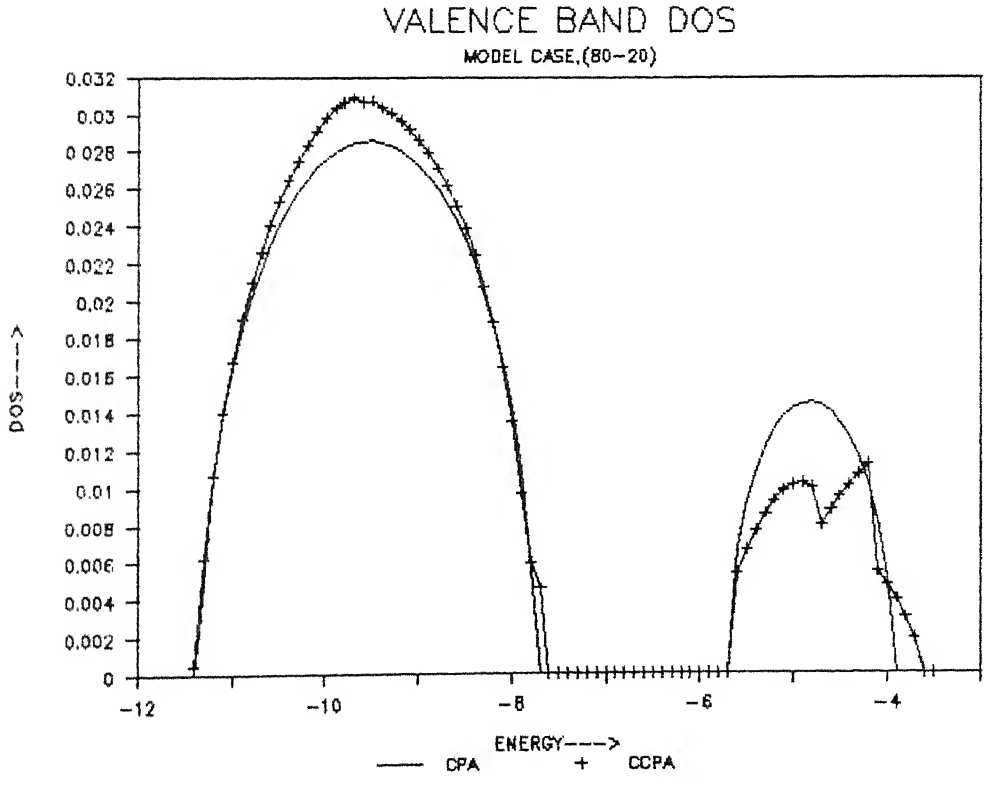

Figure 3.7.3

$$n_f(E) = \frac{(2m^*)^{3/2}}{(2\pi)^2 \hbar^3} \sqrt{E}.$$

If we choose units such that $\hbar = e = m^* = 1$, we have

$$\langle \sigma(\omega) \rangle = \frac{4\pi^2}{3} \frac{1}{\omega} \int_0^{E_o} E |\phi_{eff}|^2 \frac{2^{3/2}}{4\pi^2} \sqrt{E} \langle n_i(E-\hbar\omega) \rangle dE$$

$$= \frac{2^{3/2}}{3} \frac{1}{\omega} \int_0^{E_o} E |\phi_{eff}|^2 \sqrt{E} \langle n_i(E-\omega) \rangle dE \qquad (3.7.2)$$

From the conservation of energy we have

$$E_i + \omega = E.$$

Since $\langle n_i(E-\omega) \rangle$ is non-zero between the band edges $E_i^{min.}$ and $E_i^{max.}$ and zero outside the edges (see figure (3.7.1)), the integrand in the equation (3.7.2) is always zero outside the range between $E_i^{min.}$ and $E_o^{max.}$. If we change the variable from E to E_i, we get :

$$\langle \sigma(\omega) \rangle = \frac{2^{3/2}}{3} \frac{1}{\omega} \int_{E_i^{min.}}^{E_i^{max.}} (E_i+\omega) |\phi_{eff}|^2 \sqrt{E_i+\omega} \langle n_i(E_i) \rangle dE_i \qquad (3.7.3)$$

Let us now evaluate $|\phi_{eff}|^2$. ϕ_{eff} is given by

$$\phi_{eff}(E) = \bar{\phi}(E) + \frac{\Sigma_o(E_i)}{\delta\epsilon} \delta\phi$$

$$\bar{\phi} = c\, \phi_A(E) + (1-c)\, \phi_B(E) \qquad (3.7.4)$$

$$\delta\phi = \phi_A(E) - \phi_B(E) \text{ and}$$

$$\delta\varepsilon = \varepsilon_A - \varepsilon_B.$$

We shall choose $\phi_A(\bar{r})$ and $\phi_B(\bar{r})$ to be the wave functions (l=0) for a square well potential of width 'a' and depth $V_o^{A,B}$ (Schiff 1968).

$$\phi_A(\bar{r}) = \sqrt{\frac{\beta_A}{2\pi}} \frac{e^{-\beta_A r}}{r} \quad \text{and} \quad \phi_B(\bar{r}) = \sqrt{\frac{\beta_B}{2\pi}} \frac{e^{-\beta_B r}}{r}$$

where l is the angular momentum quantum number,

$$\beta_A = \frac{2m^*|E_A|}{\hbar^2} = (2|E_A|)^{1/2} \quad \text{and} \quad \beta_B = (2|E_B|)^{1/2}.$$

E_A and E_B are the eigenvalues of the respective atomic Hamiltonians. If we assume that the atomic potentials $V_o^{A,B}$ are not much afffected within the Winger-Seitz cell when the solid is formed, within the first approximation E_A and E_B may be taken as site energies ε_A and ε_B respectively. Thereore

$$\beta_A = (2|\varepsilon_A|)^{1/2} \text{ and } \beta_B = (2|\varepsilon_B|)^{1/2}.$$

The Fourier transform of $\phi_A(\bar{r})$ and $\phi_B(\bar{r})$ are respectively :

$$\phi_A(\bar{k}) = \frac{\sqrt{2\beta_A}}{k^2 + \beta_A^2} \text{ and } \phi_B(\bar{k}) = \frac{\sqrt{2\beta_B}}{k^2 + \beta_B^2} \qquad (3.7.5)$$

Now using the equation (3.7.3) together with the equations (3.7.4), (3.7.5) we calculate the valence band density of states $\langle n_i(E_i)\rangle$

and the self energy $\Sigma_o(E_i)$. We then calculate the optical conductivity for the model system. Then using the various relations among the response functions, described in chapter II, we calculate the other related response functions.

Figures (3.7.4) and (3.7.5) show the optical conductivity as a function of frequency of the incoming photon for the model case with concentration c=0.5 and calculated within the 1CPA and the 2CPA respectively. Figures (3.7.6) and (3.7.7) show the optical conductivity for the model case with c=0.2 and calculated within the 1CPA and the 2CPA respectively. Each of these figures clearly show the effects of disorder which arise mainly due to vertex correction associated with averaging of the kind of $\langle |g_{if\gamma}|^2 . n_i(E) \rangle$. The effect is seen in lower part of the frequency only which is expected because it is in this range of energy that $|g^{eff}_{if\gamma}(E)|^2$ has structures. In the higher frequency range the factor $1/\omega$ of the optical conductivity dominates over others making it decrease with frequency and washing out any disorder effect.

There are small double humps seen in the conductivity curve. These humps are the reflection of the double peak DOS structure and the structures in the square of the optical matrix element $|g_{if\gamma}|^2$. But these humps are much broadened because of convulation of the valence band density of states with the featureless conduction band DOS and relatively featureless optical matrix element. The effects of disorder in the case of c=0.5 is more prominent than the c=0.2 case. This is expected because in the earlier case the degree of disorder is stronger than the latter.

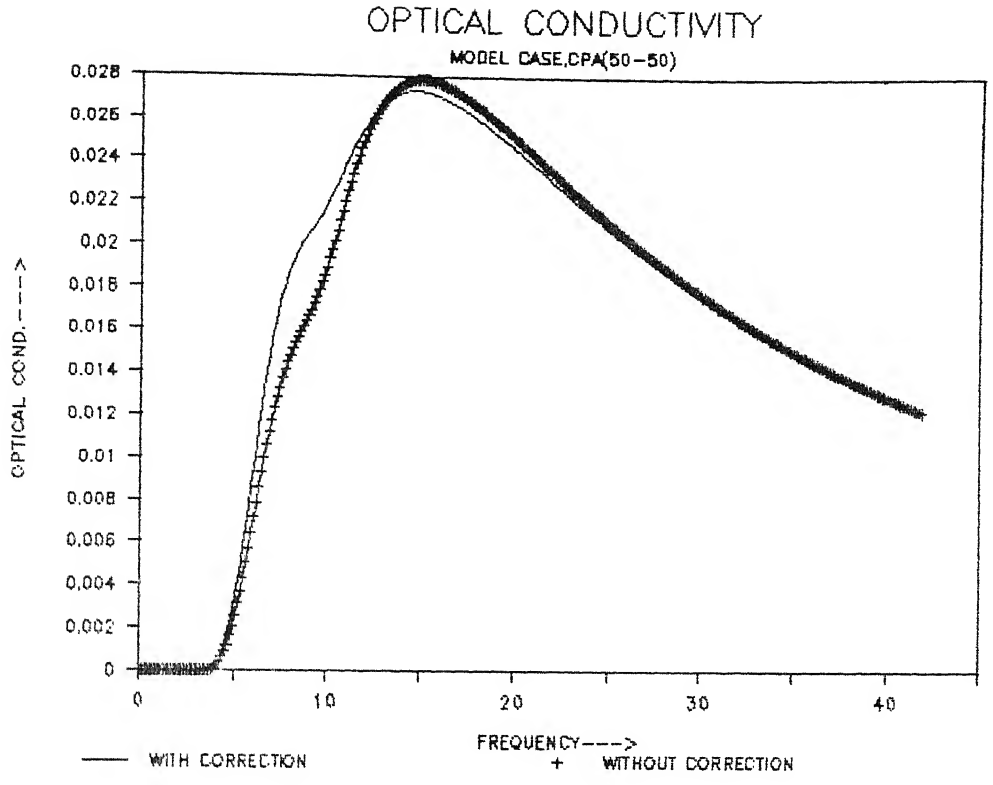

Figure 3.7.4

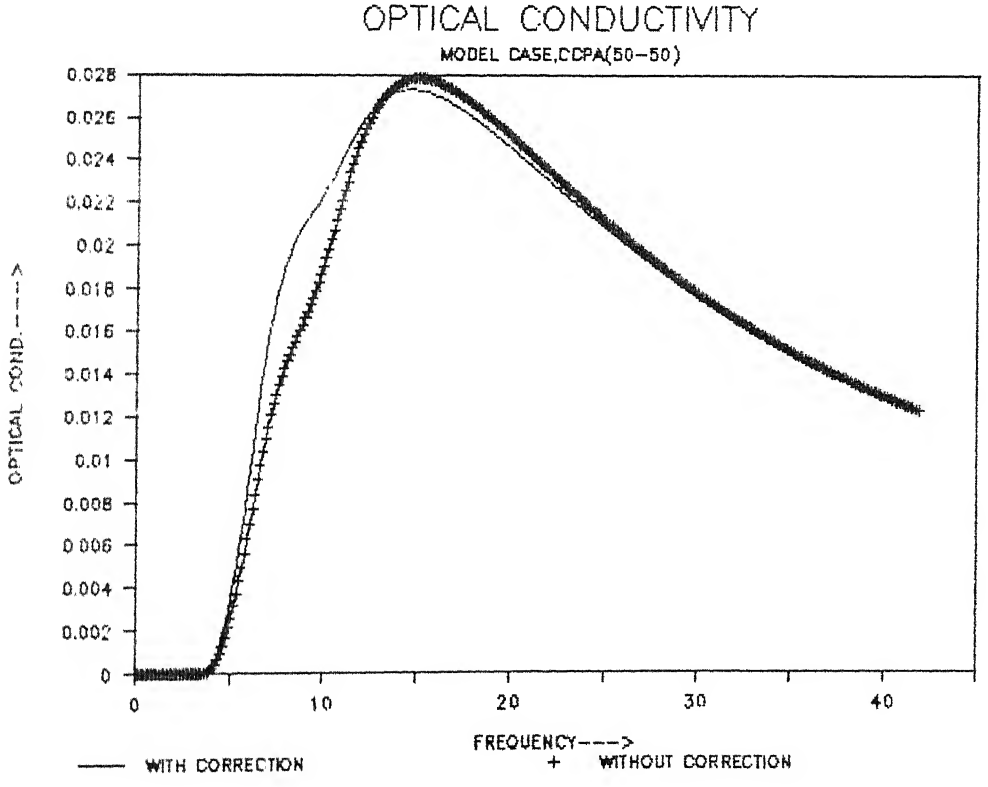

Figure 3.7.5

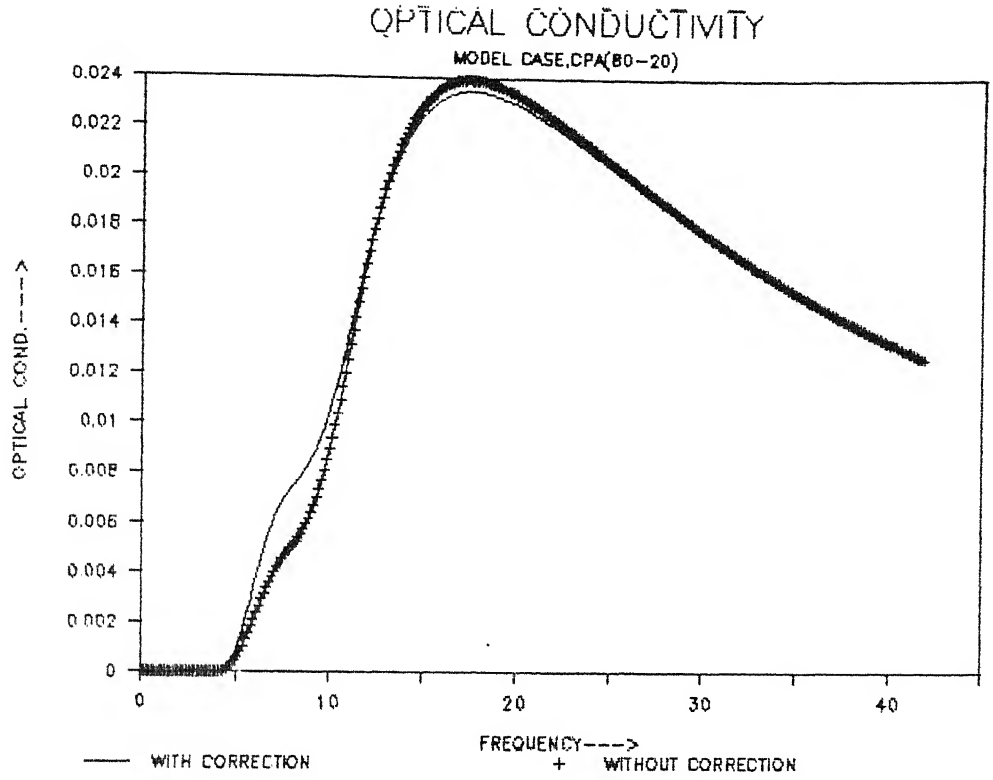

Figure 3.7.6

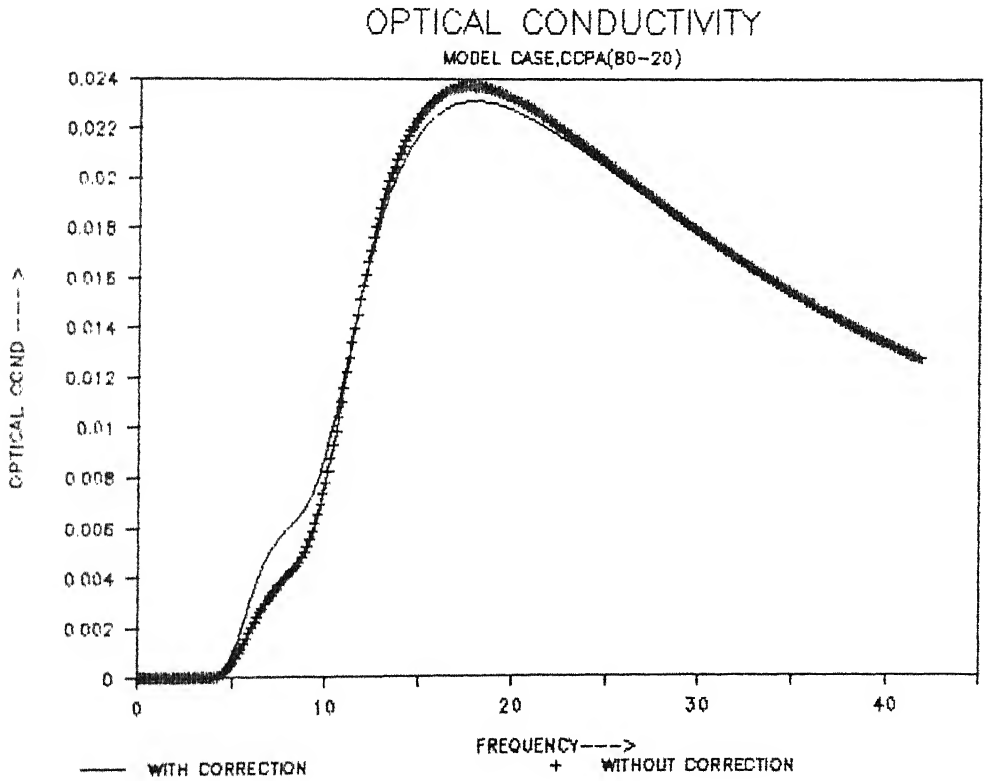

Figure 3.7.7

Figures (3.7.8) to (3.7.15) show the other related response functions like real part of the dielectric function (related to permitivity) , imaginary part of the dielectric function , refractive index and the absorption coefficient. Each of these figures shows the effects of disorder. The double hump structures are also reflected in the real part of complex dielectric function and the refractive index function.

These figures show that the 1CPA and the 2CPA results of optical conductivity and other related response functions do not differ much. They are almost the same. The structures which arise in the 2CPA DOS are not reflected in the conductivity because it is related to the integrated (convulated) density of states.

Figures (3.7.16) to (3.7.23) show the square of optical matrix element $|g_{if\gamma}|^2$ as a function of energy for different values of the concentration ,c, and the frequency of the incoming photon, ω for the 1CPA and the 2CPA calculations. Each of these figures shows that the $|g_{if\gamma}|^2$ depends on both , the energy and the disorder. The $|g_{if\gamma}|^2$ calculated within VCA has a weak dependence on energy . However , disorder effects lead to a stronger energy dependence of the optical matrix element . These figures show that the effects of disorder not only change the magnitude of $|g^{eff}_{if\gamma}|^2$ but also shows structures . These structures are more prominemt in the case of the 2CPA and c=0.5 . These are expected because in the case of CCPA the effects of cluster also come and for c=0.5 the disorder effect is more . The structures in $|g^{eff}_{if\gamma}|^2$ arise due to the self energy Σ_o , as the correction term is given by $(\Sigma_o/\delta\varepsilon)\delta\phi$. It is also clear that

because the self energy has sharp peak near the impurity band peak ,i.e. at E=-5.0 . This sharp structure is not reflected in the case when ω =4.62 because the transition takes place only from that portion of the valence band for which E_i=-4.62 to 0.0 , whereas in the case of ω =9.24 , the transition takes place also from the peak of the band.

Figures (3.7.24) to (3.7.31) show the product of valence band DOS and the square of the optical matrix element, $n_i(E_i)|g_{if\gamma}|^2$, as a function of energy, E, for different values of c and ω with the 1CPA and the 2CPA calculations . It is worthwhile to notice in these figures that , though the DOS for c=0.5 and c=0.2 are very different to each other , but when the DOS is multiplied by the square of the optical matrix element , it so happens that the product $\langle n_i(E_i)\rangle|g^{eff}_{if\gamma}(E)|^2$ look to be similar except slightly different in magnitudes . Since in an energy resolved photo emission experiment one essentially studies $\langle n_i(E_i)\rangle|g^{eff}_{if\gamma}|^2$ as a function of energy , therefore the results of such experiments do not reflect the joint DOS but very much modified by the square of the optical matrix element which arises due to energy and disorder dependence of $|g^{eff}_{if\gamma}(E)|^2$. Thus in order to get correct band structure from such experiments , one must factorize the square of the optical matrix element factor .

Though , as it has been seen above,the 2CPA calculation does not make much difference from the 1CPA calculation in the study of integrated response functions , but the results of the square of the optical matrix element show that the 2CPA result differs significantly from 1CPA result . Thus in the band structure calculations one must take into account the cluster effect.

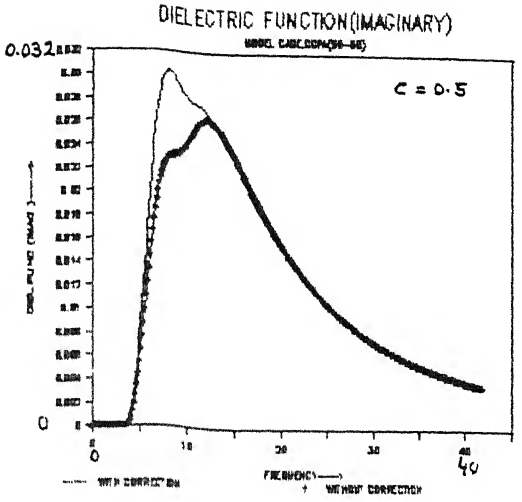

Figure 3.7.8

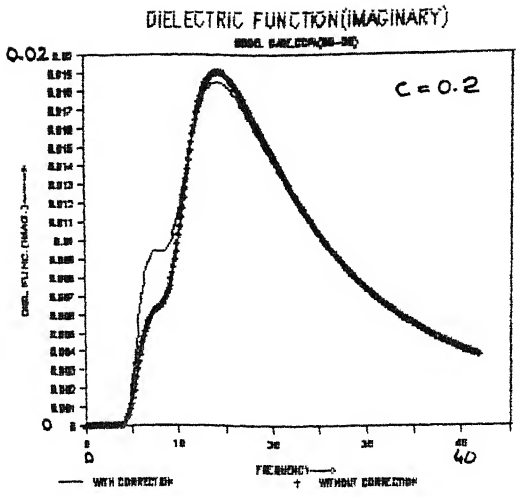

Figure 3.7.9

Imaginary part of the complex dielectric function as a function of frequency for the model case within 2CPA with c=0.5 & 0.2 respectively. — with correction
\+ without correction

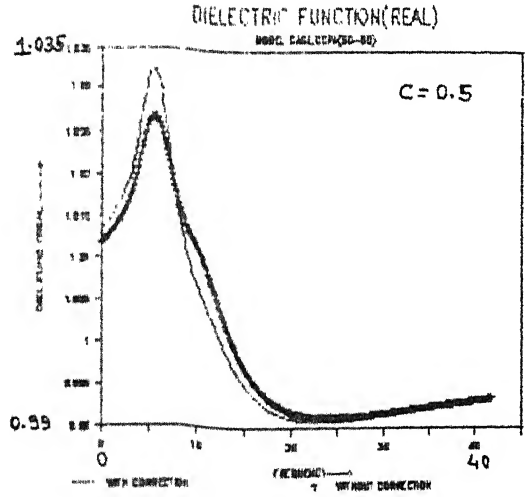

Figure 3.7.10

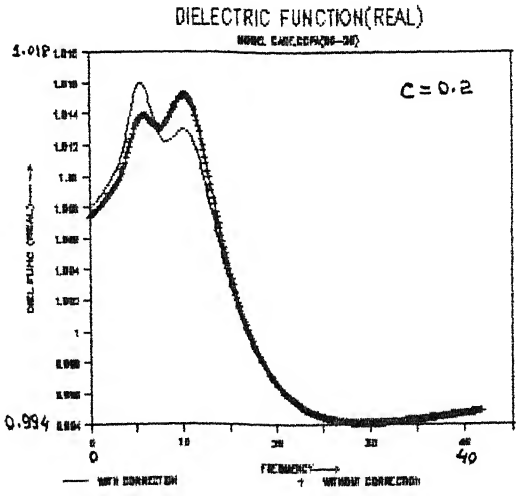

Figure 3.7.11

Real part of the complex dielectric function as a function of frequency for the model case within 2CPA with c=0.5 & 0.2 respectively.
— with correction
\+ without correction

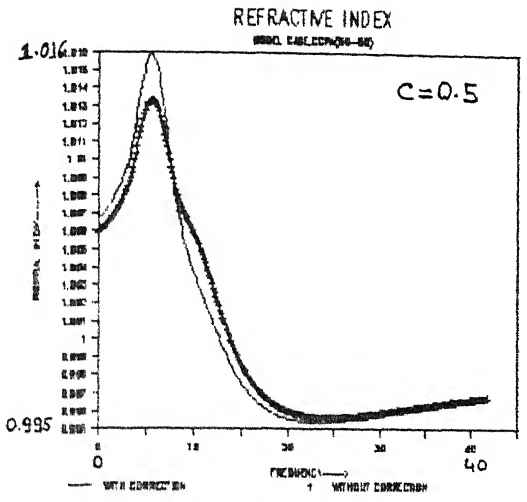

Figure 3.7.12

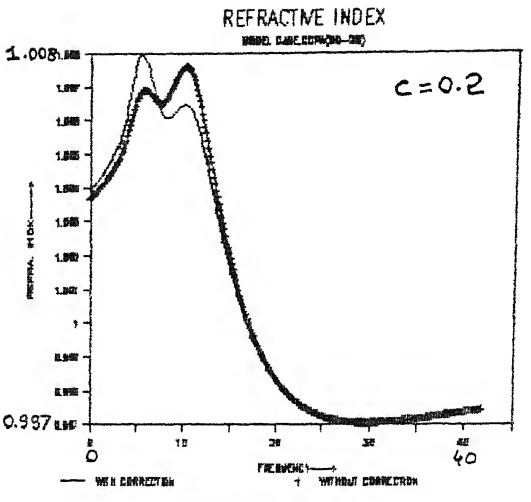

Figure 3.7.13

Refractive index function as a function of frequency for the model case within 2CPA with c=0.5 & 0.2 respectively.

— with correction
\+ without correction

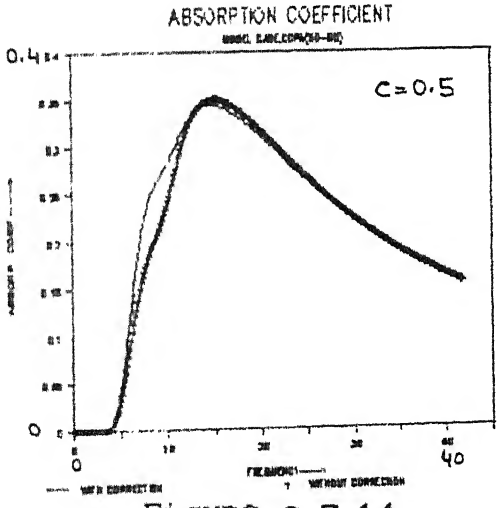

Figure 3.7.14

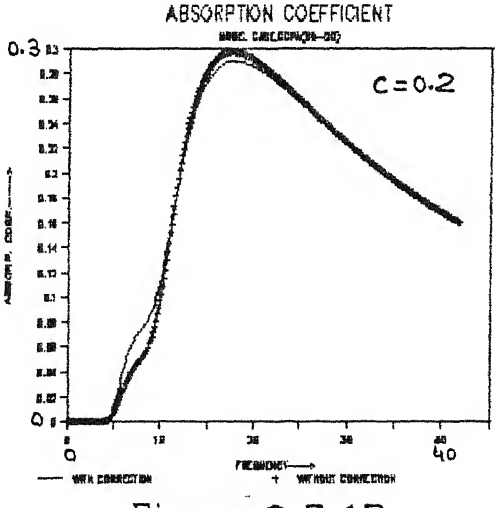

Figure 3.7.15

Absorption coefficient function as a function of frequency for the model case within 2CPA with c=0.5 & 0.2 respectively.

— with correction
\+ without correction

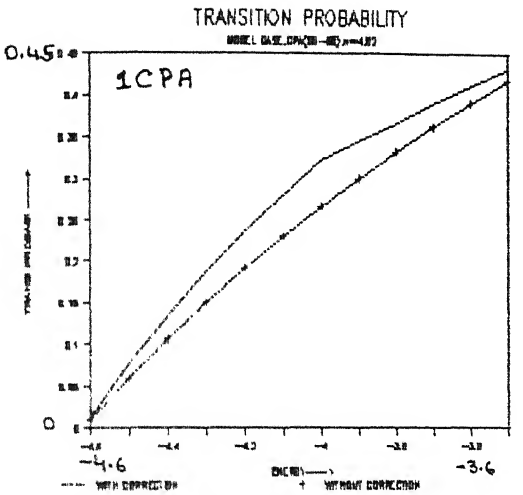

Figure 3.7.16

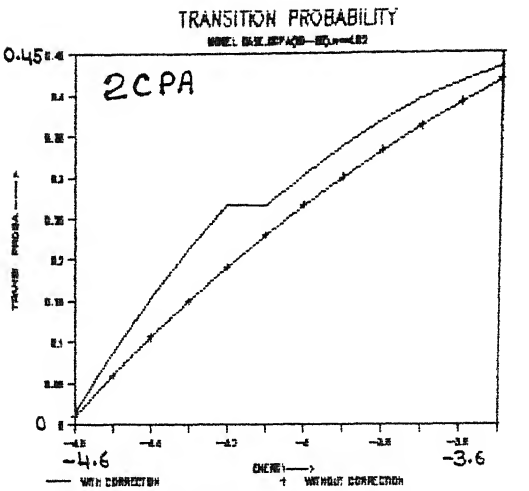

Figure 3.7.17

Square of the optical matrix element (transition probability) as a function of energy for the model case with c= 0.5 and ω = 4.62 within 1CPA and 2CPA respectively. —— with correction
+ without correction

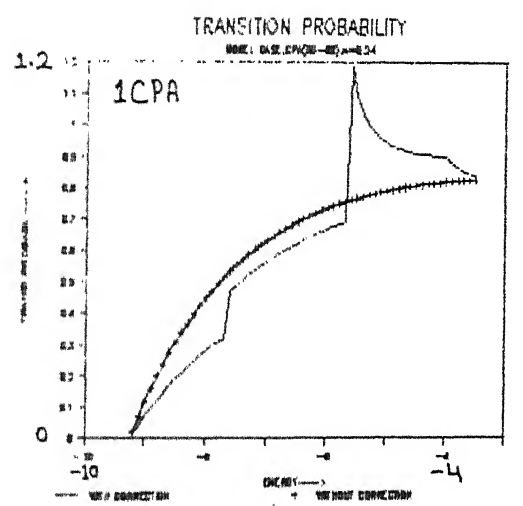

Figure 3.7.18

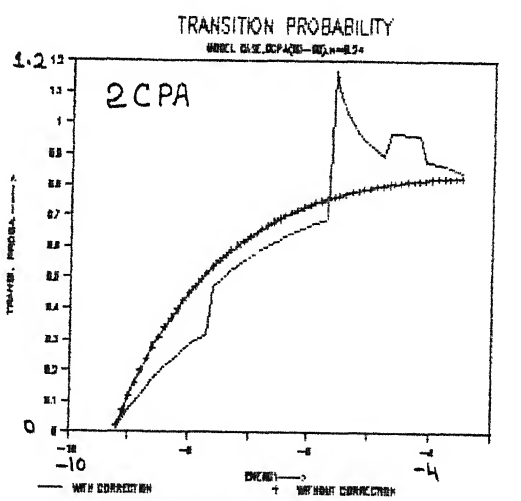

Figure 3.7.19

Square of the optical matrix element (transition probability) as a function of energy for the model case with c= 0.5 and ω = 9.24 within 1CPA and 2CPA respectively. —— with correction
+ without correction

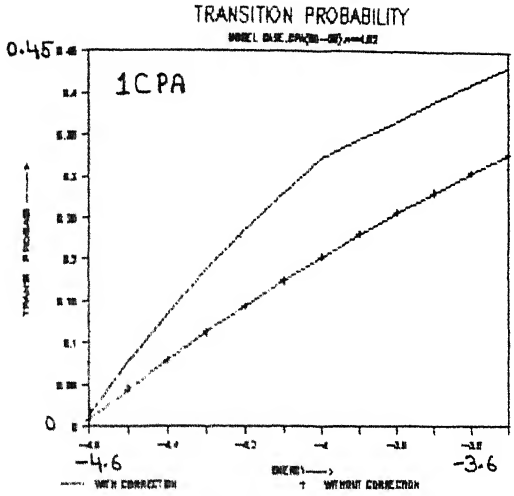

Figure 3.7.20

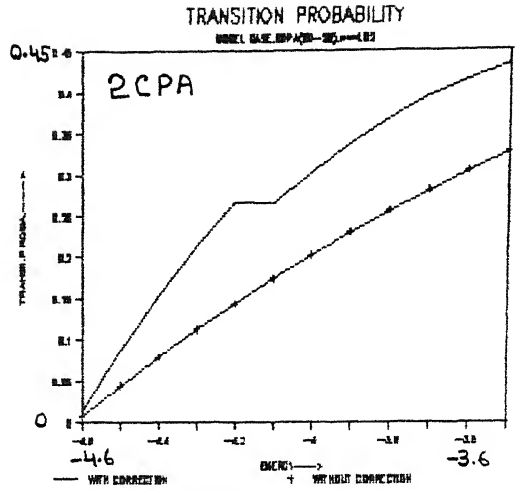

Figure 3.7.21

Square of the optical matrix element (transition probability) as a function of energy for the model case with c= 0.2 and ω = 4.62 within 1CPA and 2CPA respectively. — with correction
+ without correction

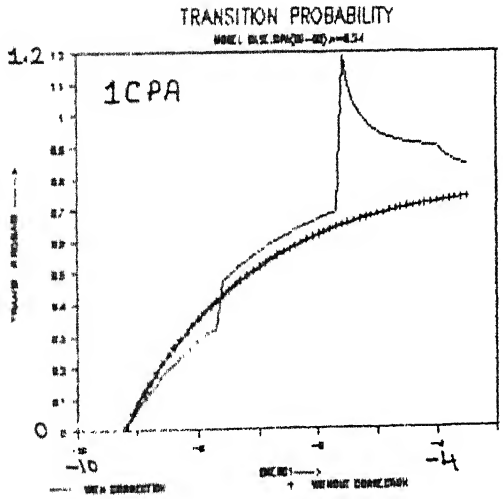

Figure 3.7.22

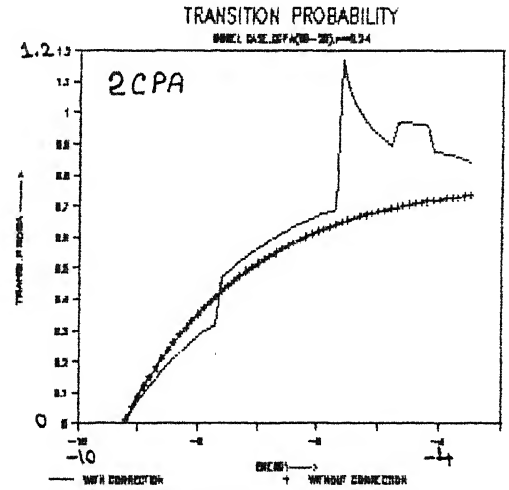

Figure 3.7.23

Square of the optical matrix element (transition probability) as a function of energy for the model case with c= 0.2 and ω = 9.24 within 1CPA and 2CPA respectively. — with correction
+ without correction

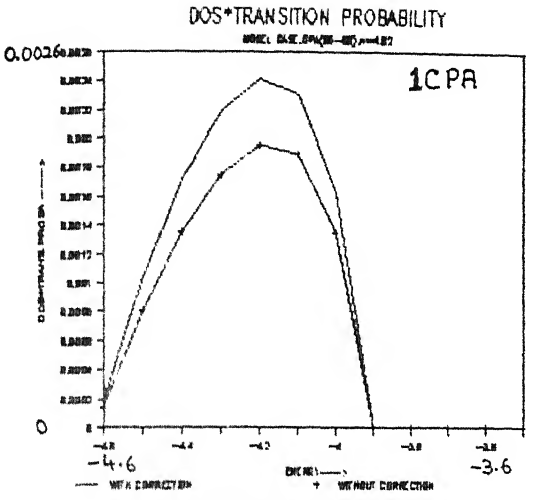

Figure 3.7.24

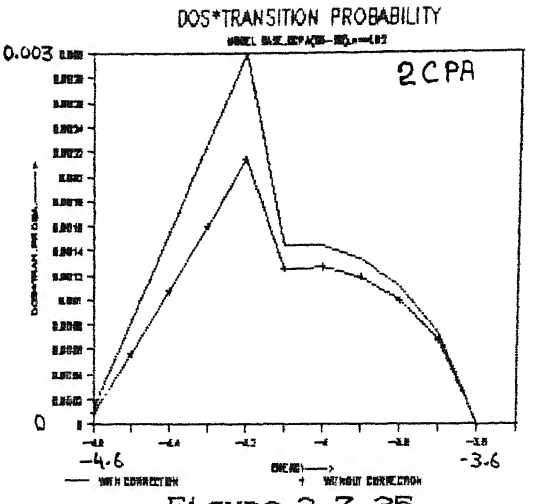

Figure 3.7.25

Product of the valence band DOS and square of the optical matrix element (transition probability) as a function of energy for the model case with c= 0.5 and ω = 4.62 within 1CPA and 2CPA respectively. —— with correction
+ without correction

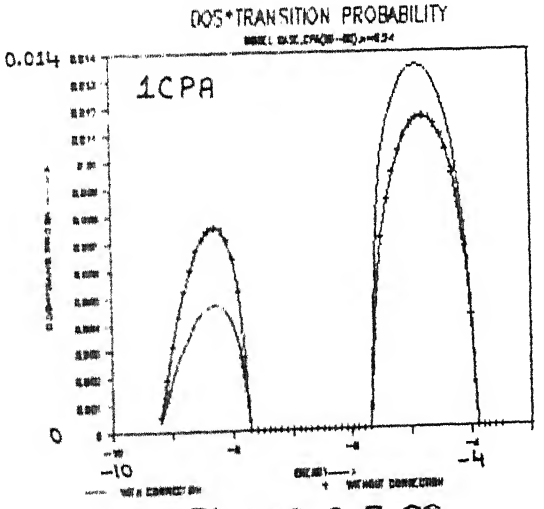

Figure 3.7.26

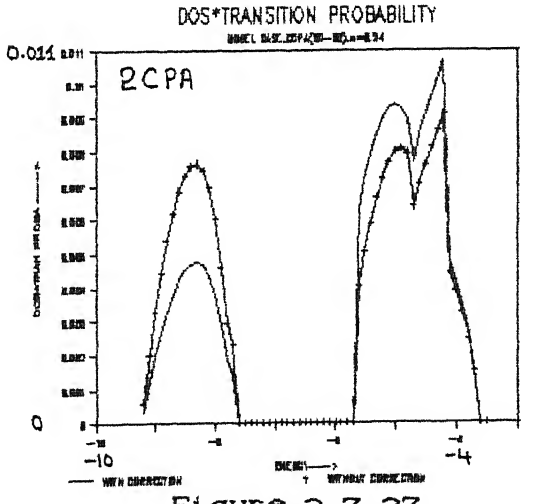

Figure 3.7.27

Product of the valence band DOS and square of the optical matrix element (transition probability) as a function of energy for the model case with c= 0.5 and ω = 9.24 within 1CPA and 2CPA respectively. —— with correction
+ without correction

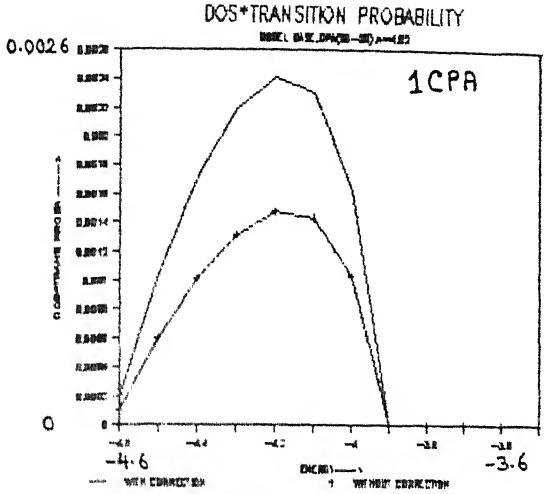

Figure 3.7.28

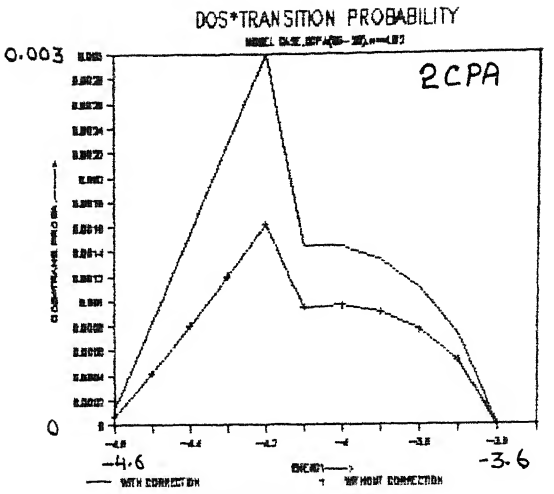

Figure 3.7.29

Product of the valence band DOS and square of the optical matrix element (transition probability) as a function of energy for the model case with c= 0.2 and ω = 4.62 within 1CPA and 2CPA respectively. —— with correction
+ without correction

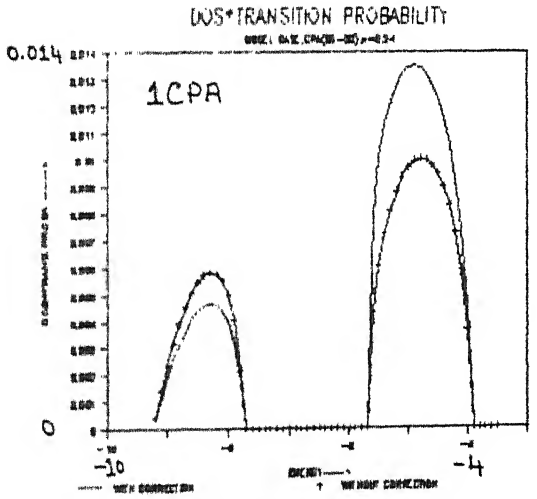

Figure 3.7.30

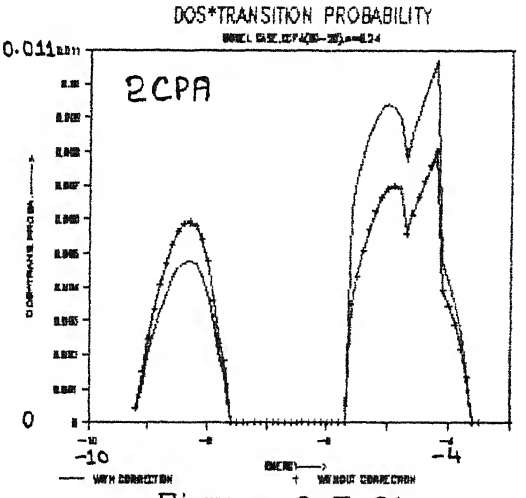

Figure 3.7.31

Product of the valence band DOS and square of the optical matrix element (transition probability) as a function of energy for the model case with c= 0.2 and ω = 9.24 within 1CPA and 2CPA respectively. —— with correction
+ without correction

CHAPTER IV

OPTICAL PROPERTIES OF III-V TERNARY ALLOYS

4.1 INTRODUCTION

The application of the Augmented Space formulation of optical conductivity on a simple model for random-semiconducting binary alloys discussed in the previous chapter gave encouraging results and it provided us with sufficient theoretical basis for applying the formulation to more realistic situations of III-V ternary alloys.

The III-V semiconductors GaAs, InAs, GaSb, GaP and InP, etc. form zinc-blende structures (see figure 4.1.1). A zinc-blende structure consists of two interpenetrating f.c.c. sublattics, the anion (e.g. As) and the cation (e.g. Ga) sublattices, which are displaced from each other by a vector $\bar{\tau}$ = (1/4, 1/4, 1/4) a, where a is the lattice constant. Consequently each anion in the crystal is surrounded by a tetrahedral arrangement of four cations and *vice versa*. A schematic picture of the flattened network of the structure is shown in figure (4.2.2).

Pairs of these semiconductors mix in all concentrations form ternary substitutional disordered alloys. The sublattice of

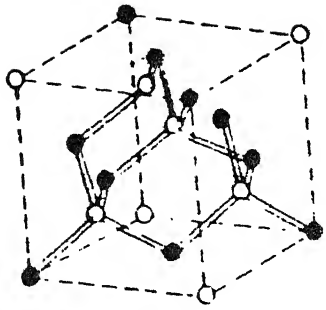

Zinc blende crystal structure

Figure 4.1.1

○ ANION
● CATION
a (0,0,0)
b (1/4,1/4,1/4)
c (1/2,1/2,0)
d (1/4,3/4,3/4)
e (0,1/2,-1/2)
f (-1/4,1/4,-1/4)
g (3/4,3/4,1/4)
h (1/2,1,1/2)
i (-1/4,3/4,-3/4)
$\bar{r}_1$ (1/8,1/8,1/8)
$\bar{r}_2$ (-1/8,-1/8,1/8)
$\bar{r}_3$ (-1/8,1/8,-1/8)
$\bar{r}_4$ (1/8,-1/8,-1/8)

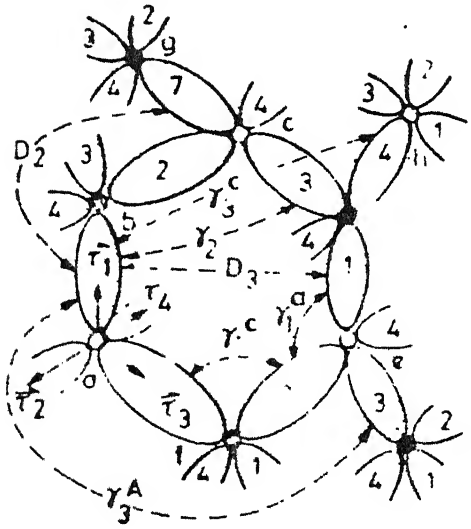

Cordinates are in the units of a, the lattice constant of the f.c.c. lattice.

Connectivities and coordinates in a flattened diagram for a zinc blende structure

Figure 4.1.2

the common ion is *ordered* while that of the other ion is occupied randomly by one of the two possible constituents.

The work reported in this chapter has two parts. In the first part, as we adopt basically a tight binding view point, we attempt with the help of the Recursion technique (§4.3) to develop a fully *real* space method for generating the various constituent Green function for GaAs, GaSb, and InSb and the alloys $GaAs_{1-c}Sb_c$ and $Ga_{1-c}In_cSb$ (for c = 0.2 and 0.5). We then use the CPA to generate the valenece band density of states for the above alloys. The basic Hamiltonian is set up in the bond orbital basis (§4.2) with parameters fitted to experiment.

In the second part we apply our formulation for optical conductivity developed in the previous chapter to calculate various optical response functions for the above alloys.

The modified square of the optical matrix element, $|g_{if\gamma}^{eff}|^2$ is calculated with the use of known numerical values of wave functions for different atoms reported by Herman and Skillman (1970). Again the wave functions are written in the bond-orbital basis.

4.2 HAMILTONIAN IN BOND ORBITAL BASIS

To illustrate what are bond basis, let us first take a simple example of a diatomic molecule. The system is formed by

two atoms A and B (see the figure 4.2.1).

The LCAO associated with A atom is $\phi(\bar{r} - \bar{r}_A)$ and that of with B atom is $\phi(\bar{r} - \bar{r}_B)$. Then the secular determinant in the LCAO basis is given by

$$\begin{vmatrix} H_{AA} - \varepsilon S_{AA} & H_{AB} - \varepsilon S_{AB} \\ H_{BA} - \varepsilon S_{BA} & H_{BB} - \varepsilon S_{BB} \end{vmatrix} = 0 \qquad (4.2.1)$$

where Hamiltonian H in LCAO basis is :

$$H = \begin{bmatrix} H_{AA} & H_{AB} \\ H_{BA} & H_{BB} \end{bmatrix} \qquad (4.2.2)$$

$$H_{AA} = \int \phi^*(\bar{r} - \bar{r}_A)\, H\, \phi(\bar{r} - \bar{r}_A)\, d\bar{r} = \varepsilon_A$$

$$H_{BB} = \int \phi^*(\bar{r} - \bar{r}_B)\, H\, \phi(\bar{r} - \bar{r}_B)\, d\bar{r} = \varepsilon_B$$

$$H_{BA} = H_{AB} = \int \phi^*(\bar{r} - \bar{r}_A)\, H\, \phi(\bar{r} - \bar{r}_B)\, d\bar{r} = V \qquad (4.2.3)$$

$$S_{AA} = \int \phi^*(\bar{r} - \bar{r}_A)\, \phi(\bar{r} - \bar{r}_A)\, d\bar{r} = 1$$

$$S_{BB} = \int \phi^*(\bar{r} - \bar{r}_B)\, \phi(\bar{r} - \bar{r}_B)\, d\bar{r} = 1$$

$$S_{AB} = S_{BA} = \int \phi^*(\bar{r} - \bar{r}_A)\, \phi(\bar{r} - \bar{r}_B)\, d\bar{r} \neq 0$$

ε_A and ε_B are site energies, V is interaction potential between A and B atoms and ε is the eigenvalues of H. Therefore a representation of $\underline{H}$ in the LCAO basis is now given by

$$\underline{H} = \begin{bmatrix} \varepsilon_A & V \\ V & \varepsilon_B \end{bmatrix} \qquad (4.2.4)$$

As an example, the solution of the secular equation for a simple case where $\varepsilon_A = \varepsilon_B = \varepsilon$ are ε^+ and ε^- where

$$\varepsilon_- = \frac{\bar{\varepsilon} - V}{1 - S}$$

$$\varepsilon_+ = \frac{\bar{\varepsilon} + V}{1 + S} \qquad (4.2.5)$$

The corresponding eigenfunctions are given by

$$\phi_-(r) = \frac{\phi_A(r - r_A) - \phi_B(r - r_B)}{\sqrt{2(1-S)}}$$

$$\phi_+(r) = \frac{\phi_A(r - r_B) + \phi_B(r - r_B)}{\sqrt{2(1-S)}} \qquad (4.2.6)$$

$\phi_-(r)$ is called *antibonding* state and $\phi_+(r)$ the *bonding* state. The representation of the Hamiltonian in the new basis (ϕ_-, ϕ_+) is diagonal, with ε_- and ε_+ in the diagonal positions

The work by Harrison and his coworkers (1973-74) has demonstrated that the systematics of bonding of various physical properties can be described by the *bond orbital model* (BOM) in covalently bonded systems. In semiconducting materials the set of bonding states spans the valence band and the set of antibonding states spans the conduction band, if the hybridising term between them is negligible. Thus the advantage of working in this basis is that if we want only the valence band structure, we can only work with the half of the space spanned by the bonding states. These basis functions are constructed by linear combinations of sp^3 hybridised orbitals on adjacent atoms.

To get the Green operator corresponding to bonding states (valence band), we may partition the Hamiltonian as

$$\underline{H} = \underline{H}_v + \underline{H}_c + \underline{H}_{vc} \qquad (4.2.7)$$

where $\underline{H}_v$ and $\underline{H}_c$ project onto the valence (or bonding) and conduction (or antibonding) subspaces respectively and $\underline{H}_{vc}$ is the hybridising term.

$$\underline{G}_v(z) = [z\underline{I} - \underline{H}_v - \underline{H}^{\dagger}_{vc}\underline{G}_c\underline{H}_{cv}]^{-P_v} \qquad (4.2.8)$$

$$\underline{G}_c(z) = [z\underline{I} - \underline{H}_c]^{-P_c} \qquad (4.2.9)$$

The valence band density of states is given by

$$-(1/\pi)\ \mathcal{I}m\ \mathcal{T}r\ \underline{G}^V \qquad (4.2.10)$$

Within the bond orbital model, it is assumed that $\underline{H}_{cv}$ is small, and so we may completely neglect the antibonding part and work exclusively in the bonding subspace to get valence band density of states. In case there is significant coupling between bonding and antibonding states, the bond orbital approximation is inaccurate, and the correction terms have to be included.

Using the notations of Chen and Sher (1978) we fix the anion f.c.c. sublattice as the reference lattice on which each lattice point is represented by a lattice vector $\bar{j}$. The four bonding orbitals surrounding it and pointing in the tetrahedral directions, may be represented by $|\bar{j}\alpha\rangle$, α = 1,2,3,4 centred at points specified by $\bar{j} + \bar{\tau}_\alpha$ where $\bar{\tau}_1$ = (1,1,1) a/8, $\bar{\tau}_2$ = (-1,-1,1) a/8, $\bar{\tau}_3$ = (-1, 1, -1) a/8 and $\bar{\tau}_4$ = (1,-1,-1) a/8, where a is the lattice constant. The bond orbitals themselves are composed of symmetric linear combinations of the hybridised atomic orbitals $|a\rangle$ and $|c\rangle$ centred at the anion and cation atomic sites respectively, i.e.

$$|\bar{j}_\alpha\rangle = (1/N_n)\ [\,|a\rangle + |c\rangle\,] = |ac\rangle \qquad (4.2.11)$$

where N_n is the normalization constant $\sqrt{2(1+S)}$ ($S = \langle a|c\rangle$, the orbital overlap of anion-cation pair), and

$$|a\rangle = (1/2)\,|s_a\rangle + (\sqrt{3}/2)\,|p_a\rangle$$
$$|c\rangle = (1/2)\,|s_c\rangle + (\sqrt{3}/2)\,|p_c\rangle \qquad (4.2.12)$$

where $|s_a\rangle$ and $|p_a\rangle$ are the s and p orbitals on the anions while $|s_c\rangle$ and $|p_c\rangle$ are those on the cations. The p-orbitals are taken to be directed along the bond in the above expressions. When expanded in terms of a bond basis set $\{|\bar{j},\alpha\rangle\}$ the BOM Hamiltonian is given by

$$\underline{H}_o = \sum_{j\alpha,j'\alpha'} \sum \sum \sum |\bar{j},\alpha\rangle \langle\bar{j},\alpha|\underline{H}_o\ |\bar{j}'\alpha'\rangle\langle\bar{j}'\alpha'| \qquad (4.2.13)$$

If we consider bond to bond overlaps upto second nearest neighbours bonds, there are five distinct overlaps $\langle\bar{j},\alpha\ \underline{H}_o|\bar{j},\alpha'\rangle$ which are defined below (see figure 4.1.2).

D : The bond energy $\langle\bar{j}\alpha|\underline{H}_o|\bar{j}\alpha\rangle$.

γ_1^a : The matrix elements between adjacent bonds with an anion in common.

γ_1^c : The matrix elements between adjacent bonds with a cation in common.

D_2 : The matrix elements between parallel second nearest neighbour bonds.

γ_2 : The matrix elements between non-parallel second nearest neighbour bonds.

Chen and Sher (1978) have shown that the inclusion of third-nearest neighbour interactions, does not change the band structure significantly. So, retaining the interactions upto second nearest neighbour parallel and non-parallel bonds only, the distinct matric elements are D, γ_1^a, γ_1^c, D_2 and γ_2

4.3 THE RECURSION METHOD

Band theory for systems, like simple metals where the interaction between electrons and atoms is weak, exploits the physics of long range periodicity of the atomic potentials to express electronic properties of the solid as a coherent superposition of the electronic properties of all the atoms. When a strong interaction is present between the electrons and the atoms, the electronic properties no longer depend on long range periodicity and thus this picture of band theory breaks down. In such cases the properties depend only on the first few shells of neighbours of each atom. The d electrons in transition metals are good examples. While the band theory is still a valid formal solution to the Schrödinger equation, the physics is better understood by means of a solution that explicitly accounts for the role of the local environment.

To do this, we have to calculate the local density of

states. The local density of states describes the effect of the rest of a solid on one region. Physically, the local density of states is the intensity of each eigenstate on a particular atom or bond. Mathematically, it is the magnitude squared of the projection of each eigenstate on a local orbital. Most properties of solids including binding energy, photoemission spectra, and magnetism can be related to the local density of states.

The basic problem is to find the local density of states from a tight-binding or localized orbital model. The physics demands that it be done in such a way that the local orbital itself has the greatest effect, and that successively more distant orbitals have lesser effect. The solution must define a hierarchy of environments so that their relative influences areexplicitely displayed in the local density of states.

The Recursion method, introduced first by Haydock *et.al.*(1973) and discussed in detail by Haydock (1980), provides one of the best real space methods to tackle the above problem. In this method, linear combinations of the local orbitals are so determined that the electron passes through each state as it diffuses away from the local orbital from which it starts. Thus it serves the demand of the physics just described above.

The sequence of environments are described by orthogonal states $\langle |u_n\rangle\rangle$, where $|u_n\rangle$ is a linear combination of basis orbitals. In practice the states $|u_n\rangle$ are localized on the shell of atoms n

hops from the atom accommodating $|\phi_o\rangle$. If the local density of states is to be obtained around a particular atom or bond described by a basis orbital $|\phi_o\rangle$, $|u_o\rangle$ is taken equal to $|\phi_o\rangle$. the rest of the orthogonal states are generated from the condition

$$\underline{H}|u_n\rangle = a_n|u_n\rangle + b_{n+1}|u_{n+1}\rangle + b_n|u_{n-1}\rangle \qquad (4.3.1)$$

where $\underline{H}$ is the Hamiltonian of the model. a_n and b_n are the coupling constants of each environment to itself and its neighbours.

The coefficients a_n and b_n are generated recursively from

$$|u_o\rangle = |\phi_o\rangle, \quad b_o = 1$$

$$a_n = \frac{\langle u_n|\underline{H}|u_n\rangle}{\langle u_n|u_n\rangle} \qquad (4.3.2)$$

$$b_{n+1} = \frac{b_n\langle u_n|u_n\rangle}{\langle u_{n+1}|u_{n+1}\rangle}$$

We have used the orthogonality of the new basis $\{|u_n\rangle\}$. The above equations are a convenient algorithm for computational generation of the coefficients a_n and b_n. It is clear, from the equation (4.3.1), that $\underline{H}$ has a tridiagonal representation in $\{|u_n\rangle\}$ basis :

$$\underline{H}_{TD} = \begin{bmatrix} a_o & b_1 & 0 & 0 \cdots\cdots \\ b_1 & a_1 & b_2 & 0 \cdots\cdots \\ 0 & b_2 & a_2 & b_3 \cdots\cdots \\ 0 & 0 & b_3 & a_3 \cdots\cdots \\ \vdots & \vdots & \vdots & \vdots \quad \ddots \end{bmatrix} \qquad (4.3.3)$$

Equivalently, given the Hamiltonian matrix $\underline{H}$ in orbital basis $\langle|\phi_n\rangle\rangle$, the Recursion method generates a unitary transformation $\underline{U}$ such that

$$\underline{U}\ \underline{H}\ \underline{U}^{-1} = \underline{H}_{TD} \qquad (4.3.4)$$

where $\underline{H}_{TD}$ is tridiagonal.

In a semi-infinite chain model described by the orbitals $\langle|u_n\rangle\rangle$ and the parameters a_n and b_n, the Hamiltonian has a tridiagonal representation and is symmetric in $\langle|u_n\rangle\rangle$ basis (Haydock 1980).

Therefore, in other words the Recursion method transforms a complicated three dimensional model into semiinfinite chain model described by the parameters a_n and b_n, thus making the problem much more simpler. A graphical representation of the chain model is shown in the figure (4.3.1).

Let us now get the expression for the local density of states $n_o(E)$. The corresponding Green function is given by

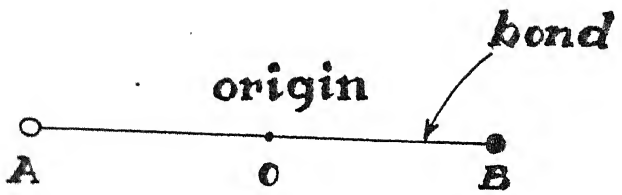

Figure 4.2.1 Co-ordinates of molecules in a diatomic molecule with respect to the origin at the centre of the bond

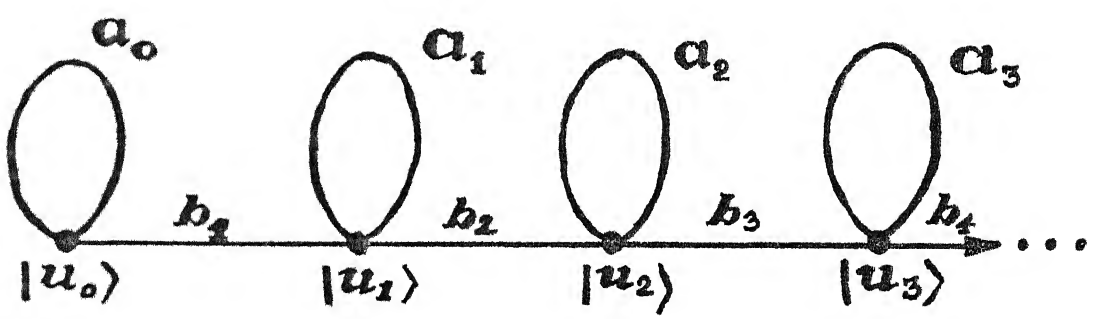

Figure 4.3.1 A graphic representation of the chain model including the states $\langle u_n \rangle$ and the recurrence parameters $\langle a_n \rangle$ and $\langle b_n \rangle$

$$G_o(z) = \langle \phi_o | (z\underline{I} - \underline{H})^{-1} | \phi_o \rangle$$

$$= \langle u_o | (z\underline{I} - \underline{H})^{-1} | u_o \rangle$$

$$= \langle u_o | \begin{bmatrix} (z-a_o) & -b_1 & 0 & 0 & \dots \\ -b_1 & (z-a_1) & -b_2 & 0 & \dots \\ 0 & -b_2 & (z-a_2) & -b_3 & \dots \\ \vdots & \vdots & \vdots & \vdots & \vdots \end{bmatrix}^{-1} | u_o \rangle \qquad (4.3.5)$$

Let us define the determinant of the matrix with the first n rows and n columns as $D_n(z)$, then

$$G_o(z) = [D_1(z) / D_o(z)]$$

$$= [D_1(z) / \{(z-a_o)D_1(z) - b_1^2 D_2(z)\}]$$

$$= 1 / [(E-a_o) - b_1^2 \, D_2(z)/D_1(z)]$$

$$= 1 / [(E-a_o) - b_1^2 \, G_1(z)]$$

If we continue this process upto n-steps, we have a continued fraction expansion for the Green function

$$\cfrac{1}{z - a_0 - \cfrac{b_1^2}{z - a_1 - \cfrac{b_2^2}{z - a_2 - \cfrac{b_3^2}{\ddots \; z - a_n - b_n^2 \, G_n(z)}}}}$$

where

$$G_n(z) = 1/[z - a_n - b_{n+1}^2 \, G_{n+1}(z)] \qquad (4.3.7)$$

The continued fraction representation, in general, may not terminate after a finite number of steps. It has been verified that for many systems the continued fraction converges very fast. When the convergence is slow or oscillatory it can be terminated by various termination schemes. Several termination schemes have been developed by Nex (1978, 1984) and Haydock and Nex (1984).

The density of states $n_o(E)$ is now given by

$$n_o(E) = -(1/\pi) \lim_{Z \to E+i0} \mathrm{Im} \; G_o(z)$$

$$= \mathrm{Im} \cfrac{-(1/\pi)}{E - a_0 - \cfrac{b_1^2}{E - a_1 - \cfrac{b_2^2}{E - a_2 - \cfrac{b_3^2}{\ddots \; E - a_n - b_n^2 \, G_n(E+i0)}}}}$$

4.4 THEORY OF CONTINUED FRACTION TERMINATORS

To get a proper terminator scheme to truncate the infinite continued fraction expansion, one needs first to examine the asymptotic behaviour of the continued fraction expansion. In the continued fraction expansion(4.3.7), one examines relations between features of the local density of states $n_o(E)$ and the coefficents $\{a_n, b_n\}$.

The asymptotic description of a_n and b_n is based on two elements :

(i) the main asymptotic behaviour depends on the band structure , *i.e.* $\{a_n\}$ and $\{b_n\}$ converges towards limits in the single band case or oscillate in a predictable way in the multiband case.

(ii) Damped oscillations are created by isolated singulatarities of n_o. The period of oscillation is related to the position of the singularity,and the rate of damping is related to the nature of the singularity.

The relation (4.3.1) defines $|u_n\rangle$ as a polynomial in $\underline{H}$ acting on $|u_o\rangle$:

$$|u_n\rangle = p_n(\underline{H})\,|u_o\rangle \qquad (4.4.1)$$

where, $p_o(\underline{H}) = \underline{I}$

$$p_1(\underline{H}) = (\underline{H} - a_o)/b_1 \text{ etc.} \qquad (4.4.2)$$

These polynomials depend only on the sequences $\{a_n\}$ and $\{b_n\}$, they are generated by the recurrence relation

$$b_1 p_1(z) = z - a_o$$

$$b_{n+1}\, p_{n+1}(z) = (z-a_n)\, p_n(z) - b_n p_{n-1}(z),\ n \geq 1 \qquad (4.4.3)$$

We shall not go into the detail of the behaviour of the polynomials $p_n(z)$. The details have been given elsewhere (Magnus, 1984). Let us only concentrate on the terminator schemes. We denote the solution of the recurrence relation (4.4.3) by $q_n(z)$ with

$$(z-a_o)\, q_o(z) - b_1 q_1(z) = 1 \qquad (4.4.4)$$

Then one has

$$q_o(z) = (z - a_o - b_1 q_1(z)/q_o(z))^{-1} \qquad (4.4.5)$$

$$[q_n(z)/q_{n-1}(z)] = b_n [z - a_n - b_{n+1}\, q_{n+1}(z)/q_n(z)]^{-1}$$

or, $$G_n(z) = b_n (z - a_n - b_{n+1}\, G_{n+1}(z))^{-1} \qquad (4.4.6)$$

$$G_o = [p^{(1)}_{n-1}/p_n] + 1/[b_n p_n (p_n/G_n - p_{n-1})] \qquad (4.4.10)$$

Thus showing that the usual continued fraction approximant $p^{(1)}_{n-1}/p_n$ corresponds to the crudest estimate $G_n = 0$ for the terminator. Much better results will be obtained with terminators coming from model continued fractions with a non-vanishing imaginary part. The models are chosen according to the behaviour of the local density of states, $n_o(E)$.

THE SQUARE ROOT TERMINATOR

In the case where the system has multiple bands (in particular single band) and $n_o(E)$ has only square-root singularities at the band edges, the widely used terminator is The Square Root Terminator. Let us consider the continued fraction expansion of a root of the quadratic equation

$$R\,G_o^2 - S\,G_o + V = 0 \qquad (4.4.11)$$

where R, S aqnd V are real polynominals.

If the root is written as :

$$G_o(z) = [S(z) - X^{1/2}(z)] / [2R(z)] \qquad (4.4.12)$$

$$X(z) = S^2(z) - 4\,R(z)\,V(z) \qquad (4.4.13)$$

$$= (z-E_1)(z-E_2)\ldots(z-E_{2m})$$

$E_1 < E_2 \ldots\ldots < E_{2m}$ also assumed to be real, G_o will have a non-vanishing imaginary part on the region where $X(z) < 0$, which is the set made of m intervals. E_{2m-1} and E_{2m} are the band edges of the m^{th} band.

The interesting feature of the form (4.4.12) is its reproducibility under the transformation (4.4.6) !

if $$S_n^2 - 4R_n\,V_n = X \qquad (4.4.14)$$

$$G_n = [S_n - X^{1/2}]/2R_n = 2\,V_n/[S_n + X^{1/2}] \qquad (4.4.15)$$

$$= b_n\left[z-a_n - b_{n-1}\frac{[2(z-a_n)V_n/b_n]-S_n - X^{1/2}}{2b_{n+1}V_n/b_n}\right]^{-1}$$

so that

$$R_{n+1}(z) / b_{n+1} = V_n(z) / b_n$$

$$S_{n+1}(z) = 2(z-a_n)\,V_n(z)/b_n - S_n(z)$$

$$b_{n+1}\,V_{n+1}(z) = b_{n+1}[S^2_{n+1}(z)/4R_{n+1}(z)] \qquad (4.4.16)$$

$$= (z-a_n)(S_{n+1}(z) - S_n(z)) / 2+b_n R_n(z)$$

Moreover, the degrees of R_n, S_n and V_n will decrease and stabilise ultimately on the values m+1, m and m-1. Indeed by putting the equation (4.4.15) in the equation (4.4.7), one obtains R_n and S_n in terms of P_n, P_{n-1}, $P^{(1)}_{n-2}$, and, after transformation using the equation (4.4.9)

$$R_n/b_n = X^{1/2} p_{n-1}q_{n-1} + Rq^2_{n-1} \qquad (4.4.17)$$

$$S_n = X^{1/2}b_n(p_{n-1} q_n + p_n q_{n-1}) + 2R b_n q_{n-1} q_n$$

As $q_n(z)$ behaves like $b_n....b_n z^{-n-1}$ when $z \to \infty$, the degrees of R_n and S_n will decrease by steps of 2 units, down m-1 and m.

The easiest case occurs when m = 1 (single band), where one has

$$R_n(z)\, b_n \equiv 1$$

$$a_{n-1} = (E_1 + E_2)/2 \qquad (4.4.18)$$

$$S_n(z) = z - (E_1 + E_2)/2$$

$$b_n = (E_1 + E_2)/4 \qquad \text{if } n \text{ is large enough}$$

The corresponding orthogonal polynomials are known as the Berstein-Szego polynomials (Chihara, 1978). Practically $(E_1+E_2)/2$ and $(E_2-E_1)/4$ must be the limits of a_n and b_n when $n \to \infty$, a very well known situation.

4.5 DENSITY OF STATES OF III-V TERNARY ALLOYS

In this section the 1CPA together with the Recursion method will be applied to calculate the valence band density of states of III-V random ternary alloys . As before the conduction band DOS will be taken to be like that for free electrons (see figure (4.5.1)).

Before calculating DOS for alloys , the valence band DOS of pure semiconductors GaAs , GaSb and InSb will be calculated using the Recursion method . The Hamiltonians for such systems in the moleculer bond basis are given by the equation (4.2.13) . The parameters like D , γ_1^a , γ_1^c, $D_2$and γ_2 (defined in § 4.2) for such

systems are taken from the work by Chen and Sher (1978) . These are shown in the table (4.5.1)

Table 4.5.1

Material	Interaction Parameters (eV)				
	D	γ_{1S}	γ_{1A}	D_2	γ_2
GaAs	-11.1687	-1.5187	-0.4250	0.3406	-0.1094
GaSb	-9.6437	-1.2687	-0.3750	0.3906	-0.0594
GaP	-10.8125	-1.3625	-0.3250	0.3812	-0.1188
InAs	-10.0562	-1.3937	-0.5125	0.3844	-0.0656
InSb	-9.5625	-1.3500	-0.3875	0.2937	-0.0563
InP	-10.2750	-1.3125	-0.4125	0.2625	-0.0375

where $\gamma_{1S} = \frac{\gamma_1^a + \gamma_1^c}{2}$ and $\gamma_{1A} = \frac{\gamma_1^a - \gamma_1^c}{2}$

The band gaps and the effective electron masses for the semiconductors GaAs , Gasb , and InSb are given in the table (4.5.2)

TABLE 4.5.2

Material	Band gap E_g (eV)	$M = (m^*/m_e)$
GaAs	1.53	0.068
GaSb	0.78	0.050
InSb	0.23	0.014

Recursion parameters (a's and b's , defined in § 4.3) for these semiconductors are calculated upto 14 steps (shown in the teble (4.5.3)) and the continued fraction expansion is terminated using the square root terminator described in § 4.4 .

TABLE 4.5.3

Recursion Parameters

	GaAs		GaSb		InSb	
(eV)	a	b	a	b	a	b
	-11.16870	15.76212	-9.64370	11.45910	-9.56250	12.38153
	-13.95030	8.29524	-11.54485	5.96766	-11.97702	5.82638
	-11.81261	11.17063	-9.49665	6.23608	-10.09841	7.00559
	-13.10205	17.32363	-9.37953	8.93029	-10.82950	13.72379
	-12.59923	6.40295	-11.73653	8.57858	-11.23511	4.23485
	-11.63092	18.17576	-8.64858	3.43360	-9.30902	10.67344
	-14.01978	7.27838	-10.12119	9.66969	-12.33525	7.46476
	-11.62677	11.47339	-11.13626	8.54560	-9.93838	5.47466
	-13.65308	15.04109	-9.49544	4.30477	-10.85169	12.51796
	-12.18002	7.72794	-9.68194	8.71177	-11.28667	6.06868
	-12.78103	14.64544	-11.26134	5.63407	-10.19797	8.54836
	-12.93502	7.77484	-10.33605	6.66237	-11.39538	7.75767
	-12.67082	7.90878	-10.05651	5.59190	-11.21823	6.87441
	-11.85587	10.77620	-11.02555	7.40693	-10.03531	4.78794

The valence band DOS per bond for pure GaAs , GaSb and InSb are shown in figures (4.5.2) , (4.5.3) and (4.5.4) respectively .It is clear from these figures that all essential features with a s-like band separated from a p-like band , which itself is split by the cubic crystal field into a e_g and a t_y like points . The heights

are in the ratio 1:1:2 as expected . There are still many oscillations which may be artifacts of the terminator , particularly in the s-like part and the upper edge of the p-like part of the band (V.K Srivastava , 1982) .

Now the valence band DOS per bond will be calculated for the random semiconducting alloys . Two alloys will be chosen : $GaAs_{1-c}Sb_c$ and $Ga_{1-c}In_cSb$ for c=0.5 and 0.2 . Table (4.5.4) shows that each of the six semiconductors have nearly the same bond length . Hence , it will be assumed that the interaction parameters corresponding to the pure materials are the same as those in the alloy . The vaccum state sets the same zero of the energy scale for all the three materials .

In an alloy the question of interaction between two different kinds of bonds arises . For example in the case of $GaAs_{1-c}Sb_c$ alloy , a configuration of the kind

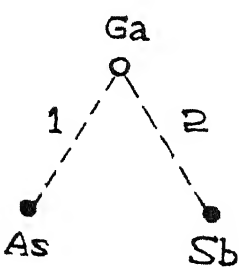

may be a part of the alloy . It is shown below that the interaction $\underline{H}_{12}^{exact}$ between bonds 1 and 2 is the average of γ_1^{α}'s , defined in §(4.2) , corresponding to pure Ga-As and Ga-Sb crystals as a reasonable approximation .

Table 4.5.4

Material	Bond length (A^o)	Bond energy (eV)	Work function (eV)
GaAs	2.45	-5.6687	5.5
InAs	2.61	-4.7562	5.3
GaSb	2.65	-4.7437	4.9
InSb	2.81	-4.7625	4.8
GaP	2.36	-5.1125	5.7
InP	2.54	-4.5750	5.7

Let the bonds 1 and 2 be described by the quantum states $|\phi_A\rangle$ and $|\phi_B\rangle$ respectively . Then

$$|\phi_A\rangle = 1/N \left[|Ga_1\rangle + |As_1\rangle\right]$$

and

$$|\phi_B\rangle = 1/N \left[|Ga_2\rangle + |Sb_2\rangle\right]$$

in terms of sp^3 hybridised orbitals at various sites directed along the respective bonds and N is the normalization constant $\simeq \sqrt{2}$,assumed to be same for the GaAs and GaSb bonds . We are concerned with H_{12}^{exact} *i.e.* ,

$$\langle \phi_A | \underline{H}_{12}^{exact} | \phi_B \rangle = (1/N^2) \left[(\langle Ga_1 | + \langle As_1 |) \underline{H}_{12}^{exact} (| Ga_2 \rangle + | Sb_2 \rangle) \right]$$

$$= (1/N^2) \left[\langle Ga_1 | \underline{H}_{12}^{exact} | Ga_2 \rangle + \langle Ga_1 | \underline{H}_{12}^{exact} | Sb_2 \rangle + \right.$$

$$\left. \langle As_1 | \underline{H}_{12}^{exact} | Ga_2 \rangle + \langle As_1 | \underline{H}_{12}^{exact} | Sb_2 \rangle \right]$$

The first term is vanishing because of the orthogonality of two different hybridised orbitals at the same sites . The middle two terms would be identical in the unalloyed case due to the geometrical symmetry of the location of the orbitals involved . Hence this part of the expression is equivalent to the average of these corresponding to the pure cases. The last term is small compared to the middle two since it involes more distant orbitals . The approximation therefore involves the neglect of the variation in this term over the constituent materials .

Therefore for these alloys interaction parameters , γ_1^a, γ_1^c, D_2 and γ_2 are given by the average of the above parameters of the respective pure semiconductors .

The band gaps and the effective electron masses for these alloys are taken as the average of the respective pure semiconductors . These and the interaction parameters are calculated and given in the table (4.5.5)

Table 4.5.5

Material	Interaction Parameters (eV)					
	γ_{1A}	γ_{1c}	D_2	γ_2	Band gap	$M=(m^*/m_e)$
$GaAs_{0.5}Sb_{0.5}$	-1.7937	-0.9937	0.3556	-0.0844	1.155	0.059
$GaAs_{0.8}Sb_{0.2}$	-1.8837	-0.9937	0.3506	-0.0994	1.380	0.064
$Ga_{0.5}In_{0.5}Sb$	-1.6906	-0.9281	0.3712	-0.0588	0.505	0.032
$Ga_{0.8}In_{0.2}Sb$	-1.6625	-0.9075	0.3712	-0.0588	0.670	0.043

Using these average values as inputs in the Recursion method , we calculate the DOS , within the virtual crystal appaoximation (VCA) , for the above alloys . Again the recursion parameters are calculated upto 14 steps of the recursion and the continued fraction expansion is terminated using the square root terminator . These DOS are then used as the input for the initial choice of $\langle G \rangle$ in the CPA equation (3.2.22) for our CPA calculation . Finally new self energy Σ_o and from this new $\langle G \rangle$ is calculated self consistently .

Figures (4.5.5) , (4.5.6) ,(4.5.7) and (4.5.8) show the CPA DOS for $GaAs_{0.5}Sb_{0.5}$, $GaAs_{0.8}Sb_{0.2}$, $Ga_{0.5}In_{0.5}Sb$ and

$Ga_{0.8}In_{0.2}Sb$ respectively . The bond energies randomness is greatest in the former set of alloys , but not enough to cause split or impurity bands . Therefore as indicated by model calculations the 50-50 GaAsSb shows the maximum effect of randomness .

4.6 OPTICAL PROPERTIES OF III-V RANDOM TERNARY ALLOYS : RESULTS AND DISCUSSION

Having calculated the valence band DOS for $GaAs_{1-c}Sb_c$ and $Ga_{1-c}In_cSb$ (for c = 0.5 and 0.2) , we shall now apply the Augmented space formalism to these alloys . Let us first write the centred orbitals for different species in the alloy . Take the example of $GaAs_{1-c}Sb_c$. The spacies A is GaAs and B is GaSb . Therefore

$$|\phi_A\rangle = |\phi_{GaAs}\rangle = (1/\sqrt{2}) \left[|\phi_{Ga}\rangle + |\phi_{As}\rangle \right] \qquad (4.6.1)$$

where $|\phi_{Ga}\rangle$ and $|\phi_{As}\rangle$ are the centred orbitals for the respective atoms and are given by the linear combinations of sp^3 hybridised orbitals (LCAO) :

$$|\phi_{Ga}\rangle = (1/2) \; |\phi^s_{Ga}\rangle + (\sqrt{3}/2) \; |\phi^p_{Ga}\rangle \quad \text{and}$$

$$|\phi_{As}\rangle = (1/2) \; |\phi^s_{As}\rangle + (\sqrt{3}/2) \; |\phi^p_{As}\rangle \qquad (4.6.2)$$

where $|\phi^s_{Ga}\rangle$ and $|\phi^p_{Ga}\rangle$ refer to the s and p states for Ga . Similarly $|\phi^s_{As}\rangle$ and $|\phi^p_{As}\rangle$ are defined . Therefore

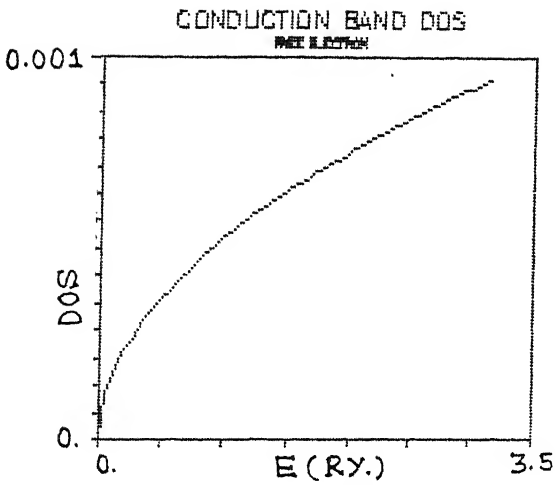

Figure 4.5.1

Conduction band DOS (to be free electron like) as a function of energy.

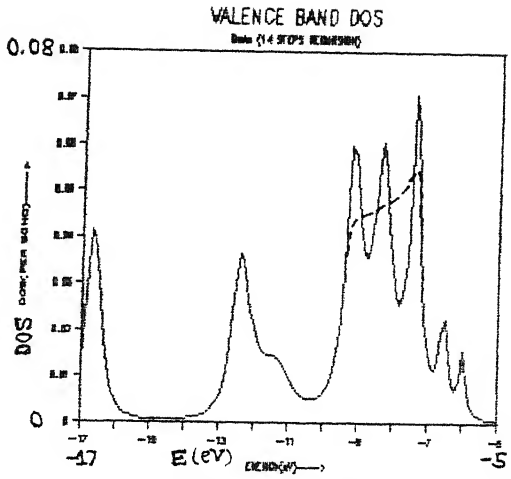

Figure 4.5.2

Valence band DOS for the pure GaAs(upto 14 steps of recursion) as a function of energy.

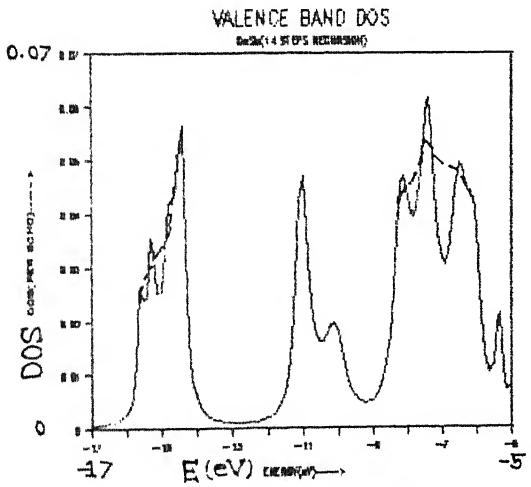

Figure 4.5.3

Valence band DOS for the pure GaSb(upto 14 steps of recursion) as a function of energy.

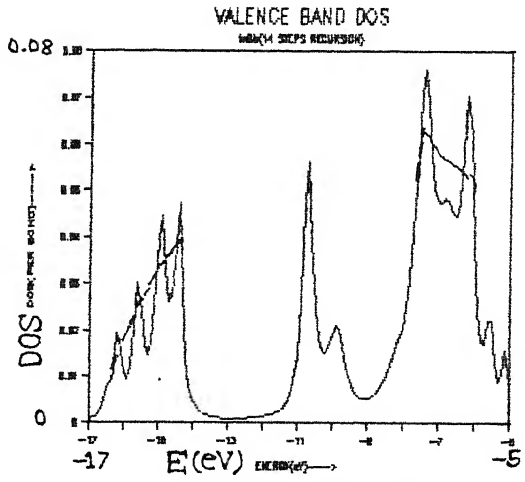

Figure 4.5.4

Valence band DOS for the pure InSb(upto 14 steps of recursion) as a function of energy.

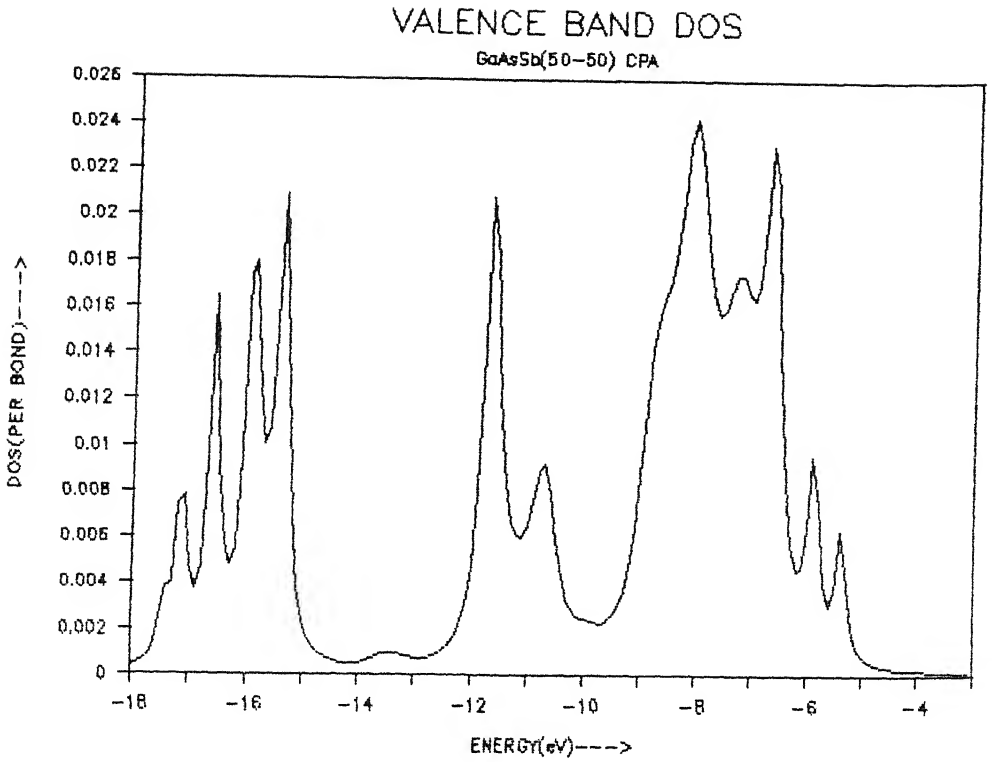

Figure 4.5.5

Figure 4.5.6

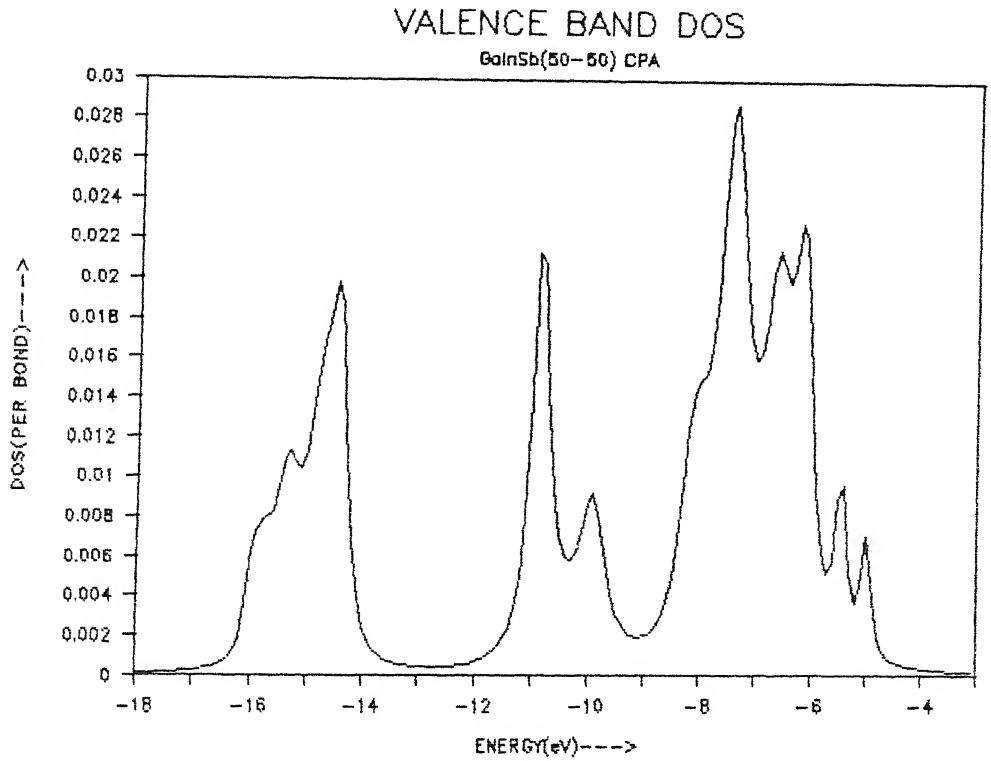
VALENCE BAND DOS
GaInSb(50-50) CPA
DOS(PER BOND)--->
0.03
0.028
0.026
0.024
0.022
0.02
0.018
0.016
0.014
0.012
0.01
0.008
0.006
0.004
0.002
0
-18
-16
-14
-12
-10
-8
-6
-4
ENERGY(eV)--->
Figure 4.5.7

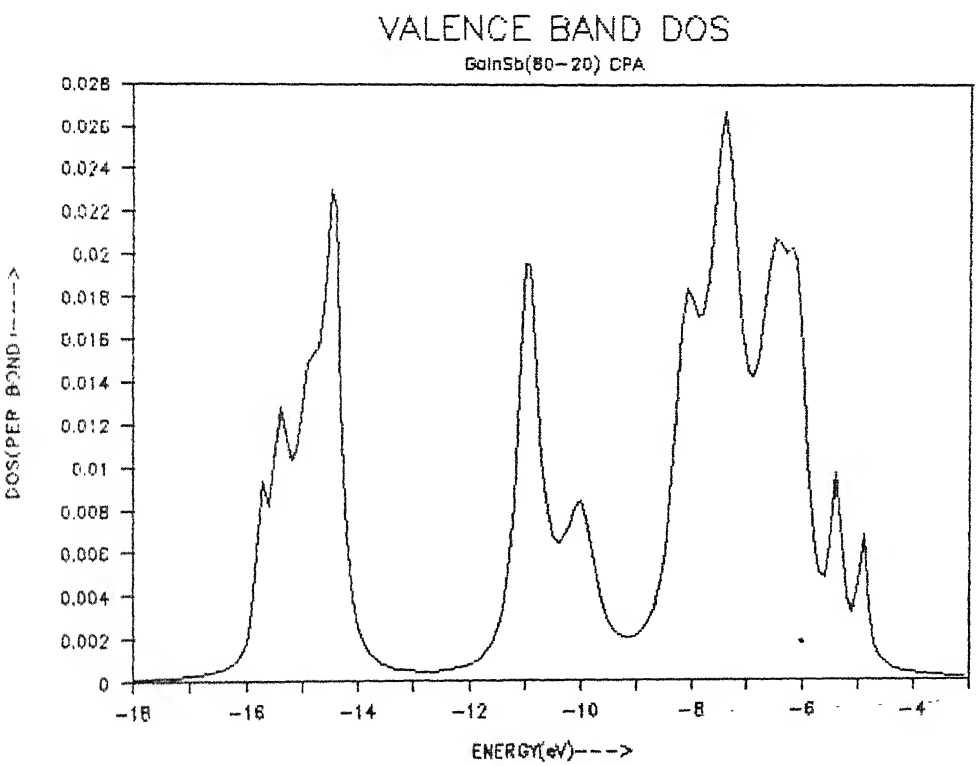
VALENCE BAND DOS
GaInSb(80-20) CPA
DOS(PER BOND)--->
0.028
0.026
0.024
0.022
0.02
0.018
0.016
0.014
0.012
0.01
0.008
0.006
0.004
0.002
0
-18
-16
-14
-12
-10
-8
-6
-4
ENERGY(eV)--->
Figure 4.5.8

$$|\phi_A\rangle = (1/\sqrt{2})\left[(1/2)\left[|\phi^s_{Ga}\rangle + |\phi^s_{As}\rangle\right] + (\sqrt{3}/2)\left[|\phi^p_{Ga}\rangle + |\phi^p_{As}\rangle\right]\right]$$

$$= (1/2\sqrt{2})\left[\left[|\phi^s_{Ga}\rangle + |\phi^s_{As}\rangle\right] + (\sqrt{3})\left[|\phi^p_{Ga}\rangle + |\phi^p_{As}\rangle\right]\right] \qquad (4.6.3)$$

Similarly

$$|\phi_B\rangle = (1/2\sqrt{2})\left[\left[|\phi^s_{Ga}\rangle + |\phi^s_{Sb}\rangle\right] + (\sqrt{3})\left[|\phi^p_{Ga}\rangle + |\phi^p_{Sb}\rangle\right]\right]$$

The Fourier transforms of $\phi_A(\bar{r})$ and $\phi_B(\bar{r})$ are given by

$$|\phi_{A,B}(\bar{k})\rangle = \int e^{i\bar{k}\cdot\bar{r}}\phi_{A,B}(\bar{r})\, d^3\bar{r}$$

$$= (1/2\sqrt{2})\left[\phi^s_{Ga}(\bar{k}) + \phi^s_{As,Sb}(\bar{k})\right] +$$

$$(\sqrt{3}/2\sqrt{2})\left[\phi^p_{Ga}(\bar{k}) + \phi^p_{As,Sb}(\bar{k})\right] \qquad (4.6.4)$$

where $\phi^S(k) = (\sqrt{\pi}/2k)\int_0^\infty r\,\sin(kr/2)\,\phi^S(r)\,dr$

(4.6.5)

$$\phi^P(k) = (i/k^2)\sqrt{3\pi}\int_0^\infty\left[\sin(kr/2) - (kr/2)\cos(kr/2)\right]\phi^P(r)\,dr$$

(r in Bhor unit)

$$k = 2\sqrt{M(E_i + \omega)}$$

Here E_i and ω are in Rydberg units and $M = m^*/m_e$.

Thus using the equation (3.6.32) and the calculated DOS $n_i(E_i)$, $n_f(E)$ and self energy together with the equation (4.6.3) ,

(4.6.4) and (4.6.5) and the values of $\phi^s(r)$ and $\phi^p(r)$ (reported by Herman and Skillman (1970)) for the various atoms in the alloys , we calculate the optical conductivities for the alloys . Since the values of $\phi^s(r)$ and $\phi^p(r)$ are given in the unequal intervals of r (in the logerthmic scale) and are zero after a finite values of r , we used trapezial rule to calculate the integrals (4.6.5) . Then using the Kramers-Krönig relations , we calculate the other response functions

Figures (4.6.1) and (4.6.2) show the optical conductivities as a function of the incoming photon for $GaAs_{0.5}Sb_{0.5}$ and $GaAs_{0.8}Sb_{0.2}$ respectively . Each of these figures show significant effects of disorder . It is clear that in the case of 50% - 50% concentration the effect is more than the 80% - 20% concentration case . In both of the cases the effect of disorder has reduced the magnitude of the conductivity . Thus we can say that the vertex correction is negative .

The calculations of the other response functions like the imaginary part of the complex dielectric function (figures (4.6.3) and (4.6.4)) ,the real part of the complex dielectric function (figures (4.6.5) and (4.6.6)) ,the refractive index function (figure (4.6.7)) and the absorption coefficient (figure (4.6.8)) also show the significant effects of the disorder .These quantities are related to one another as discussed . In these figures we see that the sharp structure of the DOS gets smoothened out because of the fact that in these properties DOS is convulated with featureless DOS

of conduction band and relatively featureless of the square of the optical matrix element .These figures also show that peak positions are shifted and widths are increased due to the disorder induced corrections .

Figures (4.6.9) , (4.6.10), (4.6.11) and (4.6.12) show the square of the optical matrix element (transition probability) as a function of energy for $GaAs_{0.5}Sb_{0.5}$ (for ω = 0.3 and 0.9Ry) and $GaAs_{0.8}Sb_{0.2}$(for ω = 0.3 and 0.9Ry) respectively .It is clear from all these figures that optical matrix element indeed depends on both the energy and disorder . Though in the case of (80-20%) composition, the magnetude due to disorder effect does not differ much (The effect is least in the weak disorder case of the dilute alloy) but there is some sharp structures seen in this case. These structures are more in the case when ω = 0.9 Ry. This is because the impurity (GaSb) has a site energy $\simeq$ 0.7 Ry which lies between 0 to 0.9 Ry and the scattering is more at impurity sites. Thus this clearly shows that in order to interpret energy resolved photo-emission experiment one must take into account of the effect of disorder, because the energy resolved experiment gives the DOS multiplied by square of the optical matrix element. Therefore the observation of photo-emission experiment will differ from the correct band structure by both the magnetude and structure.

The figures (4.6.13) to (4.6.16) for $GaAs_{0.5}Sb_{0.5}$ (ω = 0.3 and 0.9 Ry) and $GaAs_{0.8}Sb_{0.2}$ (ω = 0.3 and 0.9 Ry) respectively show how the effect of disorder make the difference of band structure

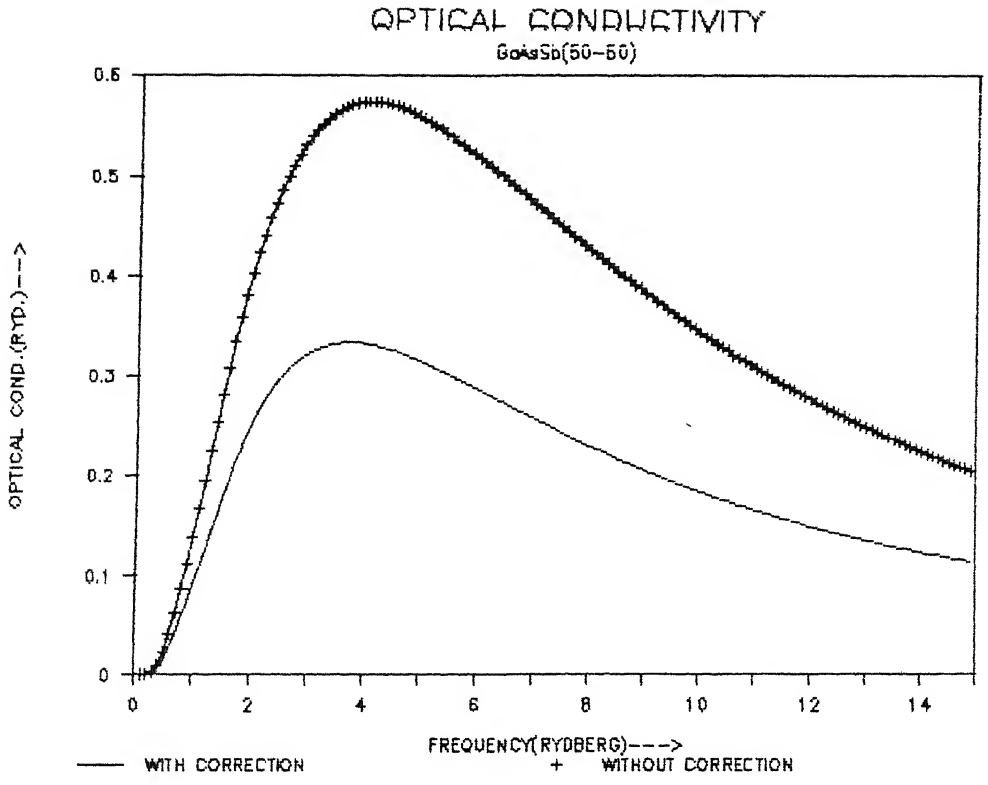

Figure 4.6.1

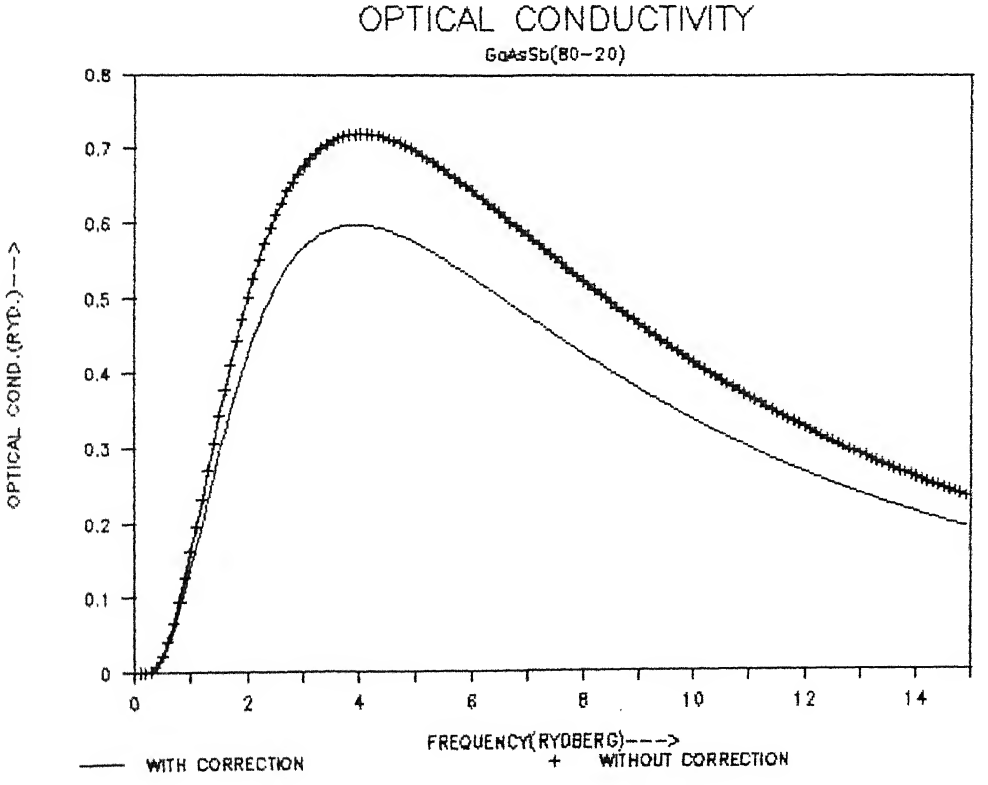

Figure 4.6.2

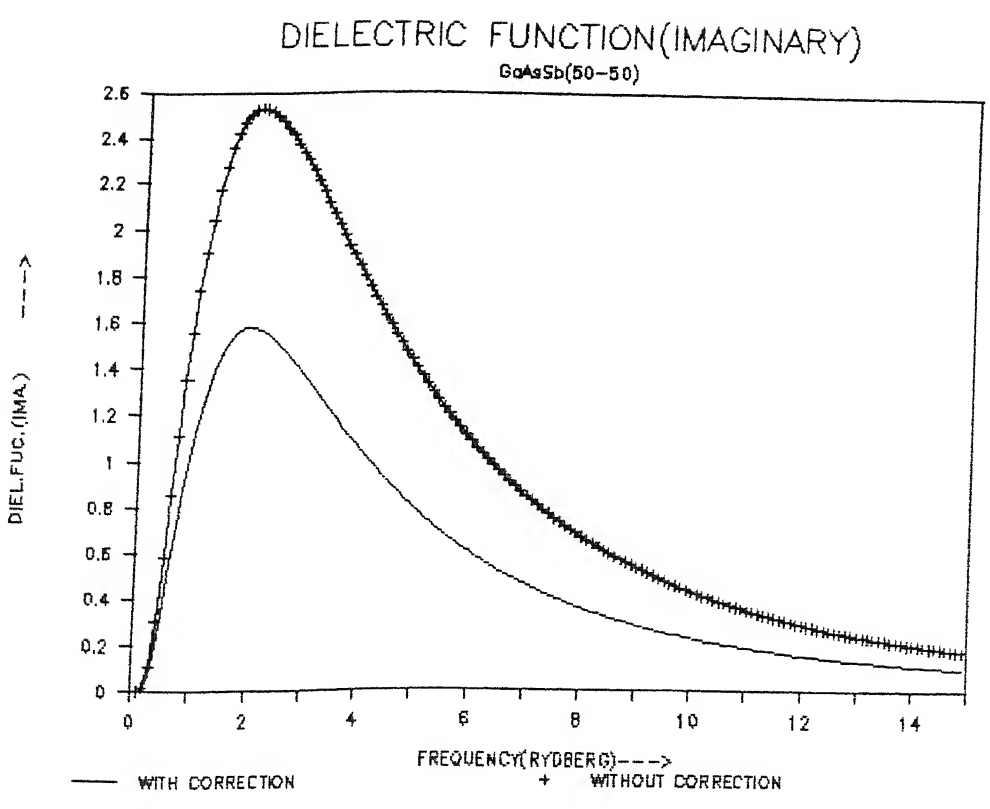

Figure 4.6.3

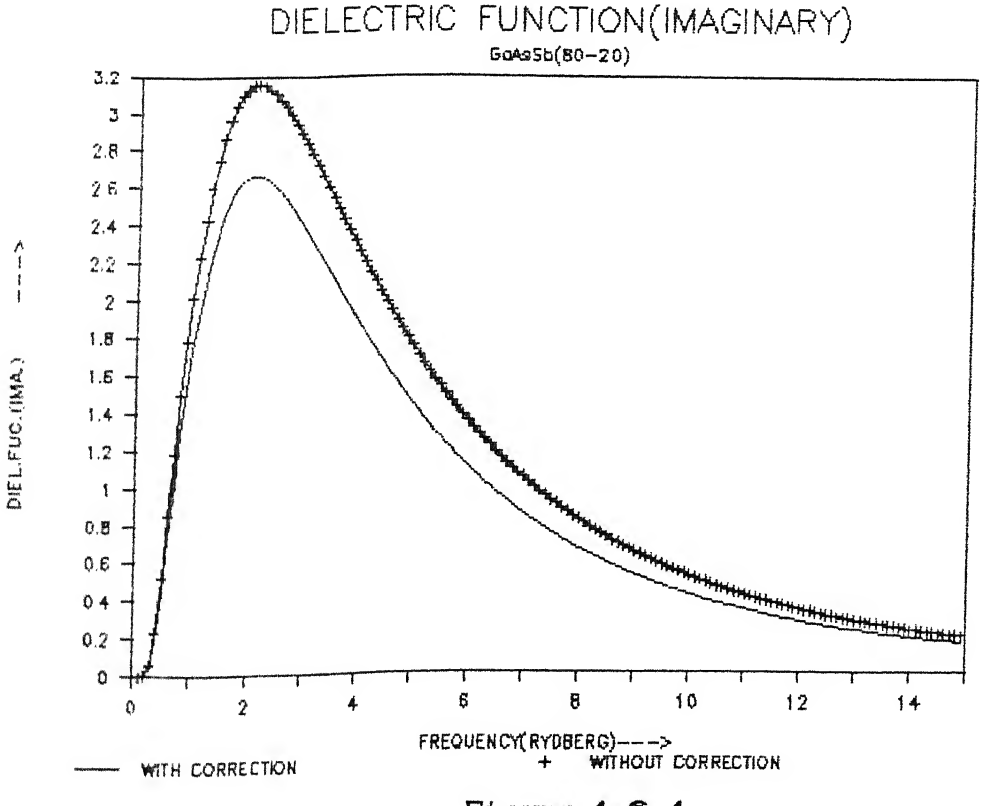

Figure 4.6.4

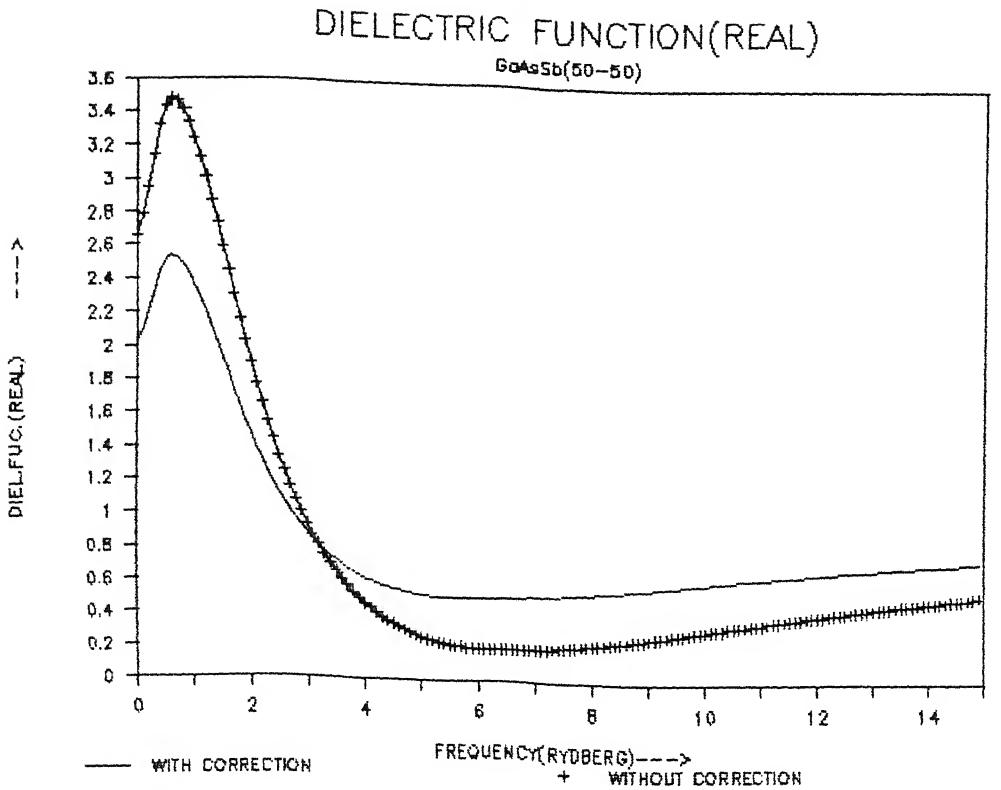
DIELECTRIC FUNCTION(REAL)
GaAsSb(50-50)
DIEL.FUC.(REAL) --->
FREQUENCY(RYDBERG)--->
WITH CORRECTION
WITHOUT CORRECTION

Figure 4.6.5

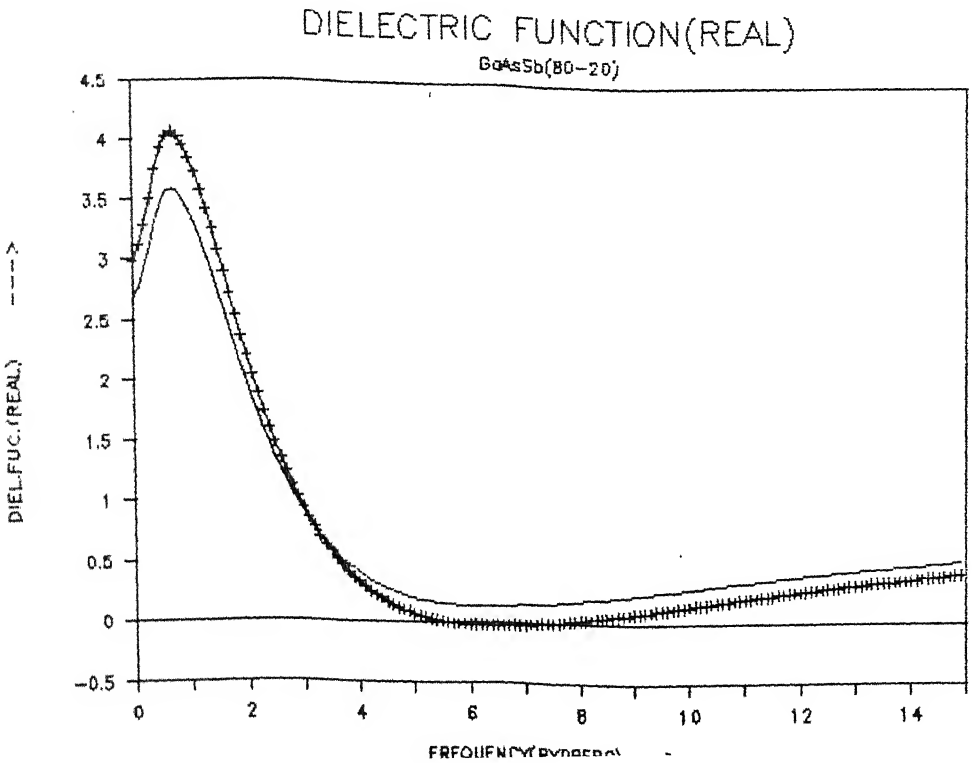
DIELECTRIC FUNCTION(REAL)
GaAsSb(80-20)
DIEL.FUC.(REAL) --->
FREQUENCY(RYDBERG)

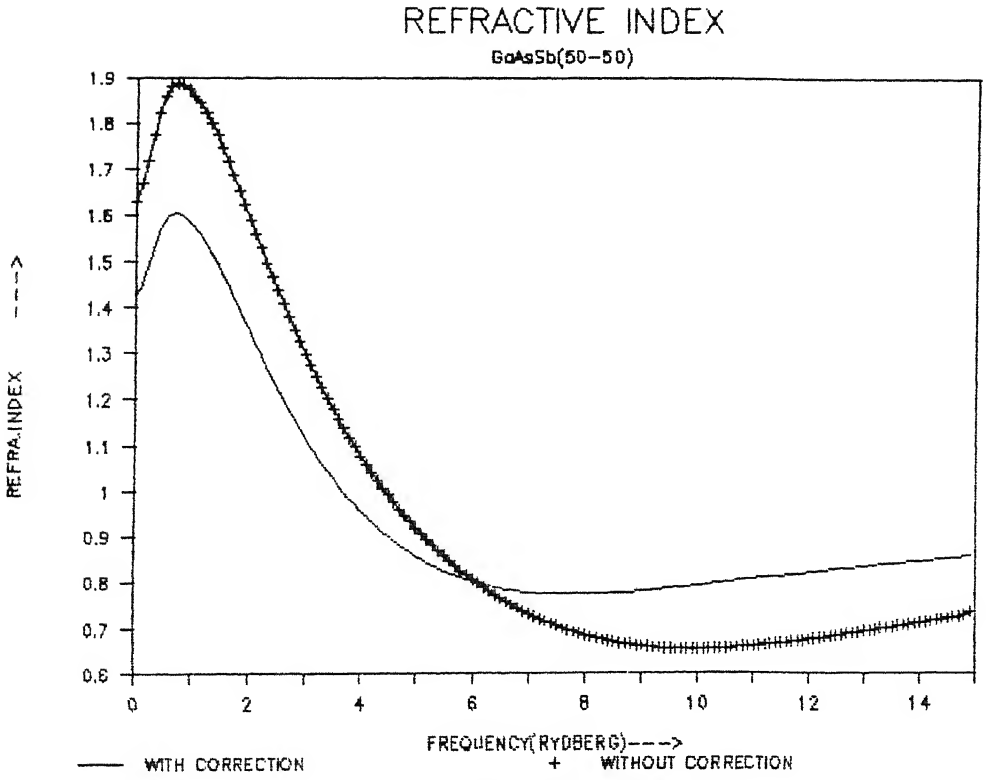

Figure 4.6.7

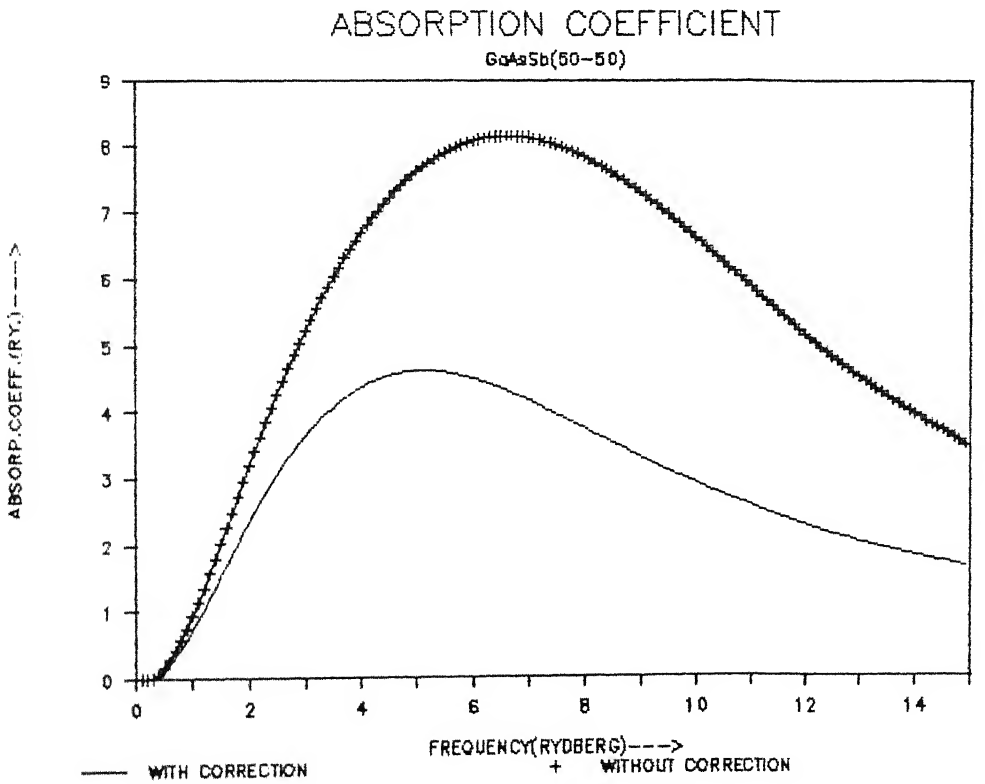

Figure 4.6.8

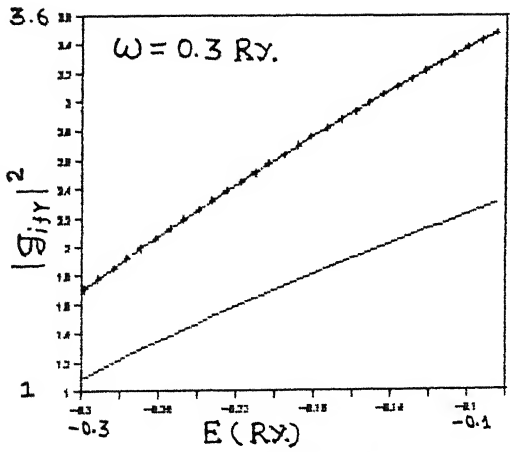

Figure 4.6.9

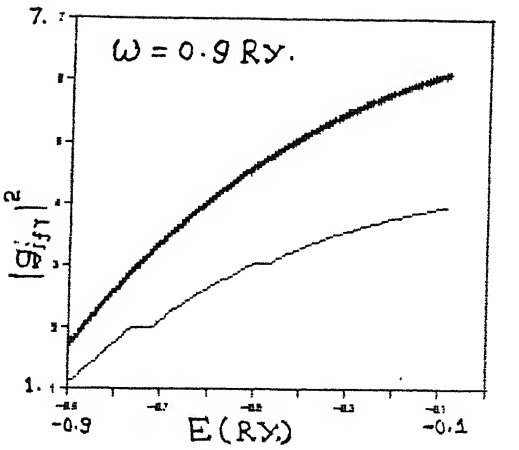

Figure 4.6.10

Square of optical matrix element(transition probability)as a function of energy for $GaAs_{0.5}Sb_{0.5}$ with ω = 0.3 Ry. and 0.9 Ry. respectively. — with correction
+ without correction

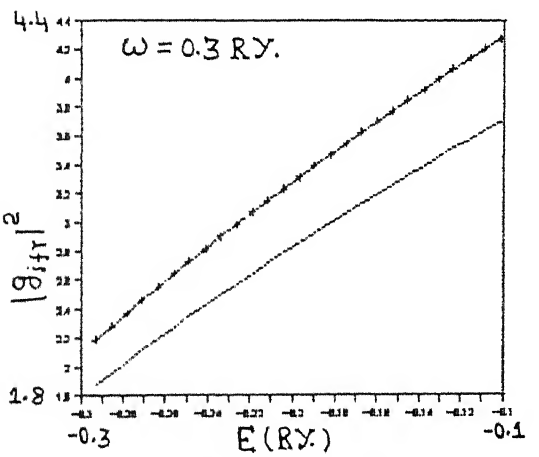

Figure 4.6.11

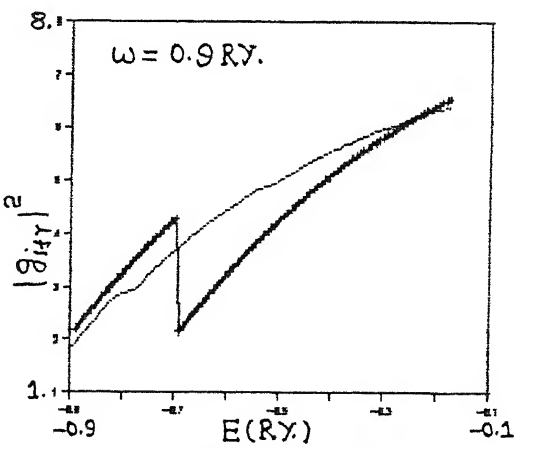

Figure 4.6.12

Square of optical matrix element(transition probability)as a function of energy for $GaAs_{0.8}Sb_{0.2}$ with ω = 0.3 Ry. and 0.9 Ry. respectively. — with correction
+ without correction

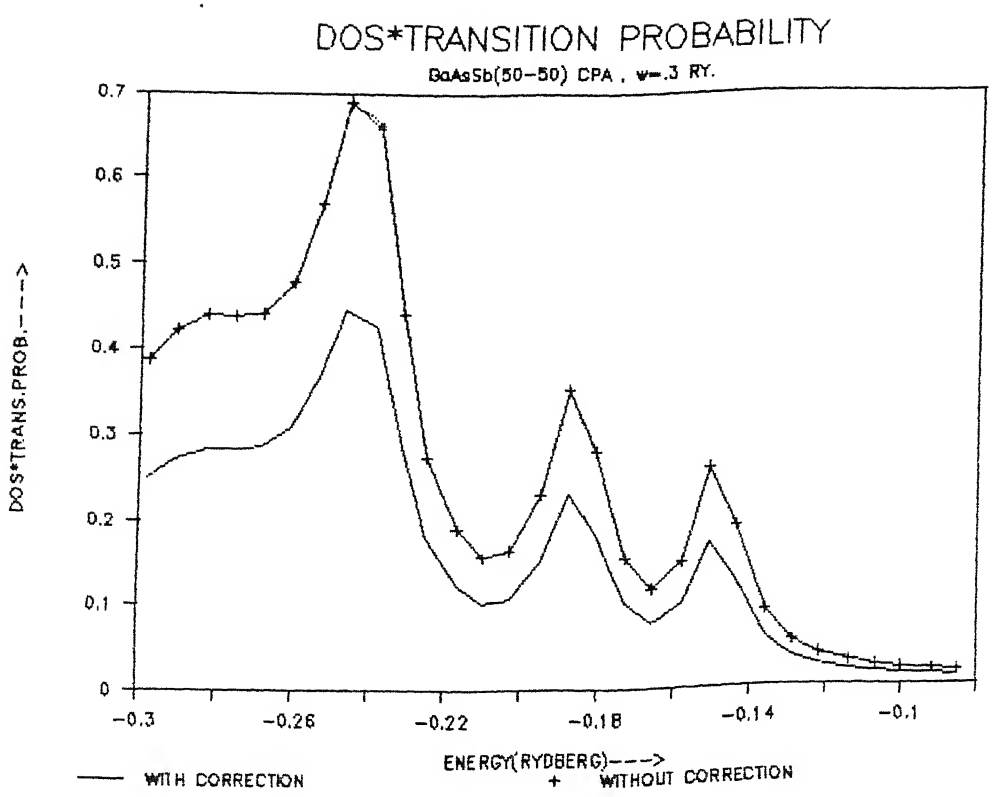

Figure 4.6.13

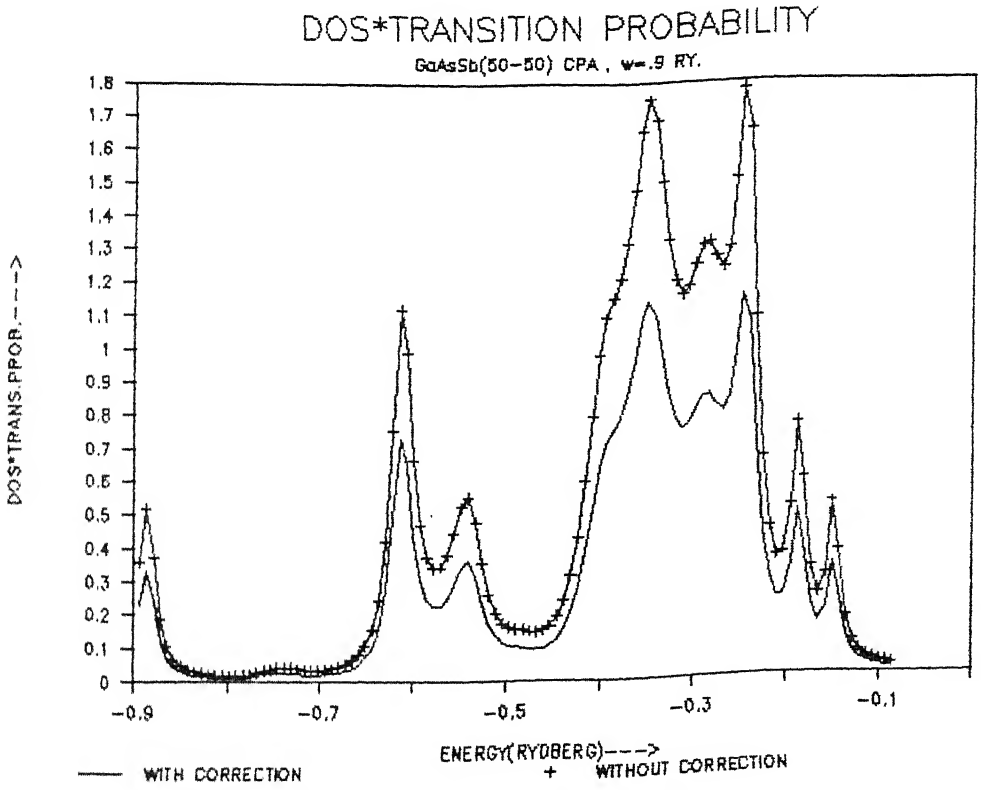

Figure 4.6.14

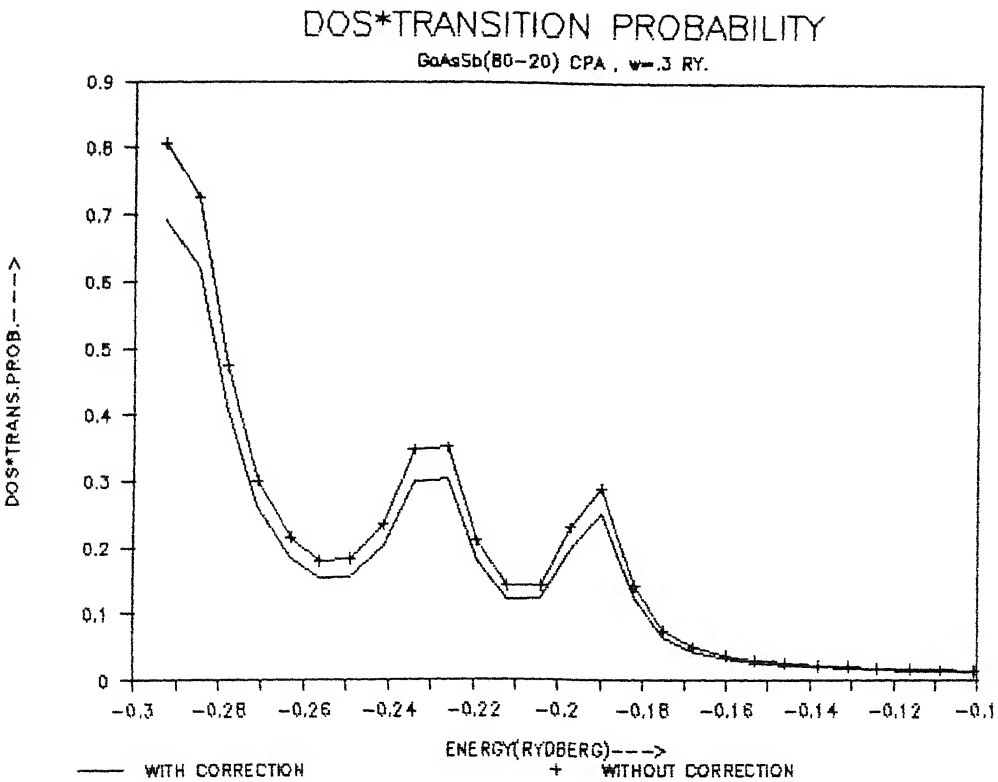

Figure 4.6.15

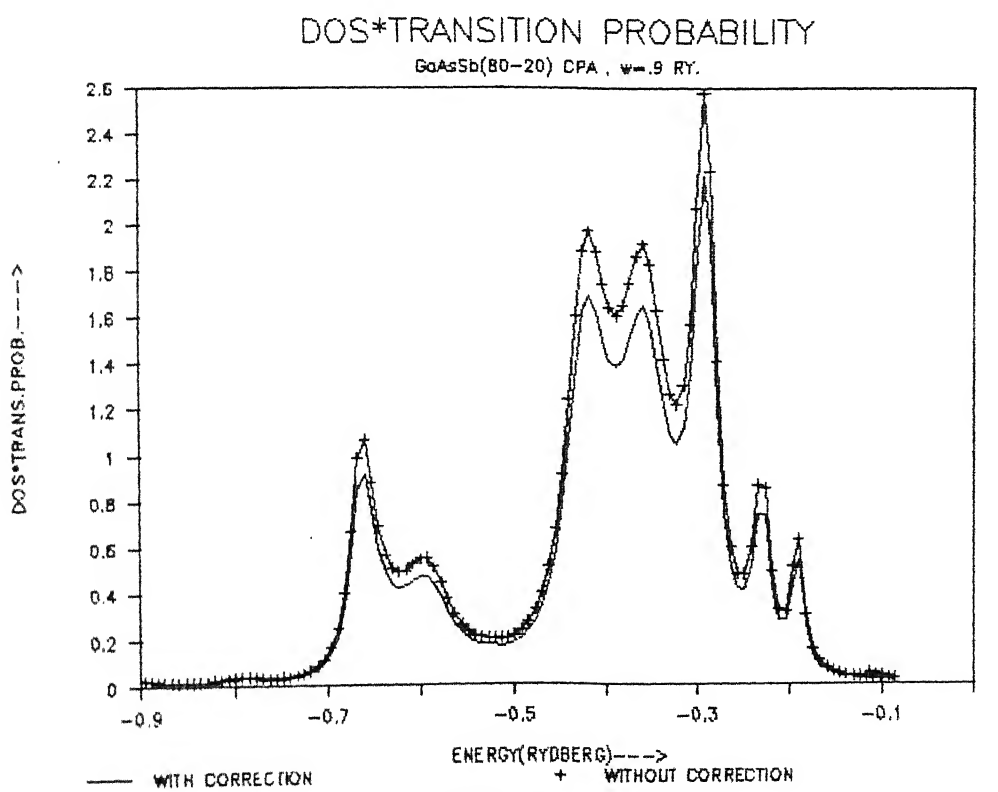

Figure 4.6.16

calculation from that of obtained from experiments. Thus to get accurate DOS one has to divide the results obtained from the experiments by the correct value of square of the optical matrix element.

Figures (4.6.17) and (4.6.18) show the optical conductivity and the dielectric function (real) respectively for $Ga_{0.5}In_{0.5}Sb$. In this case the vertex correction is almost negligible. This is because of the negligible disorder effects, as can be seen from the table (4.5.1) that various parameters of GaSb and InSb are almost the same, means the alloys of these at various concentration make a weak scattering case, *i.e.* effects of disorder over the VCA is very small. The figures (4.6.21) to (4.6.24) for self energy as a function of energy for $GaAs_{0.5}Sb_{0.5}$ and $Ga_{0.5}In_{0.5}Sb$ further make the above reasoning clear. The self energy for $Ga_{0.5}In_{0.5}Sb$ is very-very smaller than the case of $GaAs_{0.5}Sb_{0.5}$. Thus the effects of disorder in the case of alloy GaInSb is negligible.

Since the correction term to the optical matrix element is $(\Sigma_o/\delta\varepsilon)\delta\phi$ and if Σ_o, $\delta\varepsilon$ and $\delta\phi$ are very-very small, this term has to be neglected which is true in the case of the alloy GaInSb.

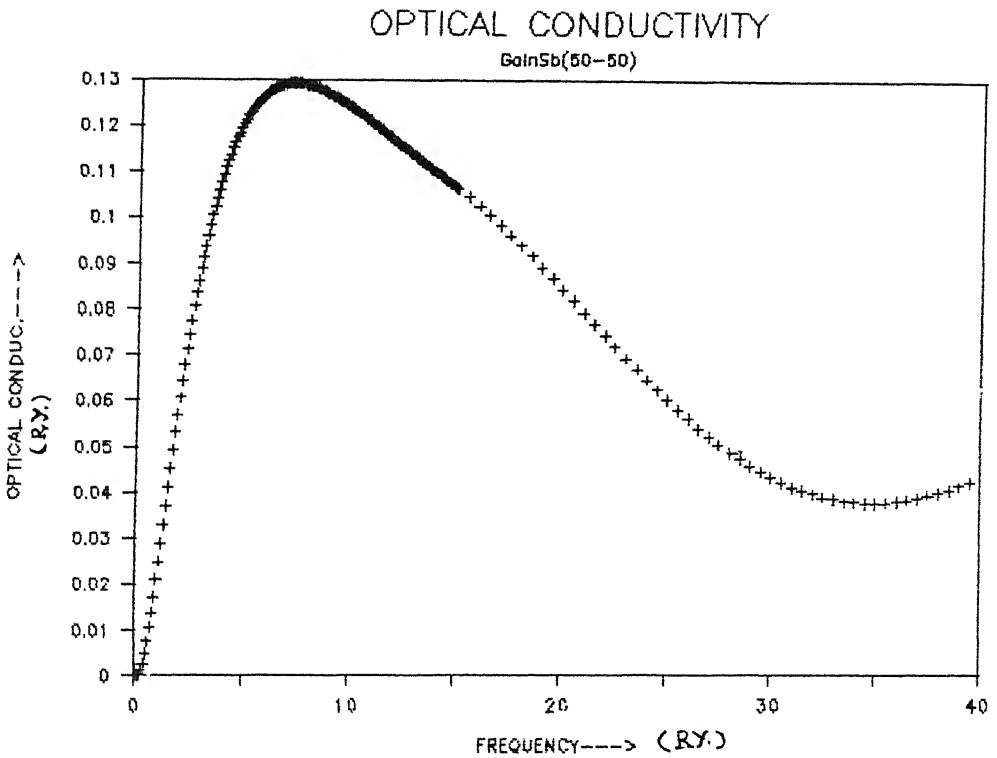

Figure 4.6.17

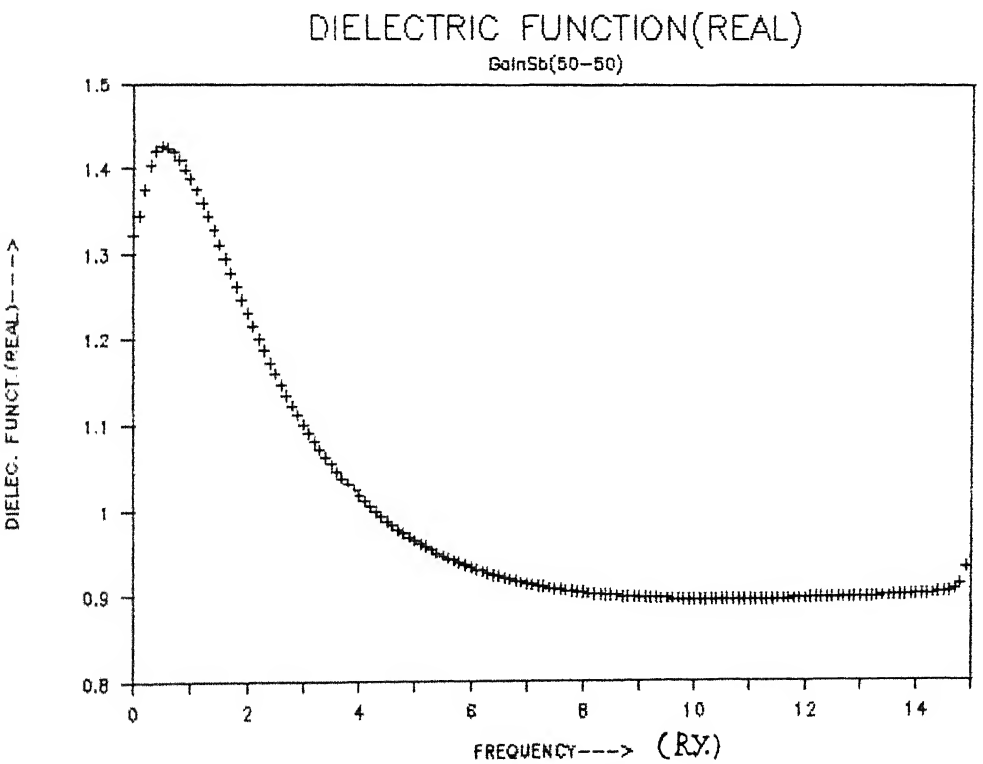

Figure 4.6.18

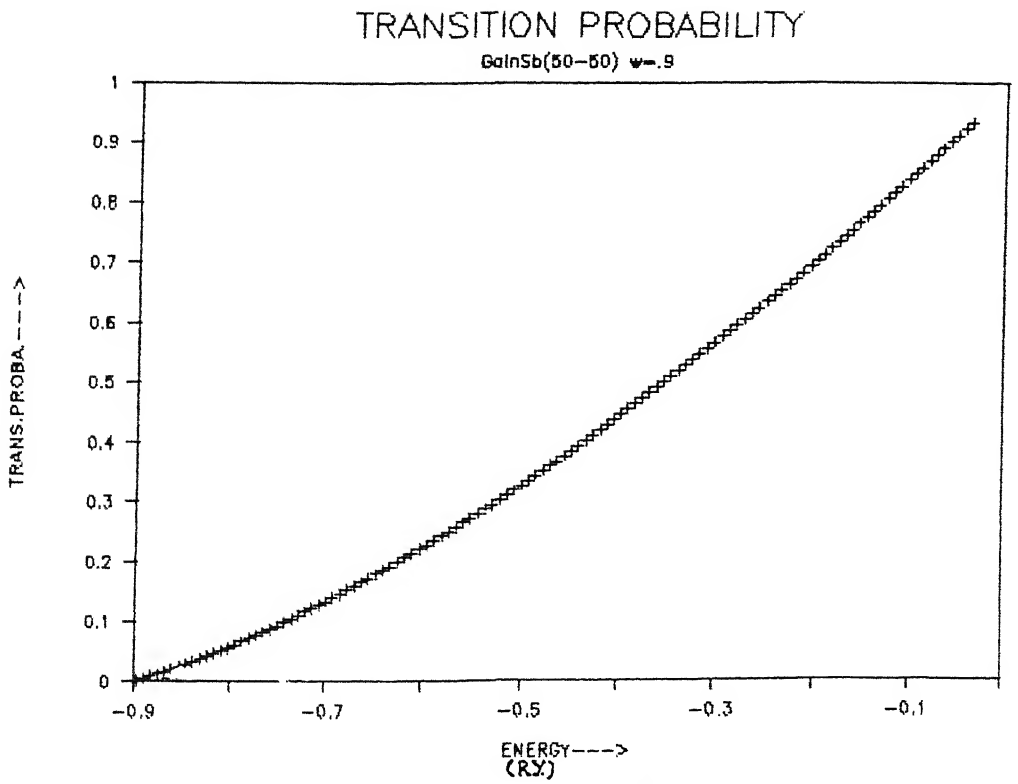

Figure 4.6.19

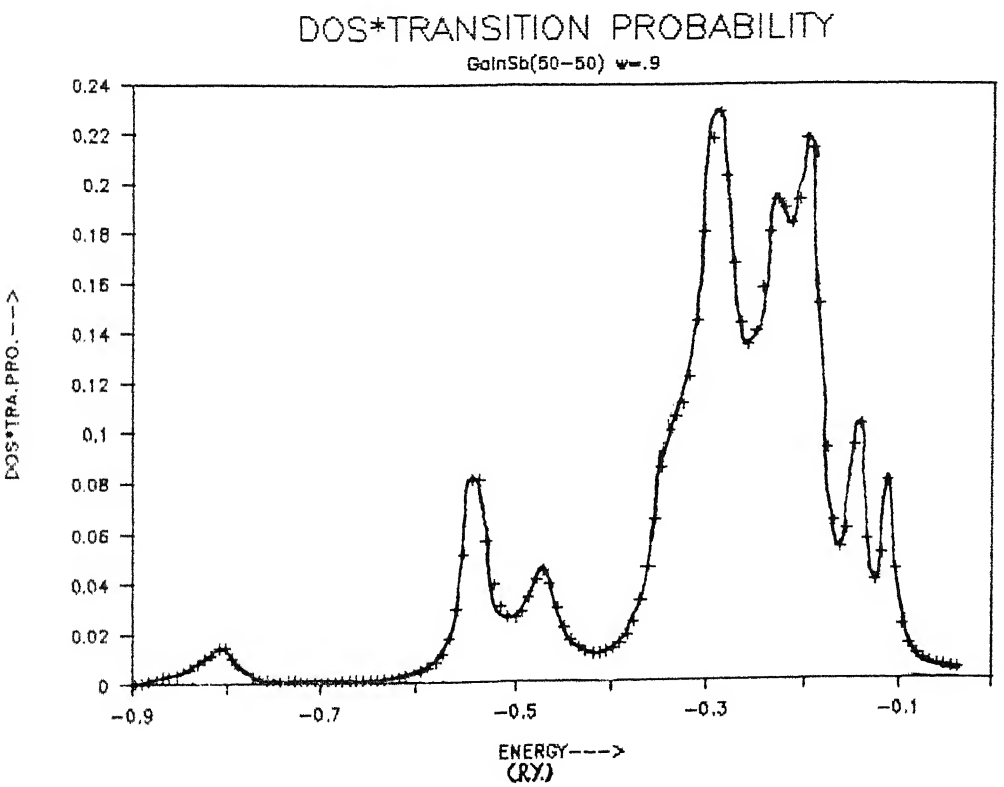

Figure 4.6.20

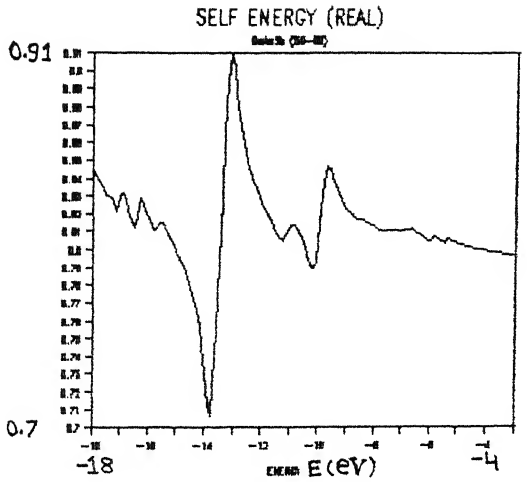

Figure 4.6.21

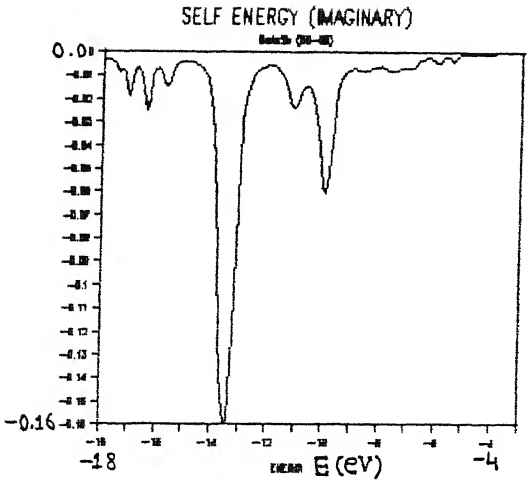

Figure 4.6.22

Self energy (Real and Imaginary parts respectively) for $GaAs_{0.5}Sb_{0.5}$ as a function of energy.

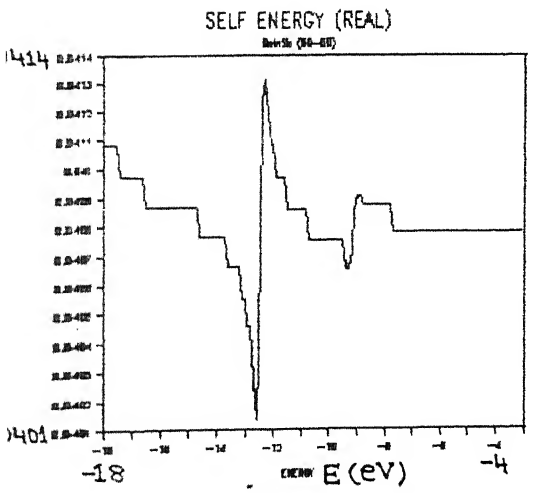

Figure 4.6.23

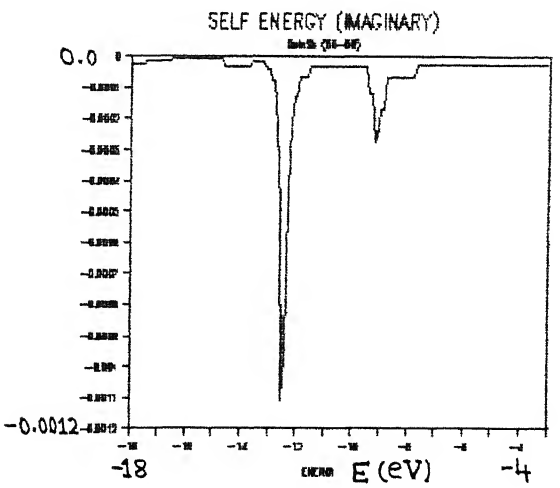

Figure 4.6.24

Self energy (Real and Imaginary parts respectively) for $Ga_{0.5}In_{0.5}Sb$ as a function of energy.

CHAPTER V

CONCLUDING REMARKS

In this work we have carried out the application of the Augmented Space Formalism (ASF) to a formulation of the optical response of random semiconducting alloys. We have shown, through the application of the formulation to a model system and III-V ternary alloys $GaAs_{1-c}Sb_c$ and $Ga_{1-c}In_cSb$ (for c = 0.5 and 0.2), that the modifications due to the effect of disorder may be significant. This effect comes from the inclusion of the vertex correction related to the averaging of the square of the optical matrix element together with the valence band DOS, *i.e.* $\langle |g_{if\gamma}|^2 n_i(E)\rangle_{av} = |g^{eff}_{if\gamma}|^2 \langle n_i(E_i)\rangle$. Therefore the assumption which was usually made in the earlier works that the optical matrix element is independent on disorder or very weakly dependent may not be correct in several situations. Thus we have been able to extend the ASF in generalizaing the study of optical properties of random semoconducting alloys.

In this work we have also included cluster coherent potential approximation (only in the model calculation) and shown that cluster effect is indeed seen in the optical matrix element.

In this work we assumed the conduction band density of states to be like nearly free electron. This needs modification. The conduction band should be treated more accurately than the nearly free electron model. Within the tight-binding model for III-V semiconductors this has been attempted by Chen and Sher (1980).

We have also ignored the vertex correction related to the averaging of the conduction band DOS together with the valence band DOS and the square of the optical matrix element, *i.e.*

$$\langle |g^{eff}_{if\gamma}|^2 G_v\ G_c \rangle = |g^{eff}_{if\gamma}|^2 \langle G_v\ G_c \rangle \neq |g^{eff}_{if\gamma}|^2 \langle G_v \rangle \langle G_c \rangle .$$

Thus the vertex correction term

$$\langle G_v\ G_c \rangle = \langle G_v \rangle \langle G_c \rangle + \langle G_v \rangle \underline{\Lambda} \langle G_c \rangle$$

has to be included maintaining the word identity $\underline{\Lambda} = \delta \underline{\Sigma} / \delta \langle G \rangle$. This can be implemented in the Augmented Space Formalism and has been discussed in some detail by Thakur et al. (1987) and Mookerjee (1986).

In our calculations of the DOS we went upto the 14^{th} steps of recursion and used the square root terminator to terminate the continued fraction expansion. But this is insufficient for more accurate calculation. Therefore the Recursion method has to be done more accurately, specially correct terminator scheme has to be used. This has been done lately by Haydock and Nex (1984, 1985).

In our calculation we used the band gap and the effective electron mass for the ternary alloys to be equal to the average of these of the respective pure semiconductors in the alloy. But this approximation is not good. One has to take the correct band gap and effective electron mass . It has been found empirically by A.G. Thompson and J.C. Woolley (1967) that the band gap $E_g(x)$ of a ternary alloy varies with concentration x as follows :

$$E_g(x) = E_{g1} + bx + cx^2$$

where E_{g1} is the band gap of the lower band gap binary and b and c are constants with $E_{g2} = E_{g1} + b + c$; E_{g2} is the band gap of the higher band gap binary. For the alloy, $GaAs_xSb_{x-1}$, the constants b and c found, at T = 300 ^oK, to be equal to -0.32 eV and 1.005 eV respectively by G.A. Antypas and L.W. James (1970).

We used the values of the interaction parameters for the pure semiconductors obtained by parametrization procedure (which is very ambiguous) of Chen and Sher. For more accurate calculation the value of these parameters obtained by the Chemical-pseudopotential approach of Anderson (1969) and Bullett (1975) may be used.

In our calculations we adopted tight binding model. We should, however, not stress too much on this, as the tight binding model calculation should indicate trends rather than really quantitatively reliable estimate. Therefore the need was felt, for future work, to go beyond the tight binding approximation. For metallic alloys, the self-consistent KKR-CPA techniques have been developed. The KKR equations have close resemblance to the tight binding method. the diagonal ε_i term in the tight binding Hasmiltonian is replaced by the inverse t-matrix, the off-diagonal hopping term V_{ij} is replaced by the structure function $B_{ij}^{LL'}$, and the Green function by the path operator.

One has to go beyond the single site approximation and consider the cluster approximation for the correct study of band structure. The generalization of the Augmented Space CCPA to KKR method has recently been carried out by Mookerjee (1987).

In cases, where the basis is not countable, an embedding technique was developed by Mookerjee and Bardhan (1989) generalizing the earlier work by Inglesfield (1981). It is essentially a generalization of the partition theorem. The Augmented Space method then allows us to develop a CCPA procedure in such cases. This work is in progress and will enable us to study systems with random distribution of extended impurities or defects.

Our calculations are at T = 0 $^{\circ}$K. However, most experimental observations are not at T = 0 $^{\circ}$K. So it could be interesting to study the optical response with varying temperatures.

Since the lattice parameters at T =300°K for GaAs and GaSb are very different from one another (5.65 A$^{\circ}$ and 6.10 A$^{\circ}$), there is a lattice mismatch in the alloy of these. In other words the alloy of these semiconductors will have high lattice deformation at the boundary between these. Because of the high lattice deformation, these alloys are not preferred for making devices and semiconductor lasers. Thus this alloy was not popular, and therefore, probably, very little experimental studies have been carried out. Hence at present,our calculation can not be compared with experimental results. But these alloys were grown up and phase diagrams were

studied extensively (Kressel and Butler (1977)). Now there is growing interest in this alloy because it can be used to produce lattice matched heterojunctions in conjunction with AlGaAsSb and also this can be prepared most easily by Liquid Phase Epitaxy (LPE) method (Kressel and Butler (1977)). Because of the large lattice parameter change with composition (7.5% across the full composition range), a miscibility gap may exist for intermediate composition values. However, excellent devices have been prepared in the 1.1 eV bandgap energy range in the As-rich composition large (Kressel and Butler (1977)).

The GaSb and InSb are continuously miscible , but there are technological difficulties in producing homogeneous $Ga_{1-x}In_xSb$ alloy with a given mixing ratio x by procedure which rely on diffusion process. The alloy has been prepared and the optical properties were investigated in number of studies (Madelung,1964) . Since in this work we are studying the disorder effect of optical matrix element, we shall not be much interested in this alloy , because the vertex correction arising due to the disorder dependence of the optical matrix element is negligible in this case.

REFERENCES

Anderson P.W. & McMillan, W.L. (1967) Proceedings of the International School of Physics 'Enrico Fermi', edited by H.Shul (Academic Press, New York).

Anderson P.W., (1969) Phys. Rev. **181**, 25.

Animalu Alexander O.E., (1978) *Intermediate Quantum Theory of Crystalline Solids* (Prentice Hall of India Private Limited, New Delhi).

Antypas G.A. & James L.W., (1970) J. Appl. Phys. **41**, 2165.

Bishop A.R. & Mookerjee A., (1974) J. Phys. **C7**, 2165.

Bullet D.W., (1975) J. Phys. **C8**, 2695.

Butler W.H., (1972) Phys. Lett. **39**, A203.

Butler W.H., (1973) Phys. Rev. **B8**, 4499.

Chandrasekhar S., (1960) *Radiative Transfer* (Dover, New York).

Chen A.B. & Sher A., (1978) Phys. rev. **B17**, 4726.

Chen A.B. & Sher A., (1980) Phys. rev. **B22**, 3886.

Chihara T.S., (1978) *An Introduction To Orthogonal Polynomials* (Gordon & Breach, New York).

Cody G.D., (1984) in *Hydrogenrated Amorphous Silicon*, edited by J. Pankove (Academic , New York)

Harrison W.A. (1973) Phys. Rev. **B8**, 4487.

Harrison W.A. & Ciraci S., (1974) Phys. Rev. **B10**, 1516.

Haydock R., (1972) *Ph.D. Thesis* (University of Cambridge).

Haydock R., Heine V. & Kelley M.J., (1972) J. Phys. **C5**, 2845.

Haydock R., (1980) *Solid State Physics* **35** (Academic Press, New York).

Haydock R., & Nex C.M.M., (1984) J. Phys. **C17**, 4783.

Haydock R., & Nex C.M.M., (1985) J. Phys. **C18**, 2235.

Haydock R., (1987) in *Electronic Band Structure and Its Applications*, edited by M. Yussouff, Lecture Notes in Physcs 283 (Springer-Verlag).

Herman F. & Skillman S., (1970) *Atomic Structure Calculations* (Prentice Hall, Inc. New Jersy).

Inglesfield J.E., (1981) J. Phys. **C14**, 3795.

Kaplan T. & Gray L.J., (1976) Phys. rev. **B14**, 3462.

Kaplan T. & Gray L.J., (1977) Phys. Rev **B15**, 3260.

Kirkpatrick S., Velicky B. & Ehrenreich H., (1970) Phys. Rev. **B1**, 3250.

Kressel H. & Butler J.K., (1977) *Semiconductor Lasers and Heterojunction LEDs* (Academic Press, New York).

Kubo , (1957) J. Phys. Soc. Japan **12**, 570.

Kumar N. & Jayannavar A.M., (1985) Phys. rev. **B32**, 3345.

Kumar N. & Jayannavar A.M., (1986) J. Phys. **C19**, 5513.

Kumar V., Mookerjee A. & Srivastava V.K., (1982) J. Phys. **C15**, 1939.

Leath P.L., (1968) Phys. Rev. **171**, 725.

Leath P.L., (1970) Phys. Rev. **B2**, 3078.

Madelung O., (1964) *Physics of III-V Compounds* , Jhon Willey & Sons (New York)

Magnus A., (1984) in the *Recursion Method and Its Applications*, edit by D.G. Pettifor and D.L. Weaire, Springer Series in Solid State Sciences, 58 (Springer-Verlag)

Mills R. & Ratanavararaksa R., (1978) Phys. Rev. **B18**, 5291.

Mookerjee A., (1973a) J. Phys. **C6**, L205.

Mookerjee A., (1973b) J. Phys. **C6**, 1340.

Mookerjee A., (1975a) J. Phys. **C8**, 24.

Mookerjee A., (1975b) J. Phys. **C8**, 1524.

Mookerjee A., (1975c) J. Phys. **C8**, 2688.

Mookerjee A., (1979) *Disordered Systems* (Hindustan Publishing Corporn., Delhi).

Mookerjee A., (1986) J. Phys. **C19**, 275.

Mookerjee A., (1986) J. Phys. **C19**, 193.

Mookerjee A., (1987) J. Phys. **F17**, 1511.

Mookerjee A., & Bardhan S., (1989) J. Phys. Condensed Matter **1**, 509.

Müller-Hartmann E., (1973) Solid State Commun. **12**, 1269.

Nex C.M.M., (1978) J. Phys. **A111**, 653.

Nex C.M.M., (1984) Computer Phys. Commun. **34**, 101.

Nickel B.G. & Krummhansl J.A., (1971) Phys. Rev. **B4**, 4357.

Nilson P.O., (1974), *Solid State Physics*, 29 (Academic Press New York).

Pickett W.E., Papaconstantopoulos D.A. & Economou E.N., (1983) Phys. Rev. **B28**, 2232.

Schiff L.I., (1968) *Quantum Mechanics*, 3rd edition (McGraw-Hill Kogakusha, Ltd., Tokyo).

Soven P., (1967) Phys. Rev. **156**, 809.

Srivastava V.K., (1982) *Ph.D. Thesis* (I.I.T. Kanpur) (Unpublished).

Stocks G.M., Williams R.W. & Faulkner J.S., (1971) Phys. Rev. Lett. **26**, 253.

Thakur P.K., Mookerjee A. & Yussouff M., (1987) in *Current Trends in The Physics of Materials*, edited by M. Yussouff (World Scientific, New Jersey).

Thompson A.G. & Woolley J.C., (1967) Can. J. Phys. **45**, 255.

Yonezawa F. & Matsubara T., (1966a) Prog. Theor. Phys. **35**, 357.

Yonezawa F. & Matsubara T., (1966b) Prog. Theor. Phys. **35**, 759.

Yonezawa F., (1968a) Prog. Theor. Phys. **39**, 1076.

Yonezawa F., (1968b) Prog. Theor. Phys. **40**, 734.

Závétova M. & Velicky B., (1976) in *The Optical Properties of Solids - New Developments*, edited by B.O. Seraphin (North-Holland Publishing Company, Amasterdam).

Zdetsis A.D., Economou E.N., Papaconstantopoulos D.A. & Flytzanis N., (1985) Phys. Rev. **B31**, 2410.

PHY-1989-D-GAN-OPT